

Dissertation  
zur Erlangung des Doktorgrades  
der Fakultät für Chemie und Pharmazie der  
Ludwig-Maximilians-Universität München



Magselectofection: A novel integrated technology of magnetic separation  
and genetic modification of target cells

Vorgelegt von

Yolanda Sánchez Antequera

aus Valencia

2010

## Erklärung

Diese Dissertation wurde im Sinne von § 13 Abs. 3 bzw. 4 der Promotionsordnung vom 29. Januar 1998 von PD Dr. Christian Plank, TUM, betreut und von Prof. Dr. Ernst Wagner an der Fakultät für Chemie und Pharmazie der LMU vertreten.

## Ehrenwörtliche Versicherung

Diese Dissertation wurde selbständig, ohne unerlaubte Hilfe erarbeitet.

München, am 13.09.2010

Yolanda Sánchez Antequera

Dissertation eingereicht am 13.09.2010

1. Gutacher: Prof. Dr. Ernst Wagner

2. Gutacher: PD Dr. Christian Plank

Mündliche Prüfung am 23.11.2010

---

## TABLE OF CONTENT

1.	INTRODUCTION .....	1
1.1.	A brief history of gene therapy .....	1
1.2.	Gene and cell therapies, ex vivo and in vivo .....	3
1.2.1.	Ex vivo and in vivo nucleic acid (gene) therapy .....	3
1.2.2.	Cell therapies.....	5
1.3.	Vectors and physical methods for nucleic acid delivery .....	6
1.3.1.	Viral vectors.....	6
1.3.2.	Non-viral vectors .....	7
1.3.3.	Physical methods, Magnetofection.....	10
1.4.	Magnetic cell separation .....	12
1.5.	Objectives of this thesis.....	14
2.	MATERIALS AND METHODS .....	15
2.1.	Material .....	15
2.1.1.	Chemicals and reagents.....	15
2.1.2.	Cell culture reagents.....	15
2.1.3.	Plasmids.....	16
2.1.4.	Chemical reagents and buffers.....	16
2.2.	Cell isolation and culture.....	17
2.2.1.	Isolation of the PBMC and CD34 <sup>+</sup> by Ficoll gradient .....	17
2.2.2.	Isolation of Wharton's Jelly stem cells (hUC-MS) .....	18
2.2.3.	Cell culture.....	19
2.3.	Magnetic nanoparticles.....	20
2.3.1.	Synthesis.....	20
2.3.2.	Characterization of magnetic nanoparticles .....	21
2.3.3.	Determination of magnetic nanoparticle concentration in terms of dry weight and iron content .....	21
2.4.	Lentivirus production and titer estimation .....	22
2.4.1.	Packaging of lentivirus vectors.....	22

---

2.4.2.	Biological titer of the lentivirus .....	23
2.4.3.	Physical titer of the lentivirus.....	23
2.5.	Preparation and characterisation of transfection complexes.....	24
2.5.1.	Assembling of magnetic non-viral complexes for magnetofection.....	24
2.5.2.	Assembling of magnetic non-viral complexes for magselectofection .....	24
2.5.3.	Assembling of magnetic virus complexes for magnetofection and standard infection.....	25
2.5.4.	Assembling of magnetic virus complexes for magselectofection .....	26
2.6.	Characterization of magnetic vectors .....	27
2.6.1.	Size and zeta potential measurements .....	27
2.6.2.	Testing vector association and magnetic sedimentation in complexes with magnetic nanoparticles.....	27
2.6.2.1.	Non-viral vectors.....	27
2.6.2.2.	Viral vectors .....	28
2.7.	Evaluation of magnetophoretic mobility.....	28
2.8.	Non-heme iron determination .....	30
2.8.1.	Non-heme iron determination in cells .....	30
2.8.2.	Non-heme iron determination in tissue samples.....	31
2.9.	Transfection/transduction experiments of Jurkat T cells and hUC-MSCs using magnetofection .....	31
2.9.1.	Standard magnetofection of suspension cells .....	31
2.9.2.	Magnetofection combined with glycerol shock.....	31
2.9.3.	Magnetofection using lentivirus and adenovirus vectors .....	32
2.9.4.	Standard infection protocols for lenti- and adenovirus .....	33
2.10.	Modification of the Miltenyi LS separation column with magnetic complexes.....	33
2.10.1.	Standard protocol.....	33
2.10.2.	Freeze-drying protocol .....	34
2.11.	Genetic modification of magnetically labelled cells by viral and non-viral magselectofection .....	34
2.11.1.	Magnetic labeling of the cells before magselectofection .....	34
2.11.2.	Magselectofection general protocol .....	34
2.11.3.	Analysis of the magnetic cell separation and gene transfer efficiency.....	35

---

2.11.4.	Magselectofection experiments using XS columns .....	37
2.11.5.	Lentiviral magselectofection versus standard infection of hCB-HSCs.....	37
2.11.6.	Testing of immobilization of the magnetic complexes at the Miltenyi <sup>®</sup> column and association with cells upon magnetic field application.....	39
2.11.6.1.	Using non-viral complexes .....	39
2.11.6.2.	Using viral complexes .....	39
2.11.7.	Analysis of cell association and internalization efficiency of the non-viral transfection complexes by flow cytometry .....	40
2.11.8.	Analysis of pDNA internalization using radioactively labeled pDNA.....	40
2.12.	Immunocharacterization of cells.....	41
2.13.	Reporter gene expression analysis.....	41
2.13.1.	Luciferin & luciferase assay .....	41
2.13.2.	eGFP expression analysis.....	41
2.13.2.1.	Fluorescence microscopy.....	41
2.13.2.2.	Analysis of transfection/transduction efficiency by fluorescence-activated cell sorting (FACS) .....	42
2.14.	Cell viability .....	42
2.14.1.	Trypan blue dye exclusion test.....	42
2.14.2.	MTT assay .....	43
2.15.	Differentiation assay .....	43
2.15.1.	Colony-forming cell (CFC).....	43
2.15.2.	Osteogenesis .....	43
2.16.	In vivo biodistribution analysis of magselectofected hUC-MSCs and magnetic labeled hCB-HSCs .....	44
2.17.	Statistics.....	45
3.	RESULTS.....	46
3.1.	Magnetic nanoparticles used in this study and their characteristics.....	46
3.2.	Magnetic vectors and their characteristics.....	49
3.2.1.	Efficient association of nucleic acids with magnetic particles after complex formation .....	49
3.2.1.1.	Non-viral magnetic lipoplexes .....	49
3.2.1.2.	Viral magnetic complexes .....	50
3.2.2.	Characteristics of non-viral magnetic lipoplexes.....	51

---

3.2.3.	Characteristics of viral complexes used for transfection using magnetofection .....	54
3.3.	Selection of magnetic vectors for magselectofection (results from 2D transfection) .....	56
3.3.1.	Correction for the autofluorescence of the transfection reagent is needed for true percentage of eGFP-positive Jurkat T cells.....	57
3.3.2.	Magnetic lipoplexes transfect Jurkat T cells more efficiently than magnetic polyplexes.....	58
3.3.3.	Reporter gene expression in Jurkat T cells is increased by magnetofection without causing cell toxicity.....	60
3.3.4.	Transfection efficiency of Jurkat T cells is not increased by combination of magnetofection with glycerol or DMSO shocks.....	63
3.3.5.	Magnetic lipoplexes are better internalized in Jurkat T cells upon gradient magnetic field application, as compared to non-magnetic lipoplexes .....	64
3.4.	Establishing magselectofection .....	67
3.4.1.	Reversible immobilization of transfection complexes and association with the cells at the Miltenyi® column .....	67
3.4.2.	Efficient association and internalization of magnetic lipoplexes in Jurkat T cells after magselectofection .....	70
3.4.3.	Modification of the LS column yields gene delivery specific to the target cell population without compromising the cell separation efficiency.....	72
3.4.4.	Optimal parameters for the magselectofection procedure yielding the highest transfection efficiency .....	74
3.4.5.	Magselectofection results in high transfection efficiency in Jurkat T cells. ....	77
3.5.	Magselectofection of therapeutically relevant cells .....	79
3.5.1.	Human umbilical cord mesenchymal stem cells (hUC-MSCs).....	79
3.5.2.	Human cord blood hematopoietic stem cells (hCB-HSCs) .....	83
3.5.3.	Human peripheral blood mononuclear cells (hPBMCs) .....	87
3.5.4.	Magselectofection in hUC-MSCs results in higher transduction efficiency compared to magnetofection and standard infection.....	89
3.6.	Upscale from LS to XS and CliniMACS is possible.....	90
3.7.	Preliminary study of the in vivo biodistribution of the hUC-MSCs and hCB-HSCs: first pilot study .....	94
3.7.1.	Biodistribution of the magnetically labeled hUC-MSCs after magselectofection .....	94
3.7.2.	Biodistribution of hCB-HSCs post- magnetic cell labeling .....	98
4.	DISCUSSION .....	101
4.1.	The role of magnetic nanoparticles and enhancers in gene delivery efficiency .....	101

---

4.2.	Development of magnetic vectors .....	102
4.3.	Establishment of the magselectofection procedure .....	104
4.3.1.	Modification of LS Miltenyi's columns with magnetic vectors.....	104
4.3.2.	Genetic modification of different cell types using magnetofection and magselectofection procedures.....	105
4.3.2.1.	Jurkat T cells.....	105
4.3.2.2.	Primary and stem cells.....	108
4.4.	Internalization of the magnetic complexes.....	110
4.5.	Critical parameters in optimizing magselectofection.....	112
4.6.	Other applications of magselectofection .....	113
4.7.	Conclusions.....	115
5.	SUMMARY .....	117
6.	ABBREVIATIONS.....	118
7.	REFERENCES .....	121
8.	ACKNOWLEDGEMENTS .....	133
9.	CURRICULUM VITAE .....	134
9.1.	Publications .....	136
9.1.1.	Original papers .....	136
9.1.2.	Oral presentations.....	136
9.1.3.	Poster presentations .....	137

## 1. INTRODUCTION

### 1.1. *A brief history of gene therapy*

In 1868, the nucleic acids were discovered by Friedrich Miesche. This material was called 'nuclein' since it was found in the nucleus of cells (Dahm, 2005). Since Watson and Crick described the structure of deoxyribonucleic acid (DNA) in 1953 (Watson and Crick, 1953b), the importance of the DNA within living cells has been undisputed. Watson and Crick also postulated that “DNA is the carrier of a part of (if not all) the genetic specificity of the chromosomes and thus the gene itself” (Watson and Crick, 1953a). In 1961, ribonucleic acid (RNA) was described to be responsible for the regulated translation of this information into structural and functional molecules. However, it was not until 1966 when the genetic code was deciphered.

Nucleic acids carry the building plans of living systems. Given this distinguished role of nucleic acids, one can conclude that any cellular process may be influenced to some particular purpose by the introduction of nucleic acids into cells from outside. Already in 1966, the year when the genetic code had finally been deciphered, Tatum formulated the concepts of nucleic acid therapy: “I would define genetic engineering as the alteration of existing genes in an individual. This could be accomplished by directed mutation or by the replacement of existing genes by others.” (Tatum, 1966) However, numerous scientific discoveries and technological breakthroughs were required until the first gene therapy treatment in human patients was technically feasible. This was in 1990 when Blaese and colleagues treated two children suffering from adenosine deaminase (ADA) deficiency applying an *ex vivo* gene therapy strategy with genetically engineered T lymphocytes (Blaese et al., 1995). In the meantime, more than 1400 gene therapy trials have been conducted worldwide, 66.5% of which were in cancer indications (<http://www.wiley.co.uk/genetherapy/clinical/>). The most convincing therapeutic success but also disastrous outcomes were observed in the treatment of monogenic diseases. Hence, the development of the field has been compared to a roller-coaster ride by many authors, characterized by impending promise and grave setbacks (Dunbar and Larochelle, 2010), (Editorial, 2003).



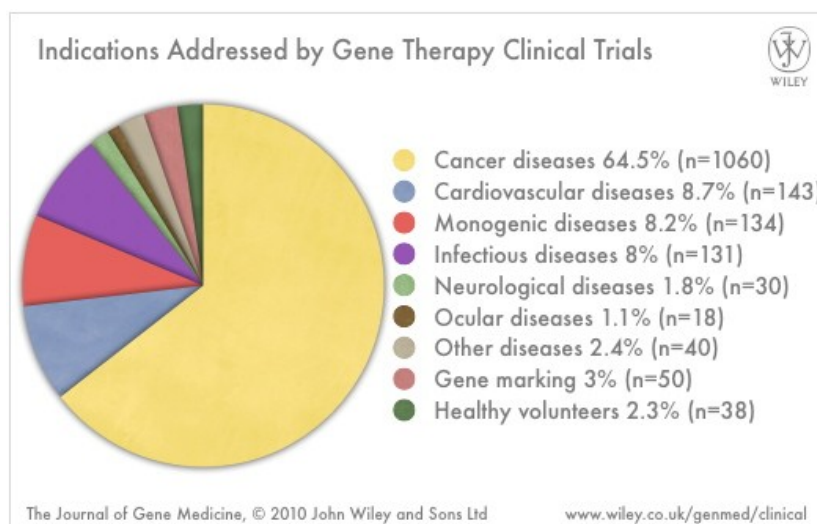


**Figure 1. Clinical targets for gene therapy (from: The journal of Gene Medicine (2010) <http://www.wiley.co.uk/genetherapy/clinical/>)**

This is for example highlighted by the clinical trial conducted by Fischer, Cavazzana-Calvo and colleagues who treated children suffering from a severe combined immunodeficiency (SCID-X1) with genetically engineered hematopoietic stem and progenitor cells (Cavazzana-Calvo and Fischer, 2007; Cavazzana-Calvo et al., 2005). This treatment yielded effective and life-saving immune reconstitution in 18 out of 20 patients based on a strong selective advantage of the gene modified cells. While the positive therapeutic outcome was celebrated as a breakthrough for gene therapy, a serious set back subsequently became evident (Hacein-Bey-Abina et al., 2003). Five of the 20 patients (four in France and one in England) developed a lympho-proliferative disease after proviral integration into proto-oncogenes (Staal et al., 2008). Similarly severe complications have been observed most recently with an *ex vivo* gene therapy of chronic granulomatous disease (CGD) (Stein et al., 2010). On a more positive note, in another clinical trial ten patients suffering from adenosine deaminase (ADA) deficiency, which is a fatal autosomal recessive form of severe combined immunodeficiency (SCID), were treated successfully in a similar manner without complications and demonstrated a safe and effective treatment in ADA deficiency (Aiuti et al., 2009). Adoptive transfer of antigen-specific T lymphocytes has recently shown clinical success in the treatment of viral infections and tumors (Walter et al., 1995), (Savoldo et al., 2000), (Yee et al., 2002), (Dudley et al., 2005). Different research groups have demonstrated that transfer of TCR $\alpha\beta$  genes into T cells (e.g., genetic T cell retargeting) represents a feasible and attractive alternative to provide

tumor-specific immunity (Clay et al., 1999), (Willemsen et al., 2000), (Cooper et al., 2000), (Orentas et al., 2001), (Schaft et al., 2003). Furthermore, gene-modified T cells have become as a promising tool as immunotherapy for multiple myeloma and acute myeloid leukemia. Strategies to enhance the efficacy of this treatment, such as the use of T cells engineered with improved and modified receptors (Cohen et al., 2007), (Sebestyen et al., 2008), (Varela-Rohena et al., 2008) and/or the *ex vivo* treatment of T cells with common- $\gamma$  cytokines (Kaneko et al., 2009) are currently scheduled for clinical testing.

Promising gene-therapy approaches for the treatment of Leber's congenital amaurosis (LCA) using recombinant adeno-associated virus (AAV) carrying RPE65 gene has been investigated by different research groups yielding positives results (Bainbridge et al., 2008), (Maguire et al., 2008).

Forty-four years after concepts of gene therapy have been lined out for the first time, its merits begin to live up to expectations. However, two essential deficiencies limit a safe and widespread application of nucleic acid therapies, probably for many years to come. One is our incomplete knowledge of the complex biology that governs nucleic acid delivery into target cells, intracellular trafficking and the regulation of nucleic acid action inside cells. The other limitation, in part resulting from the first one, is the lack of efficient and safe technologies for the genetic manipulation of target cells using exogenous nucleic acids. Efficient, meaning that minimal effort yields the desired therapeutic outcome and minimal effort to be understood as a minimal consumption of materials, goods and manpower. Therapies need to be standardized and cost effective.

To tackle these challenges, the principal task of this thesis was establishing a novel technology for the combined isolation and manipulation of target cells with nucleic acids in one integrated procedure.

## *1.2. Gene and cell therapies, ex vivo and in vivo*

### **1.2.1. Ex vivo and in vivo nucleic acid (gene) therapy**

The two traditional classifications of gene therapy methods have been *ex vivo* and *in vivo* gene therapy (Felgner, 1997). The latter approach may appear more straightforward because the shuttles ("vectors") for nucleic acid delivery are directly

administered to the patient. However, depending on the target of therapeutic intervention and the route of administration, this approach can be technically more challenging than the *ex vivo* approach.

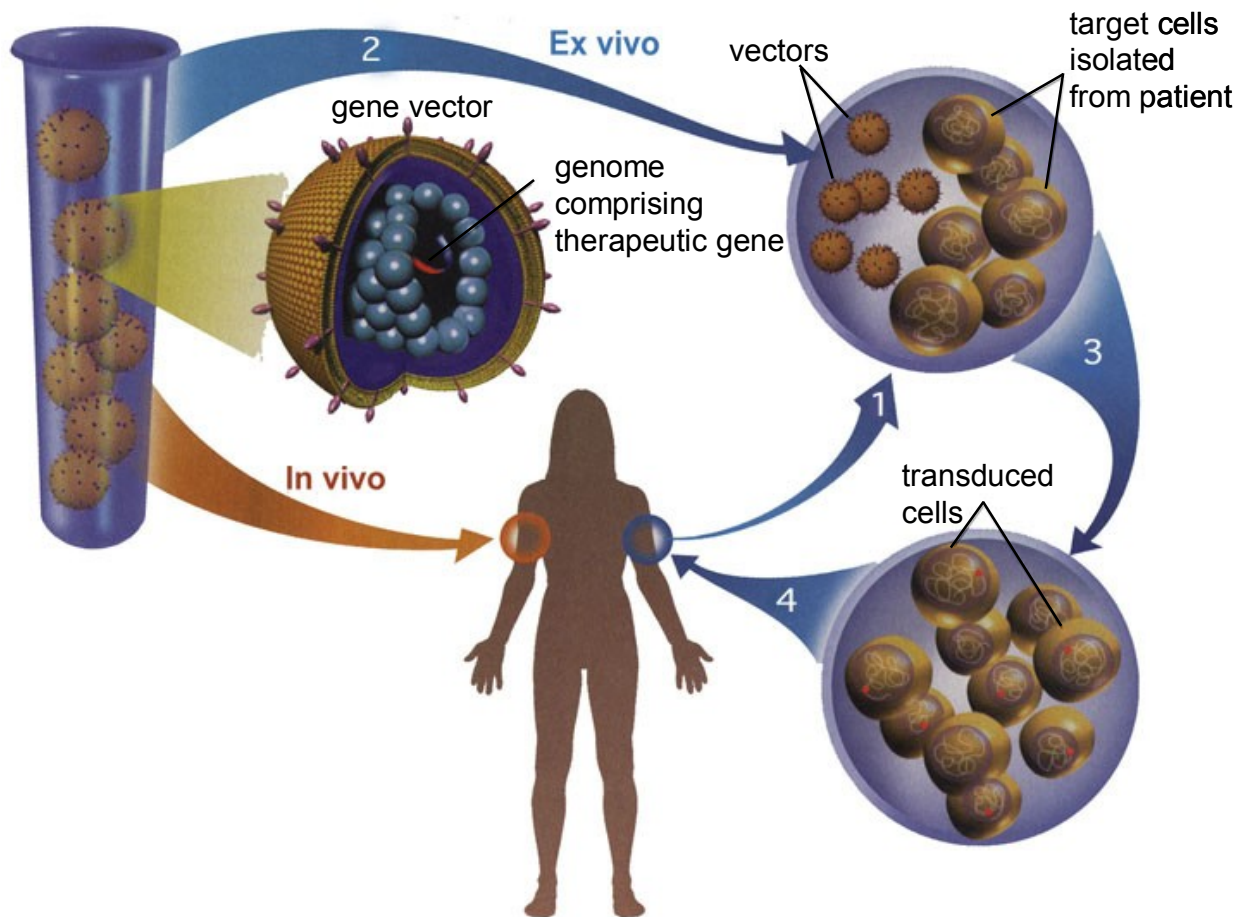


**Figure 2. Strategies for delivering therapeutic transgenes into patients (courtesy of PD Dr. Christian Plank)**

Vectors first need to find their target cells in order to deliver. This first and essential step is physically enforced by magnetic means using the integrated method of cell isolation and genetic modification described in this thesis. Already Tatum in 1966 pointed out “Hence, it can be suggested that the first successful genetic engineering will be done with the patient’s own cells [...] grown in culture”. And justly he adds later in his keynote address: “The efficiency of this process and its potentialities may be considerably improved [...] by increasing the effectiveness of DNA uptake and integration by recipient cells.” As mentioned above, the first gene therapies in man have involved the *ex vivo* approach and notably have involved stem cells.

### 1.2.2. Cell therapies

In the last years, cellular therapies involving stem cells have been used in several clinical trials. The transplantation of hematopoietic stem cells (HSC) from an HLA-identical sibling donor is the treatment of choice for severe combined immunodeficiencies (SCID) and other types of primary immunodeficiencies with poor prognosis. Despite improvements in cell transplantation, patients continue to experience long-term complications after transplant (Neven et al., 2009), and the use of alternative donors is still associated with high morbidity and mortality (Antoine et al., 2003). Large-scale clinical use of MSC-based therapies still awaits strategies that maximize therapeutic benefit and safety, while at the same time minimize production and processing costs (Wagner et al., 2009).

Cell therapies using *ex vivo* engineered cells is supposed to overcome some of these problems like for example, reduce the number of cells per dose or increase secretion of cytokines (Wagner et al., 2009). However, therapies with *ex vivo* engineered cells have not yet become widely practised. Conventional tools involving cellular genetic modification are neither efficient enough, nor affordable, nor simple to practice, require high vector doses and time. There is a need to develop new technologies that allow to obtain engineered cells in an efficient, simple and practicable way with minimum number of single working processes for cell manipulation (Goverdhana et al., 2005). This thesis has been dedicated to this task.

Gene and cell therapies fields have been unified in the last years. An example of that is the renaming of the European Society of Gene Therapy to European Society of Gene & Cell Therapy and an analogous renaming of the American Society. Because the fields of gene and cell therapies evolve so successfully, integrated procedures for cell isolation and genetic modification of therapeutically relevant cells, such as HSC and MSC, are urgently needed. This was one of the tasks of this thesis. The novel technology described in this thesis was supposed to be a standardized method for separation and genetic manipulation of cells of interest, such as human cord blood hematopoietic stem cells (hCB-HSC), human umbilical cord mesenchymal stem cells (hUC- MSC) and human peripheral blood mononuclear cells (hPBMCs). The novel technology described here is supposed to reduce the number of cell manipulation steps and hence, the cost.

### 1.3. *Vectors and physical methods for nucleic acid delivery*

Nucleic acid delivery into cells, also known as transfection (in the case of non-viral vectors) or transduction (in the case of viral vectors), is in most cases used to achieve the overexpression of introduced genes, the on/off regulation of endogenous genes or gene repair. The ultimate aim of such modifications is to assign function to a nucleic acid sequence of interest or its expression product, or to produce therapeutic benefit in patients (known as gene therapy). The term vector is most often understood to comprise a nucleic acid sequence to be delivered and additional elements that help it to be delivered. In the case of non-viral vectors, these are synthesised to mimic essential viral functions for overcoming cellular barriers and to protect the nucleic acids from degradation during the delivery process (Plank et al., 2005).

Standard physicochemical methods used for cell transfection include chemical methods, such as cationic lipids and polymers, and physical methods, like electroporation and magnetic drug targeting (magnetofection) (Plank et al., 2000).

#### 1.3.1. **Viral vectors**

Vectors derived from a variety of viruses with diverse properties have been used as gene transfer vehicles. The common characteristic of all viruses is their natural ability to deliver genetic material to cells, which is exploited in viral-vector design. This is mediated by proteins of the viral envelope that interact with cell surface receptors. However, important considerations, principally regarding biosafety issues, have arisen over time (Recillas-Targa et al., 2004), (Hawley, 2001). The main problems related to viral gene transfer are their pathogenicity, immunogenicity, insertional mutagenesis (in case of retroviral vectors) and practical concerns (large-scale virus production) (Klein and Baum, 2004), (Baum et al., 2003).

For gene therapy application, both DNA and RNA viruses are used. DNA viruses provide non-integrative means of transferring therapeutic genes. Adenovirus (Ads) can successfully infect a wide variety of cells including respiratory epithelial cells, myoblasts, macrophages, hepatocytes, and glial cells (Engelhardt et al., 1994), (Horellou et al., 1994), (Castel-Barthe et al., 1996). In 1986, Haj-Ahmad *et al.* (Haj-Ahmad and Graham, 1986) reported that Ads can be used as efficient vehicles, or vectors, for carrying and delivering foreign genes into target cells *in vitro*.

Unfortunately, the *in vivo* use of these vectors has suffered from serious drawbacks including toxic or even lethal results (Smith et al., 1993), (Raper et al., 2003).

Lentiviruses count among the most efficient gene vectors. HIV, SIV, and FIV are all examples of lentiviruses. An important feature of lentiviruses is its ability to permanently integrate into the mammalian cell genome and consequently, to enduringly modify their genetic character. Another feature is that lentiviruses can infect both non-dividing and dividing cells (Naldini et al., 1996). This characteristic distinguishes them, for example, from onco-retroviruses which can only infect dividing cells (Lewis and Emerman, 1994). One of the risks associated with using retroviruses and lentiviruses for gene therapy is the occurrence of insertional mutagenesis (Cavazzana-Calvo and Fischer, 2007), (Hacein-Bey-Abina et al., 2003), (Hacein-Bey-Abina et al., 2008). However, the lentivirus vector strategy was successfully applied to several types of non-dividing cell populations *in vitro*, *ex vivo* and *in vivo*. These included central nervous system neurons (Nanou and Azzouz, 2009), fetal cardiac myocytes (Rebolledo et al., 1998), cells from retina (Ikeda et al., 2009), (Miyoshi et al., 1997), skeletal muscles and liver (MacKenzie et al., 2002). Concerning biosafety of lentivirus, several generations of lentivirus have been developed in the last years (Naldini, 1998). The most advanced third generation self inactivating (SIN) packaging construct includes many design features that make it safe for gene therapy applications (Kappes and Wu, 2001).

Since adenovirus and lentiviral vectors are promising vectors for gene/cell therapy, another task of this thesis was to validate the novel technology in the cells of interest (hCB-HSCs, hUC-MSCs and hPBMCs) using both adeno- and lentiviral vectors.

### **1.3.2. Non-viral vectors**

The use of non-viral vectors for clinical applications has considerable advantages over viral vectors. Plasmid vectors usually have a low immunogenicity. Moreover, non-viral vectors are more cost-efficient, easier to scale-up and to quality-control. Non-viral vectors do not have host cell specificity except when equipped with special targeting moieties or nucleic acid sequences that make them active only in specific cell types. Transfection of resting cells using lipofection is usually quite inefficient and remains a challenge in the construction of non-viral systems (Brunner et al., 2002). On the other hand, Floch et al. have reported that the transfection efficiency in

CD34+ cells (which was one of the major target cell types in this thesis) using phosphonolipids is independent of whether these cells divide or not (Floch et al., 1997). For polyfection the results are less clear (Pollard et al., 1998), (Godbey et al., 1999) (Brunner et al., 2000). Plasmids have been used in basic research for transfecting cultured cells for a long time. Their use in gene therapy applications *in vivo* is more recent and is still limited by some disadvantages compared to viral vectors. With respect to the copy number of a nucleic acid per target cell required to genetically modify that target cell, non-viral vectors for gene delivery are orders of magnitude less efficient than most viral vectors (Kichler et al., 2001), (Singh et al., 2008), (Pollard et al., 1998). Furthermore, plasmids usually are lost rapidly from highly proliferating cells since they lack mitotic stability (Nishikawa and Hashida, 2002). Considerable improvements of non-viral vector systems have been achieved during the past years. These include improved and targeted cellular uptake by virtue of receptor ligands (Ward, 2000), (Blessing et al., 2001), (von Gersdorff et al., 2005), improved endosomal release and intracellular shuttling by virtue of exploiting chemical and biological triggers (Meyer et al., 2007), (de Bruin et al., 2008) and improved mitotic stability by virtue of certain nucleic acid sequences such as S/MARs (scaffold/matrix attachment regions)(Jenke et al., 2002), (Conese et al., 2004).

Two kinds of non-viral vectors are broadly used for gene/cell therapy: lipoplexes and polyplexes. Cationic lipid transfection reagents are widely used for gene therapy, both *in vivo* and *in vitro* (Hoare et al., 2010), (Floch et al., 1997), (Zhu et al., 1993), (Liu et al., 1997). Hundreds of compounds are described in the literature and many of them are commercially available and confer good results with various cell types. Examples are Lipofectamine, Fugene or Dreamfect-Gold (used in this thesis and provided by OZ Biosciences, <http://www.ozbiosciences.com/>). The efficiency of lipoplexes in nucleic acid delivery is thought to rely on displacement reactions between negatively charged lipids of cellular membranes with the cationic lipids comprised in lipoplexes. It is believed that this triggers membrane fusion events (which can be further supported by fusogenic lipids such as DOPE) and ultimately leads to the intracellular release of nucleic acids compacted in a lipoplex (Xu and Szoka, 1996), (Zelphati and Szoka, 1996a), (Zelphati and Szoka, 1996b).

The other major class of non-viral delivery systems is polyplexes. They consist of a polycation which compacts the nucleic acid to be delivered and, depending on the

construct, further functional modules for receptor targeting, endosomal release and nuclear transport. Among the many polycations which have been described as transfection reagents, the most commonly used is polyethylenimine (PEI). Its high efficiency in nucleic acid delivery relies on its chemical structure which entails buffering capacity at the acidic pH of endosomes. The endosomal escape of PEI was explained by the “proton sponge hypothesis” (Boussif et al., 1995) which was experimentally confirmed by Sonawane et al. (Sonawane et al., 2003). Briefly, because of the buffering capacity the endosomal proton pump ( $H^+$  ATPase) needs to pump way more protons into the endosome until the natural endosomal pH is reached. Because of  $H^+/Cl^-$  charge coupling, endosomal  $Cl^-$  entry is increased as well and consequently osmotic swelling and endosomal leakage/lysis is promoted. An additional mechanic destabilization may be provided through swelling of the internalized polymer itself due to electrostatic repulsion of its protonated amino groups.

Due to the high gene transfer efficiency that can be achieved with PEI on the one hand and due to its major disadvantage, which is its high toxicity, on the other hand, many variations of its essential structural motif have been described in the literature. Prof. Wagner group was deeply engaged in this topic. For example, Boeckle et al. showed that covalent attachment of the membrane-active peptide all-(L)-melittin to polyethylenimine (PEI) polyplexes yielded an enhanced gene transfer efficiency (Boeckle et al., 2005). Zintchenko et al. reported that highly efficient siRNA carriers with low toxicity can be achieved by introducing simple modifications of branched PEI (Zintchenko et al., 2008). Furthermore, a novel purification method for PEI polyplexes based on electrophoresis has been developed (Fahrmeir et al., 2007). It has been shown that purified polyplexes can mediate *in vitro* gene transfer with high transfection efficiencies while demonstrating lower cellular toxicity (Fahrmeir et al., 2007).

Both lipoplexes and polyplexes, when applied intravenously in mice, lead to systemic gene delivery with a strong passive tropism for the lung. For both vector types, shielding and receptor targeting is used to achieve specificity for other organs and in particular for tumors (Ogris and Wagner, 2002), (Fella et al., 2008), (Hyndman et al., 2004), (Conwell et al., 2008)



While lipoplexes and polyplexes have been used with great success for transfecting adherent cell lines in culture, their efficiency in suspension cells is often low. And in particular many primary cell types in culture, notably HSCs, are quite resistant to non-viral gene delivery with lipoplexes and polyplexes. Hence, the suitability of these vector types for the genetic engineering of cells for therapeutic purposes has been limited so far. Therefore, researchers have developed physical methods of gene delivery which are either applied for naked nucleic acids or which are used to enhance the efficiency of lipoplexes and polyplexes.

The method developed in this thesis exploits magnetofection which is a physical method to enhance nucleic acid delivery.

### **1.3.3. Physical methods, Magnetofection**

Independent of vector type, vector contact with target cells is the primary event in, and a prerequisite for, a successful transfection/ transduction process. During the last 20 years, an intense research in non-viral vectorology has yielded excellent tools for nucleic acid delivery. Physical methods such as particle bombardment, microinjection, electroporation and ultrasound have been used for gene delivery. From all these methods electroporation techniques have been applied in gene therapy. Electroporation has some advantages such as high transfection efficiency (Van Tendeloo et al., 2000), can be used in nearly all cell types and species (Nickoloff, 1995) and has been successfully applied *in vivo* (Andre et al., 2008), (Mir, 2009). In contrast, the disadvantages of electroporation are high toxicity and non-specific transport (Weaver, 1995). Hence, further improvements with respect to the efficiency/toxicity and specificity of nucleic acid delivery are required and can be achieved.

Magnetofection is a physical method that uses magnetic forces to attract and concentrate the nucleic on the cell surface (Plank et al., 2003b), (Plank et al., 2003c). As diffusion is a slow process and many vector types are subject to time-dependent inactivation under cell culture conditions (as well as being toxic in very high concentrations), measures to overcome this limitation can greatly improve transfection/transduction efficiency (Plank et al., 2003a). The magnetofection method was designed to overcome the limitations in cell-binding, efficiency of nucleic acid uptake and low transfection efficiency. Magnetofection was inspired by the concept of

magnetic drug targeting. In 1963, Meyers described how they were able to accumulate small iron particles intravenously injected into the leg veins of dogs, using a large, externally applied horse shoe magnet (Meyers et al., 1963). Several research groups have independently developed magnetofection methods (Hughes et al., 2001), (Mah et al., 2002), (Pandori et al., 2002), (Chan et al., 2005), (Isalan et al., 2005), and the generic term 'magnetofection' is widely used in the scientific literature in the context described earlier. The term magnetofection was first introduced by Dr. Plank in the year 2000 (Plank et al., 2000) and has since become a widely used technical term in the literature.

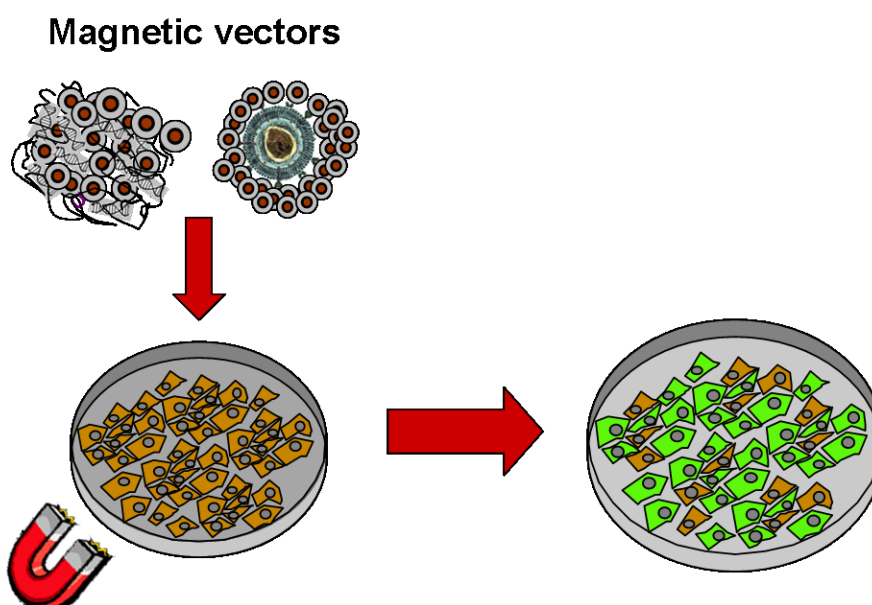


**Figure 3. Scheme of a magnetofection. Magnetic vectors are added to the cells. Magnetic field is applied in order to attract and sediment the magnetic vector on the cell surface.**

Magnetofection has come out as a highly efficient method for genetic modification of numerous cell lines and primary cells *in vitro* and *in vivo*. Magnetofection use non-viral and viral delivery vectors associated with magnetic nanoparticles combined with the application of a gradient magnetic field to concentrate vectors at the cell membrane (Huth et al., 2004) and to efficiently deliver them into the cells (Scherer et al., 2002), (Plank et al., 2003a), (Xenariou et al., 2006), (Mykhaylyk et al., 2007a), (Lee et al., 2008). Enhancement of viral gene delivery to suspension cells using magnetofection with cationic chitosan-coated iron oxide nanoparticles has also been reported (Bhattarai et al., 2008). Advantages of the use of magnetofection for gene delivery are: 1) the diffusion limitation to delivery is overcome; 2)

transfection/transduction is synchronized and greatly accelerated; and 3) the vector dose requirement for efficient transfection/transduction is considerably reduced. These features together constitute a substantial improvement of transfection/transduction efficiency. The mechanism of vector uptake into cells is probably the same during magnetofection as for standard transfection/transduction methods (Huth et al., 2004); magnetic nanoparticles are co-internalized with vectors into cells. It is known that iron oxide-based magnetic nanoparticles are biodegradable over long periods *in vivo* when injected intravenously (Weissleder et al., 1989). Whether the biodegradability is dependent on the type of particle surface coating and whether cells in culture can mediate particle degradation is not known. Magnetofection is well established and widely used for *in vitro* applications, which include overexpressing a transduced/transfected gene using almost any vector type and for gene silencing (siRNA) (Plank et al., 2003c), (Dobson, 2006), (Mykhaylyk et al., 2008). In contrast, major improvements are still required to make the method efficient enough to be widely used in *in vivo* applications (Scherer et al., 2002). The development of new magnetic nanoparticles is, however, expected to lead to further improvements of the technique.

#### **1.4. Magnetic cell separation**

The first work using magnetic particles with surface markers against cell receptors was reported in 1978 by Kronick et al. (Kronick et al., 1978). Since this day, many different kits for the sample preparation, extraction, enrichment and analysis of entire cells based on surface receptors, and subcellular/molecular components such as proteins, mRNA, DNA are available. Magnetic cell separation or magnetically-activated cell sorting (MACS) was developed by S. Miltenyi in the beginning of the 90's (Miltenyi et al., 1990) and is the method of choice for isolating specific cell populations from tissue samples in laboratory and clinical practice, such as CD34<sup>+</sup>, CD4<sup>+</sup>, CD8<sup>+</sup> or CD105<sup>+</sup> cells (Prince et al., 2002). In this technology, superparamagnetic MicroBeads coupled with highly specific monoclonal antibodies are used to label the target cell populations magnetically. The labeled cells are retained on magnetic cell separation column (MACS separator) exposed to the magnetic field and thus separated from the non-labelled cells. The *CliniMACS*® instrument is an automated cell selection device utilized for clinical applications, based on magnetic cell separation (MACS) technology. It enables large scale

magnetic cell selection in a closed and sterile system. Nearly every cell type, e.g. specific lymphocyte subpopulations, can be isolated via the Flexible Labeling System using a primary biotinylated antibody and *CliniMACS*® Anti-Biotin Reagent or *CliniMACS*® Anti-Biotin MicroBeads for magnetic cell separation on the *CliniMACS*®. The *CliniMACS*® System has received CE-approval for clinical use in Europe and many other countries for the selection of therapeutically relevant CD34+, CD133+ and CD14+ cells from human peripheral blood and bone marrow. In the United States *CliniMACS*® products for clinical use are available only under an approved Investigational Device Exemption (IDE).

One of the important applications of magnetic cell separation is the selection of specific lymphocyte subsets with potential antileukemic activity. The therapeutic applications of immunomagnetic cell selection are based on antibodies that bind to cancer cell antigens such as CD10, CD19 or CD20 (Frag, 2002).

Since magnetofection and magnetic cell separation rely on the use of magnetic nanoparticles and magnetic forces, it makes sense to combine the two independent technologies in one integrated technology. This has been the major objective of this thesis.

### *1.5. Objectives of this thesis*

The goal of this work is to provide a methodology that produces, in a single standardized technology, genetic modification and cell isolation. We have named this novel procedure “Magselectofection”. The approach is based on magnetic cell separation and magnetically-guided gene delivery (magnetofection). It was expected that magselectofection results in an enhanced target gene expression and minimization of the number of cell manipulations and time required.

In order to develop magselectofection technology, it was focussed on the following issues:

**Selection of magnetic vectors for magselectofection using 2D transfections (magnetofection) in Jurkat T cells.** It is known that magnetofection is a highly efficient method for the genetic modification of cells. As magnetofection is a part of the magselectofection technology, it can be assumed that efficient magnetic vectors to transfect/transduce the cells using magnetofection will also be efficient in transfections/transductions using magselectofection.

For this purpose, Jurkat T cells were selected as T lymphocyte model cell and used to select efficient magnetic lipoplexes by using a modified magnetofection protocol. NIH3T3 cells were selected for testing magnetic viral complexes by magnetofection.

**Establishing magselectofection.** The principal idea behind magselectofection technology is to associate the magnetic vector with the cells into the LS separation column. Cell separation efficiency and cell recovery must not be impaired.

**Validation of magselectofection in therapeutically relevant cells and upscale to use with the CliniMACS instrument.** This step is intended to provide proof of principle for future clinical applications.

## 2. MATERIALS AND METHODS

### 2.1. *Material*

#### 2.1.1. Chemicals and reagents

Polyethylenimin 25-kD branched (PEI), Pluronic F-127, 1,9-Nonanedithiol, fluorinated surfactant ZONYL FSA and methylthiazoyldiphenyl-tetrazolium (MTT), Trypan blue dye, propidium iodide (PI) and Alizarin red S were purchased from Sigma-Aldrich (St.Louis, USA).

D-luciferin was obtained from Roche Diagnostics.

Liposomal transfection reagent Dreamfect-gold (DF-Gold), SM4-31, Ecotransfect, PolyMag-41/1, CombiMag magnetic nanoparticles and 96-well magnetic plates was acquired from OZ Biosciences (Marseille, France). Lipofectamine 2000 transfection reagent and DNA-intercalating dye YOYO<sup>®</sup>-1 iodide (491/509) were purchased from Invitrogen (Carlsbad, USA).

BioRAD protein assay reagent was purchased from Bio-Rad Laboratories (Hercules, USA).

LS separation columns, MidiMACS<sup>®</sup> Cell Separator, Cytostim, human CD2, CD15 CD45, CD34 and CD105 Microbeads and PE- CD4 human CD2-PE, CD4-PE, CD15-PE, CD34-PE and CD45-PE antibodies were purchased from Miltenyi Biotec (Bergisch Gladbach, Germany). Human CD3-PE, CD90-PE and CD105-PE antibodies were obtained from AbD serotec (United Kingdom).

Sodium <sup>125</sup>Iodide in 40 mM NaOH with an activity of 2 mCi in 20µl was acquired from Hartmann Analytics, cat. no. I-RB-31 (Braunschweig, Germany).

#### 2.1.2. Cell culture reagents

PBS-Dulbecco (1x w/o Ca<sup>2+</sup>, Mg<sup>2+</sup> LE), Dulbecco's MEM (1x, w/o Ca<sup>2+</sup>, Mg<sup>2+</sup>, w 3.7g/L NaHCO<sub>3</sub> w 4.5 g/L D-Glc, w stable glu, LE, w/o Na-pyruvate), RPMI 1640 medium (w 2.0g/L NaHCO<sub>3</sub>, w stable glu), Trypsin/EDTA solution, (0.5%/0.2% in PBS w/o Ca/Mg) Penicillin/Streptomycin (10.000 IE/10.000 µg/mL) and L-Glutamine (200 mM) were purchased from Biochrom AG (Berlin, Germany).

OptiMEM<sup>®</sup> medium was acquired from Invitrogen.

Fetal calf serum Sera Plus (FCS) was obtained from PAN-BIOTECH (Aidenbach, Germany)

DMEM + GlutaMAX™-I (1x, (+) 4.5g/L Glc, (+) Pyruvate) culture medium were purchased from Invitrogen (Carlsbad, USA).

X-Vivo-10 cell culture medium was purchased from Lonza (Basel, Switzerland).

### 2.1.3. Plasmids

Luciferase reporter plasmid p55pCMV-IVS-luc+ containing firefly luciferase cDNA under the control of the cytomegalovirus (CMV) promoter, PlasmidFactory, Bielefeld, Germany, eGFP reporter plasmid containing enhanced green fluorescence protein (eGFP) under the control of the CMV promoter, transfer plasmid pL771-eGFP, *gag-pol* plasmid pMD.GP, *Rev* plasmid pRSV-rev and *Env* plasmid pMD.G were expanded in *E. coli* and purified using the Qiagen plasmid purification kit (Hilden, Germany). pCMV-kk was kindly provided by Dr. Ian Johnston from Milteny Biotec.

### 2.1.4. Chemical reagents and buffers

10% Hydroxylamine hydrochloride (Sigma-Aldrich, St.Louis, USA) in water

*Ammonium acetate buffer for iron determination:*

Dissolve 25 g ammonium acetate (Sigma, St.Louis, USA) in 10 mL water, add 70 mL glacial acetic acid and adjust volume to 100 mL with water.

*0.1% Phenanthroline solution:*

Dissolve 100 mg 1,10-phenanthroline monohydrate (Sigma, Steinheim, Germany) in 100 mL water, add 2 drops of concentrated hydrochloric acid (Fluka, Steinheim, Germany). If necessary, warm to obtain a clear solution.

*Iron stock solution:*

Dissolve 392.8 mg ammonium iron (II) sulfate hexahydrate (Sigma, Steinheim, Germany) in a mixture of 2 mL concentrated sulfuric acid and 10 mL water, add 0.05N KMnO<sub>4</sub> dropwise until pink color persists and adjust the volume to 100 mL with water.

*Standard iron solution (make fresh as required):*

Dilute iron stock solution from 25 to 1 with water just before calibration measurements.

*0.05N KMnO<sub>4</sub> solution:*

Dissolve 0.790 g KMnO<sub>4</sub> in 100 mL water.

*2 x HBS-buffer, pH 7.05:*

Mix 6.5 g HEPES with 8.0 g NaCl and dissolve in 10 mL Na<sub>2</sub>HPO<sub>4</sub> stock (5.25 g in 500mL ddH<sub>2</sub>O). Adjust pH to 7.0 with sodium hydroxide and volume to 50 mL with water

## 2.2. Cell isolation and culture

### 2.2.1. Isolation of the PBMC and CD34<sup>+</sup> by Ficoll gradient

To isolate Peripheral Blood Mononuclear Cells (PBMC), 35-50 mL of buffycoat or cord blood was transferred into a 50 mL Falcon tube and centrifuged 35 minutes at 445 rcf without brake. The plasma phase (around 15 mL) was discarded and the leukocyte phase (white band) was transferred to a 50 mL Falcon tube prepared with 16 mL Ficoll solution. The Falcon tube was filled up with PBS/ 2mM EDTA solution to 50 mL. Afterwards, the tubes were centrifuged for 10 minutes at 1000 rcf without brake. Then, the PBMC phase (white phase) was pipetted into a new 50 mL Falcon tube and filled up to 50 mL with PBS/ 2mM EDTA solution. The Falcon tubes were centrifuged again for 15 minutes at 300 rcf with brake. The supernatant was discarded and washed with 50 mL PBS/EDTA buffer for 10 minutes at 200 rcf (thrombocytes washing). Then, the supernatant was discarded and the cell pellet was resuspended in 10-20 mL PBS/EDTA buffer, cell number was counted using a Neubauer chamber (Optik Labor).



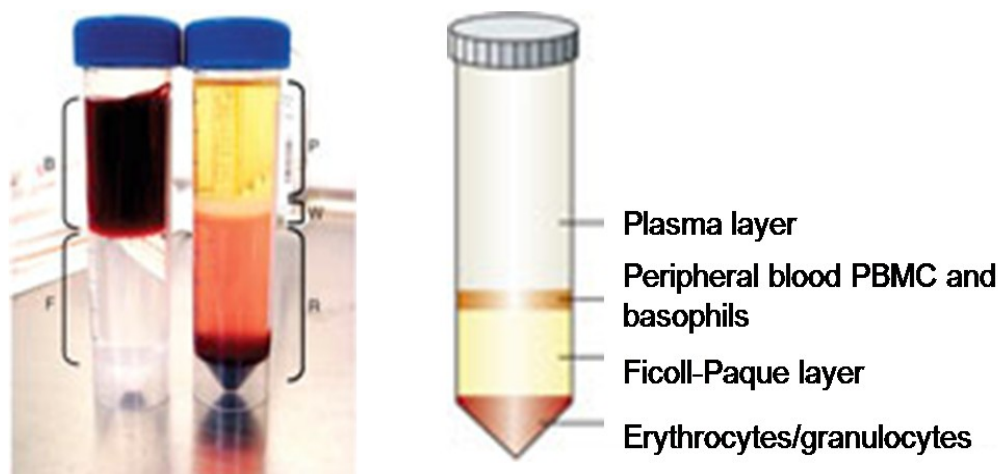


**Figure 4. Separation of granulocytes from PBMC and basophils by Ficoll-Paque centrifugation.** (Adapted from: Munoz, N. M. & Leff, A. R. (2006) Nat Protoc. 1(6): 2613-20).

### 2.2.2. Isolation of Wharton's Jelly stem cells (hUC-MSC)

Human mesenchymal stem cells of fetal origin (hUC-MSCs) were isolated from umbilical cord Wharton's jelly and kindly provided by Prof. Pojda (Department of Experimental Hematology and Cord Blood Bank M. Sklodowska-Curie Memorial Cancer Center, Warsaw, Poland). Fragments of umbilical cord were collected during Cesarean section delivery, transported in Penicillin/Streptomycin – supplemented buffered salt solution (PBS) at 4°C, and processed not later than 24 h following collection. Umbilical cords were cut into 2 cm - long fragments, rinsed with PBS supplemented with 15% fetal bovine serum (FBS, Invitrogen) and, after removing blood vessels, Wharton's jelly fragments were dissected, minced into 1-3 mm fragments, suspended in Dulbecco's Modified Eagle Medium (DMEM, Invitrogen) plus 20% FBS, and cultured in 25 cm<sup>2</sup> flat-bottom vented culture flasks (Nunc) at 37°C, 5% CO<sub>2</sub> fully-humidified atmosphere. Every 7 d, ½ medium volume was gently aspirated from the culture flask, and replaced with identical volume of newly-prepared medium, pre-warmed up to 37°C. Plastic-adherent hUC-MSC expanded from Wharton's jelly fragments, until forming a monolayer in approximately 3 weeks. Flask contents were then trypsinized (0,05% Trypsin, Sigma-Aldrich), remaining tissue fragments removed, and cells re-planted into 25 cm<sup>2</sup> flasks (Nunc) (1,5 x 10<sup>5</sup> cells per flask). From second passage, culture time until reaching the monolayer stage was 7-10 d. Cells were growing without changing their characteristics (phenotype, surface markers, differentiation potential) until 12-17 passage, depending on the donor. Cells

from 2-5 passage were used for the further experiments. Cultivation without antibiotic was of importance to efficiently label the cells magnetically with CD105 magnetic MicroBeads for further separation and magnetofection at the LS Miltenyi separation column. When cultivated in the medium supplemented with 100 U/mL penicillin and 100 µg/mL streptomycin the cells loosed the ability to bind CD105 magnetic MicroBeads efficiently and to be trapped in a separation column.

### 2.2.3. Cell culture

Jurkat T cells and K562 cells were obtained from DSMZ (Deutsche Sammlung von Mikroorganismen und Zellkulturen GmbH, cat no. ACC 282 and ACC 10, respectively) and maintained at 37°C and 5% CO<sub>2</sub> in RPMI 1640 medium (Biochrom AG, Berlin, Germany) supplemented with 10% fetal calf serum (FCS), 2 mM D-glutamine, 100 U/mL penicillin and 100 µg/mL streptomycin (further referred to as complete medium). Every 2-3 days, the cells with a density of 1-1.5 x 10<sup>6</sup> cells/mL were split at 1:2 ratio and used for transfection experiments until 13-15 passages after thawing.

CMS5 (Methylcholanthrene-induced fibrosarcoma cells of BALB/c origin) and 293T human embryonic kidney (HEK) cells were obtained from DSMZ (ACC 10) and maintained at 37°C; 5% CO<sub>2</sub> in DMEM high glucose medium containing 10% fetal calf serum, 2 mM D-glutamine, 100 U/mL penicillin and 100 µg/mL streptomycin. Cells were split 1:5-1:10 every 2-3 days until passage 15-20 after thawing.

Blood samples were purchased from DRK Hagen and were kindly provided by Miltenyi Biotec. PBMC were isolated by Ficoll gradient procedure. PBMCs were grown in RPMI 1640 medium with 10% FCS. Cell density was adjusted to 5 x 10<sup>6</sup> cells per mL per cm<sup>2</sup>. Cytostim from Miltenyi Biotec, a bi-specific antibody conjugate that crosslinks the TCR on T cells with MHC molecules on antigen presenting cells, was used to activate PBMC following the protocol described by Miltenyi Biotec.

Human Umbilical Cord Mesenchymal Stem Cells (hUC-MSCs) from Wharton's Jelly surrounds were isolated from umbilical cord and kindly provided by Prof. Pojda (M. Skłodowska-Curie Memorial Cancer Center, Warsaw, Poland). Cells were maintained in 75 cm<sup>2</sup> flasks at 37°C and 5% CO<sub>2</sub> environment in DMEM medium (Glutamax II, Invitrogen Gibco®, Carlsbad, USA) containing 20% fetal calf serum (FCS) without

antibiotics. Every 5-7 days, cells were split at a density of  $1.4 \times 10^4/\text{cm}^2$  in 75  $\text{cm}^2$  flasks and cultured up to 80-90% confluence.

Human Cord Blood Hematopoietic Stem Cells (hCB-HSCs) were isolated from umbilical cord blood by Ficoll gradient. Cells were maintained at 37°C and 5%  $\text{CO}_2$  environment in X-Vivo-10 medium containing 10% fetal calf serum (FCS), 50 ng/mL Flt3, 50 ng/mL TPO and 20 ng/mL SCF (complete X-Vivo-10 cell culture medium).

### **2.3. Magnetic nanoparticles**

Magnetic nanoparticles were synthesized and characterized by Dr. Olga Mykhaylyk from the Experimental Oncology Department at the Klinikum rechts der Isar (Dr. Plank's group).

#### **2.3.1. Synthesis**

Core/shell-type iron oxide magnetic nanoparticles (MNPs) were synthesised by precipitating Fe(II)/Fe(III) hydroxide from an aqueous salt solution, followed by transformation into magnetite in an oxygen-free atmosphere with immediate spontaneous adsorption or condensation of the shell components, as described elsewhere (Mykhaylyk et al., 2007a), (Mykhaylyk et al., 2007a), (Mykhaylyk et al., 2010). Particles with a surface coating consisting of the fluorinated surfactant ZONYL FSA (lithium 3-[2-(perfluoroalkyl)ethylthio] propionate) combined with 25-kDa branched polyethylenimine (PEI-25<sub>Br</sub>) will hereafter be referred to as PEI-Mag2. Those synthesised with a surface coating formulated of ZONYL FSA and 1,9-nonandithiol will be further referred to as NDT-Mag1. The particles synthesised in the presence of ZONYL FSA and Pluronic F-127 will be referred to as PL-Mag1 particles. The particles further referred to as PalD1-Mag1 were synthesised as described elsewhere (Mykhaylyk et al., 2009b) using palmitoyl dextran (PalD1) as a shell component to stabilise the particles. PalD1 with an esterification level of 10 palmitoyl groups per 100 dextrans was synthesised from Dextran 10 (Amersham Biosciences) using a modification of Suzuki's procedure (Suzuki et al., 1977). The particles referred to as SO-Mag2 particles have a surface coating resulting from the condensation of tetraethyl orthosilicate and 3-(trihydroxysilyl)propylmethylphosphonate at the surface followed by surface decoration of nanomaterial via spontaneous adsorption of PEI-25<sub>Br</sub> (Mykhaylyk et al.,

2010). The aqueous MNP suspensions were sterilised using  $^{60}\text{Co}$  gamma-irradiation (Dosage 25 kGy) (Kowalski and Tallentire, 1999).

### **2.3.2. Characterization of magnetic nanoparticles**

The mean hydrodynamic diameter and the zeta ( $\xi$ ) potential of the MNP suspension in water were determined by PCS using a Malvern 3000 HS Zetasizer (UK). The mean magnetite crystallite size ( $\_d\_$ ) was calculated from the broadening of the X-ray diffraction peaks using the Scherrer formula. The magnetization and hysteresis loop measurements were performed at 298 K using a vibrating sample magnetometer (Oxford Instruments Ltd.) in a  $\pm 1.0$  T applied field.

### **2.3.3. Determination of magnetic nanoparticle concentration in terms of dry weight and iron content**

The MNP concentration was determined in terms of the dry weight per unit volume, the iron content of the dry nanoparticles and the iron content in suspensions of the nanoparticle stock suspension in water, as described previously (Mykhaylyk et al., 2007a), (Mykhaylyk et al., 2009b). To determine the magnetic nanoparticle concentration in suspension in terms of iron content, 20  $\mu\text{l}$  aliquots of the magnetic nanoparticle suspension were taken and added to 200  $\mu\text{l}$  of concentrated hydrochloric acid and 50  $\mu\text{l}$  of water. Volume was adjusted to 5 mL with water after magnetic nanoparticles were completely dissolved. 20  $\mu\text{l}$  of the solution were transferred to an Eppendorf tube and 20  $\mu\text{l}$  of concentrated hydrochloric acid, 20  $\mu\text{l}$  of 10% hydroxylamine hydrochloride solution, 200  $\mu\text{l}$  of ammonium acetate buffer, 80  $\mu\text{l}$  of 1,10-phenanthroline solution, and 860  $\mu\text{l}$  of water were added, well mixed and incubated for 20 min at room temperature. After that time, the optical density was measured at the maximum of the spectrum of iron (II)–1,10-phenanthroline complex (510 nm) using the spectrophotometer (Beckman DU 640) and the blank was subtracted. Blank sample was prepared by mixing 20  $\mu\text{l}$  of concentrated hydrochloric acid, 20  $\mu\text{l}$  of hydroxylamine hydrochloride solution, 200  $\mu\text{l}$  of ammonium acetate buffer, 80  $\mu\text{l}$  of 1,10-phenanthroline solution, and 880  $\mu\text{l}$  of water.

To construct a calibration curve for determining the iron concentration, increasing amounts of iron standard solution were added to microcentrifuge tubes (e.g., 50, 70, 90 up to 150  $\mu\text{l}$ ) and the volume was adjusted to 150  $\mu\text{l}$  with water. 150  $\mu\text{l}$  of water

instead of iron solution was used to prepare a blank sample. To each tube, 20  $\mu\text{L}$  of concentrated hydrochloric acid, 20  $\mu\text{L}$  of 10% hydroxylamine hydrochloride solution, 200  $\mu\text{L}$  of ammonium acetate buffer, 80  $\mu\text{L}$  of 0.1% 1,10-phenanthroline solution, and 730  $\mu\text{L}$  of water was added and stood for 20 min. The absorbance was measured at 510 nm against the blank. The absorbances at 510 nm were plotted as a function of the iron concentration in the standard samples and linear regression as an approximation function to calculate the iron concentration in the magnetic nanoparticle samples was used.

To determine the iron concentration per dry weight of magnetic nanoparticles, freeze-dry protocol under high vacuum was performed as follows: transfer 1 mL aliquots of magnetic nanoparticle suspensions into pre-weighed glass vials, freeze the samples (at  $-80^{\circ}\text{C}$  or in liquid nitrogen) and dry overnight under high vacuum using a lyophilizer. Weigh the vials again to calculate the dry weight. Add 1 mL of concentrated hydrochloric acid, wait until the magnetic nanoparticles are completely dissolved, and then transfer 20  $\mu\text{L}$  of the resultant solution to a microcentrifuge tube and determine the iron content as described above. Calculate the iron concentration per dry weight of magnetic nanoparticles.

## *2.4. Lentivirus production and titer estimation*

### **2.4.1. Packaging of lentivirus vectors**

For lentivirus production a modified protocol from Barry, SC et al. (Barry et al., 2001) was followed. Packaging of these viruses was performed by transient transfection of 293 T cells. The day prior to transfection  $2.5 \times 10^6$  cells were seeded in 10 cm dishes. Self inactivated (SIN) lentivirus vectors were generated by calcium phosphate cotransfection of the transfer vector, HIV gag/pol packaging construct, a rev expression plasmid, and the VSV-G expression plasmid. Briefly, for each 10 cm dish 10  $\mu\text{g}$  of transfer vector (peGFP), 6.6  $\mu\text{g}$  of pMDL (gag/pol) packaging plasmid, 5  $\mu\text{g}$  of pRSV-REV, and 3  $\mu\text{g}$  of pVSVG envelope were mixed. 30  $\mu\text{L}$  of the plasmid DNA mixture was resuspended in 409  $\mu\text{L}$  ddH<sub>2</sub>O and 61  $\mu\text{L}$  CaCl<sub>2</sub> (2M). The DNA-CaCl<sub>2</sub> solution was added dropwise to 500  $\mu\text{L}$  of HBS (2x; pH7.12) under vigorous bubbling with a pipette and once slightly turbid the solution was immediately added to the cells. All transfection proceeded for 16 h, with medium replacement from 10 mL to 4

mL after 16 h and virus collection 48 h later. Viral supernatants were filtered through 0.45- $\mu$ m pore size filter and stored at -80°C.

#### **2.4.2. Biological titer of the lentivirus**

Biological titer or number of infectious vector particles in a unit volume of vector preparation, called transducing units per mL (TU/mL), and an average number of TU per cell, called Multiplicity of Infection (MOI), are the parameters used to quantify dosage of the virus and optimize transduction experiments. Biological titer of the eGFP lentivirus was determined following a modified protocol of Barry et al. (Barry et al., 2001). CMS5 cells were infected in the presence of polybrene followed by fluorescence-activated sorting (FACS) analysis 3 days later. Briefly,  $3.6 \times 10^5$  CMS5 cells were seeded in 25 cm<sup>2</sup> flasks in DMEM containing 10% FCS, 2 mM D-glutamine and 100U/mL penicillin and 100  $\mu$ g/mL streptomycin the day before infection. At the day of infection culture medium was aspirated and serial dilutions of the lentivirus stock in a final volume of 1 mL each in DMEM containing 10% FCS, 2 mM D-glutamine and 100U/mL penicillin and 100  $\mu$ g/mL streptomycin and 8  $\mu$ g/mL of polybrene were added to the cells in the flasks. Every 30 min the flasks were swirl gently. 2 h post-infection, 4 mL of culture medium was added to the cells and the flasks were incubated for further 72 h. Afterwards, the cells were trypsinized and after washing once with a FACS buffer (PBS supplemented with 1% FCS) fixed using the Cytofix solution and analysed for eGFP positive cells by flow cytometry.

Biological titer (TU/mL) was calculated according to the following formula:  $TU/mL = (P \times N \times DF) / 100 \times V$ , where P = % GFP<sup>+</sup> cells, N = number of cells at time of transduction =  $3.6 \times 10^5$ , V = volume of dilution added to each flask = 1 mL and DF = dilution factor = 1 (undiluted), 10 (diluted 1/10), 100 (diluted 1/100), and so on.

#### **2.4.3. Physical titer of the lentivirus**

Physical titer of the lentivirus preparation (virus particles/mL) was determined using Quick Titer<sup>TM</sup> Lentivirus Quantitation Kit developed for detection and quantitation of the lentivirus associated HIV-1 p24 core protein only. Lentivirus particle concentration in the stock was calculated from the data on lentivirus associated HIV-1 p24 core protein concentration assuming that there are approximately 2000

molecules of p24 capsid protein per Lentiviral Particle (LVP) and at a molecule weight of 24kDa 1 ng p24 corresponds to  $1.25 \times 10^7$  LVPs.

## *2.5. Preparation and characterisation of transfection complexes*

### **2.5.1. Assembling of magnetic non-viral complexes for magnetofection**

For transfection experiments in 96-well plates, the magnetic transfection complexes were prepared by mixing 20  $\mu\text{L}$  of a MNP suspension in water with 90  $\mu\text{g Fe mL}^{-1}$  and 40  $\mu\text{l}$  of the enhancer. We then added 300  $\mu\text{l}$  of the plasmid DNA solution at 12  $\mu\text{g DNA mL}^{-1}$  in a serum- and supplement-free RPMI 1640 medium to the mixture of the particles and the enhancer. The enhancer was prepared by mixing 14.4  $\mu\text{l}$  of the DF-Gold (or Lipofectamin 2000) with 25.6  $\mu\text{l}$  of water just prior to the transfection experiment. This resulted in 360  $\mu\text{l}$  of the complex having a liposomal transfection-reagent-to-nucleic-acid ratio of 4:1 (v/w) and an iron-to-plasmid ratio of 0.5:1 (w/w). To prepare the lipoplexes, 20  $\mu\text{L}$  of the magnetic nanoparticle suspension was substituted with water. To prepare the polyplexes, a solution of 10 mg/mL PEI-25<sub>Br</sub> was used as an enhancer, resulting in a complex nitrogen-to-phosphate ratio of 10:1. After mixing the components, the mixture was further incubated at RT for 20 min to allow self-assembling, then 2:1 dilutions with serum- and supplement-free RPMI 1640 were performed, resulting in DNA concentrations of 500-62.5 ng plasmid/well after adding 50  $\mu\text{l}$  of the prepared complexes to each well with cells seeded for transfection. DNA-polymer or DNA-lipid duplexes were used as reference complexes.

### **2.5.2. Assembling of magnetic non-viral complexes for magselectofection**

To ensure the complete immobilization and homogenous distribution of the magnetic vector within the MACS separation column, we prepared magnetic transfection/transduction complexes for loading onto the LS column in a total volume of 400  $\mu\text{l}$  which approximately corresponds to the dead volume of an LS column. To prepare magnetic lipoplexes for non-viral magselectofection, we used eGFP or luciferase plasmid DNA, DF-Gold lipid transfection reagent and in-house synthesized, core-shell type magnetic nanoparticles PEI-Mag2 and SO-Mag2. The particle stock concentration in terms of iron content was determined as described previously. For complex formation, we diluted 20  $\mu\text{g}$  of plasmid DNA in a total volume of 100  $\mu\text{l}$  RPMI without additives and mixed the solution well. In another tube, we diluted 20  $\mu\text{g}$

magnetic nanoparticles from a stock suspension to a total volume of 100  $\mu\text{l}$  with deionized water. In a third tube, we mixed 80  $\mu\text{l}$  of DF- Gold lipid transfection reagent with 20  $\mu\text{l}$  of water. Then, we added 100  $\mu\text{l}$  of the magnetic particle dilution to the second tube containing plasmid DNA and mixed the suspension well with a pipette. After this, we added 100  $\mu\text{l}$  of the diluted DF-Gold from the third tube, mixed well with a pipette again, added 100  $\mu\text{l}$  of RPMI 1640 media without additives, mixed again with a pipette and finally incubated the suspension at room temperature for 20 min to allow complex assembly. The resulting ratio of components in the complex (MNPs/DF-Gold/pDNA) is 1:4:1 (Fe w/v/w).

### **2.5.3. Assembling of magnetic virus complexes for magnetofection and standard infection**

To prepare lentivirus magnetic complexes to be added to the cells, we mixed 29  $\mu\text{l}$  virus stock containing  $1.2 \times 10^9$  VP/mL with infectivity of  $1.7 \times 10^6$  TU/mL and 0.5  $\mu\text{l}$  of the SO-Mag2 particle suspension containing 1.4  $\mu\text{g}$  Fe/ $\mu\text{l}$  in an Eppendorf tube, mixed well, incubated at RT for 20 min and added 170  $\mu\text{l}$  of the DMEM-Glutamax media without additives. We performed 1-to-2 dilutions of the complexes with DMEM-Glutamax media without additives. This resulted in MOI from 0.5 to 0.0625 and particle-to-VP ratio of 20 fg Fe/VP when 100  $\mu\text{l}$  of the dilutions were added to the cells. For standard infection, we substituted the particle stock with the medium and made dilutions in the same way as for magnetic complexes and added to each 100  $\mu\text{l}$  of the virus dilution polybrene stock solution to receive final concentration of 8  $\mu\text{g}$  polybrene/mL.

To assemble adenovirus magnetic complexes with SO-Mag2 nanoparticles for magnetofection of  $1.3 \times 10^6$  hUC-MSCs at MOI of 0.5, 1 or 2 pfu/cell and iron-to-virus particle ratio of 5 fg Fe/VP in 10 cm dish, we diluted adenovirus stock 1-to-10 resulting in  $2.5 \times 10^8$  pfu/mL and  $1.59 \times 10^{11}$  VP/mL. We sampled per 2.6, 5.2 or 10.4  $\mu\text{l}$  of the diluted virus stock into three Eppendorf tubes and mixed with 1.43, 2.86 or 5.72  $\mu\text{l}$  of the SO-Mag2 particle stock (1.4  $\mu\text{g}$  Fe/ $\mu\text{l}$ ), respectively, diluted the mixture in each tube with an OptiMEM® to a final volume of 400  $\mu\text{l}$  and incubated at room temperature for 20 min to allow complexes assembling. To prepare virus dilutions for standard infection, we substituted the particle stock with the medium. Prior giving to the cells, we adjusted volume of the virus or magnetic virus complexes to 1.5 mL.



#### 2.5.4. Assembling of magnetic virus complexes for magselectofection

To formulate magnetic virus complexes for magselectofection of Jurkat T cells and hUC-MSCs we have used magnetic nanoparticles SO-Mag2 and the third generation self inactivated lentivirus vector LVpHIV-7SFeGFP (LV.eGFP) with a virus stock containing  $1.2 \times 10^9$  VP/mL and biological titer of  $1.7 \times 10^6$  TU/mL or adenoviral vector AdmCMVeGFPLuc (eGFP encoding adenovirus aliquots were kindly provided by Dr. Martina Anton from the Experimental Oncology Department at the Klinikum rechts der Isar) with a virus stock containing  $1.59 \times 10^{12}$  VP/mL and infectivity of  $2.5 \times 10^9$  pfu/mL, both coding for eGFP.

To assemble magnetic complexes of LV.eGFP lentivirus with SO-Mag2 nanoparticles, referred to as SO-Mag2/LV.eGFP, for magselectofection of  $1 \times 10^6$  hUC-MSCs at MOI of 1 pfu/cell and iron-to-virus particle ratio of 10 fg Fe/VP using LS column, we calculated that total pfu to be applied was of  $1 \times 10^6$  TU that with account for biological virus titer of  $1.7 \times 10^6$  TU/mL corresponded to 588  $\mu$ l of the virus stock. This volume with account for physical titer of  $1.9 \times 10^9$  VP/mL contained  $1.9 \times 10^9$  VP/mL  $\times$  0.588 mL =  $7.06 \times 10^8$  VP. We further calculated that to ensure nanomaterial-to-VP ratio of 10 fg Fe/VP, SO-Mag2 nanomaterials suspension containing 7.1  $\mu$ g Fe has to be associated with 588  $\mu$ l of the virus preparation. 588  $\mu$ l of the LV.eGFP stock was added to 5.1  $\mu$ l of the particles suspension with concentration of 1.4  $\mu$ g Fe/ $\mu$ l, mixed well with a pipette and incubated at room temperature for 20 min. This resulted in assembling of SO-Mag2/LV.eGFP complexes. To ensure complete immobilization and homogenous distribution of the magnetic vector at the MACS separation matrix, volume of the complex was further adjusted to 400  $\mu$ l. The tube containing the complexes was fixed at the magnet at 24-well magnetic plate and the complexes were sedimented magnetically for 15-20 min. Afterwards, 193  $\mu$ l excessive supernatant was removed to get a final volume of 400  $\mu$ l. The tube was removed from the magnet and the complexes were resuspended to be loaded into the LS column positioned out from the MidiMACS magnet.

To assemble adenovirus magnetic complexes with SO-Mag2 nanoparticles for magselectofection of  $2.5 \times 10^6$  hUC-MSCs at MOI of 0.5, 1 or 2 pfu/cell and iron-to-virus particle ratio of 5 fg Fe/VP using LS column, adenovirus stock was diluted 1-to-10 resulting in  $2.5 \times 10^8$  pfu/mL and  $1.59 \times 10^{11}$  VP/mL. The diluted virus stock was sampled per 5, 10 or 20  $\mu$ l into three Eppendorf tubes and mixed with 2.75, 5.5 or 11

$\mu\text{l}$  of the SO-Mag2 particle stock ( $1.4 \mu\text{g Fe}/\mu\text{l}$ ), respectively. The mixture was further diluted in each tube with OptiMEM® to a final volume of  $400 \mu\text{l}$  and incubated at room temperature for 20 min to allow complexes assembling.

To prepare virus magnetic complexes for modification of the column for magselectofection of another cell number, at different MOI or particle-to-VP ratio each time the volume of the virus stock, volume of the nanoparticle suspension was accordingly adjusted and finally the volume of the complex to be loaded into the LS column was adjusted to  $400 \mu\text{l}$ .

## 2.6. Characterization of magnetic vectors

### 2.6.1. Size and zeta potential measurements

For size and zeta potential measurements, DNA transfection complexes prepared as described in p. 2.5.1-2.5.4, were diluted to a volume of 2 mL with RPMI 1640 medium with or without additives. The mean hydrodynamic diameter of the complexes and the  $\xi$ -potential of the magnetic nanoparticles were determined by photon correlation spectroscopy using a Malvern Zetasizer 3000 (UK).

### 2.6.2. Testing vector association and magnetic sedimentation in complexes with magnetic nanoparticles

#### 2.6.2.1. Non-viral vectors

To evaluate plasmid association with magnetic nanoparticles in the presence of DF-Gold as an enhancer, the stock suspension of MNPs was diluted in water to a concentration of  $720 \mu\text{g iron mL}^{-1}$ . Then,  $20.2 \mu\text{l}$  of DF-Gold was mixed with  $119.8 \mu\text{l}$  of water. This resulted in an enhancer-to-nucleic-acid volume/weight ratio of 4:1. For DNA stock solutions,  $12 \mu\text{g mL}^{-1}$  total DNA in an  $^{125}\text{I}$ -labelled DNA solution containing  $2 \times 10^5 \text{ CPM mL}^{-1}$  of  $^{125}\text{I}$  was resuspended in RPMI medium without supplements. Aliquots ( $10 \mu\text{l}$ ) of a 2:1 dilution series of the MNPs were added to wells in a 96-well round bottom plate starting from the iron concentration in the stock suspension of MNPs. A  $10\text{-}\mu\text{l}$  water sample was added to the reference well. Afterwards,  $20 \mu\text{l}$  of enhancer solution was added to each well and thoroughly mixed. Finally,  $150 \mu\text{l}$  of  $^{125}\text{I}$ -labelled DNA was added to each well and mixed, followed by incubation for 15 min to allow for complex formation. To sediment the magnetic transfection

complexes, the 96-well plate was placed on the 96-well magnetic plate (OZ Biosciences) for 30 min. Afterwards, 50  $\mu$ l of the supernatant was carefully transferred along with the pipette tip into the scintillation vial. Radioactivity was measured in each vial using a gamma counter device. Magnetically sedimented nucleic acid associated with the magnetic nanoparticles was calculated as follows:

*Magnetically sedimented DNA (siRNA) (%) =*  $[1 - CPM_{sample}/CPM_{ref}] \times 100$ , where  $CPM_{ref}$  is the radioactivity measured in the reference well.

### **2.6.2.2. Viral vectors**

The appropriate ratios of magnetic particle and viral vector were found by serial titrations of transducing units of lentivirus with magnetic particles followed by magnetic sedimentation of the complexes and determination of the lentiviral vector fraction remaining in the supernatants. Viral magnetic complexes were prepared by mixing 150  $\mu$ L LVPs with 50  $\mu$ L MNP (corresponding to 40 fg Fe/LVP) at MOI 0.5, 1 and 2 and at iron-to-lentivirus particles ratios of 40, 20, 10, 5, 2.5, 1.25 and 0.625 fg Fe/VP in wells of 96-round bottom plates. After 15 min of incubation, an Nd-Fe-B 96-well magnet was placed underneath each plate and the samples were exposed to the magnetic field for 30 min. Without removing the magnet, 150  $\mu$ L supernatant from each well was carefully sampled and analyzed for p24 HIV associated ELISA. In every well 50  $\mu$ L remained in order not to disturb the pellet containing LVP/MNP complexes. The ELISA provides information about the amount of p24 protein and thus the viral titer. If the LVPs form complexes with the MNPs they are magnetically attractable towards the magnet and within minutes magnetic viral complexes are sedimented. Hence, only free LVP can be detected via the HIV p24 ELISA and the magnetically sedimented LVPs directly correspond to the amount of LVPs associated with MNPs. In this manner, the percentage of LVP associated with MNPs and thus the ideal ratio for transfection of MNP to LVP could be identified. Results are compared to the reference one and thus, the viral titer of each sample is determined.

### **2.7. Evaluation of magnetophoretic mobility**

The sedimentation stability and magnetic responsiveness of the magnetic transfection/transduction complexes and magnetically labelled cells were determined using a turbidity measurement both without magnetic field application and when subjected to inhomogeneous magnetic fields, respectively, as recently described

((Mykhaylyk et al., 2008) (Mykhaylyk et al., 2009b)). Briefly, a gradient field was generated by positioning two mutually attracting packs of four quadrangular neodymium-iron-boron permanent magnets symmetrically on each side of a cuvette holder and parallel to a light beam for optical density measurements. The magnetic field between the magnets was measured along a grid with a 1-mm step size and an average magnetic field of 213 mT, and a resulting field gradient of 4 mT was calculated for the measuring window. Aliquots (500  $\mu$ L) of the magnetic lipoplexes or magnetically labelled cells (500.000 cells per 500 $\mu$ l medium) were transferred to the optical cuvettes, which were then placed into a spectrophotometer and exposed to the gradient magnetic field. The change in optical density or turbidity was then recorded at 360 nm. The clearance velocity under the influence of magnetic field gradient is related to the magnetophoretic mobilities of the objects, which in turn are proportional to their magnetic moments. Briefly, magnetic force that acts on a magnetic particle assemblies or magnetic lipoplexes or magnetic viral complexes comprising multiple magnetic particles in the presence of the magnetic field gradient  $\nabla\vec{B}$  is given by  $\vec{F}_m = (\vec{M} \cdot \nabla)\vec{B}$ . The total magnetic moment,  $\vec{M}$ , is the product of the effective magnetic moment,  $m_{eff}$ , of the MNP under the magnetic field,  $\vec{B}$ , and the total number,  $N$ , of magnetic particles associated with the magnetic lipoplexes or magnetic viral complexes ( $\vec{M} = N \cdot \vec{m}_{eff}$ ). Above the saturation magnetization of the MNPs, which is achieved with fields exceeding 200 mT for magnetite, the magnetic force experienced by the magnetic dipole is a linear function of the field gradient. Magnetic lipoplexes or magnetic viral complexes must move in the direction of the maximum magnetic field and are subject to a hydrodynamic drag force that can be described by Stokes law as  $\vec{F}_d = -3\pi\eta D_h \vec{v}$ , where  $\eta$  is the viscosity of the carrier liquid,  $D_h$  is an average hydrodynamic diameter of the objects, and  $\vec{v}$  is the velocity. In a stationary regime, hydrodynamic drag force counterbalances the magnetic force. The average magnetic moment,  $M$ , can then be calculated from the magnetically induced velocity in a magnetic field gradient as described by Wilhelm *et al.* (Wilhelm et al., 2002). At an average magnetic field  $\langle B \rangle$  of 213 mT, which we have used in our experimental setup, the magnetization of the nanoparticles according to the experimentally measured magnetization curve corresponds to 97% of the saturation value. Thus, the effective magnetic moment of each particle is  $m_{eff} = (0.97 M_s) P_{part}^{Fe}$ ,

where  $M_s$  is the specific saturation magnetization per unit iron weight and  $P_{part}^{Fe}$  is the content of iron in one particle with a known core size. Thus, the number of particles associated with magnetic lipoplexes or magnetic viral complexes can be calculated from the magnetophoretic mobility,  $\bar{v}$ , estimated from the clearance curves as

$$N = \frac{3\pi\eta D_h v}{\nabla B \cdot m_{eff}}$$
. An average velocity,  $v_z$ , under a magnetic field gradient was evaluated

from the magnetic responsiveness curves as  $v_z = \langle L \rangle / t_{0.1}$ . Here  $\langle L \rangle = 1$  mm is the average path of the complexes' movement perpendicular to the measuring light beam symmetrically in both directions to the surface of the magnets arranged from both sides of the 4-mm-wide optical cuvette and  $t_{0.1}$  is the time required for a 10-fold decrease in optical density.

## 2.8. Non-heme iron determination

### 2.8.1. Non-heme iron determination in cells

To analyze the associated/internalized iron after the cells were associated with MNPs and thus magnetically labeled, approximately 200,000 cells were washed with PBS and then sedimented by centrifugation in a Falcon tube ( $2 \times 10^6$  untreated cells were used as a reference for determination of basal non-heme iron level). Optionally,  $10^5$  cells could be also used. The supernatant was discarded and 250  $\mu$ l of an acid mixture containing 3M HCl and 0.6 M trichloroacetic acid was added to the pellet. The probe was incubated overnight at 65 °C. Fifty microliter samples of the clear supernatant were sampled and analyzed for the iron content. Briefly, 20  $\mu$ l of an hydroxylamine-hydrochloride solution, 100  $\mu$ l of ammonium acetate buffer (25 g ammonium acetate and 70 mL glacial acetic acid adjust to a volume of 100 mL with de-ionized water), and 50  $\mu$ l of a 0.2 % 1,10-phenantroline solution were added. The mixture was incubated for 10 min, after which time the optical density was measured at the maximum of iron(II)-1,10-phenantroline complex (510 nm) and the blank was subtracted. Calibration curve was measured as described in item 2.3.3 for iron determination in suspensions of MNPs.

### **2.8.2. Non-heme iron determination in tissue samples**

15-40 mg tissue samples were covered with 100-200  $\mu$ l acid mixture (3M HCl and 0.6 M trichloroacetic acid) and incubated at 65°C during 24 h. Then, 20-50  $\mu$ l of acid extract was used for non-heme iron determination with 1,10-phenanthroline as described for non heme iron determination in cells. Tissue samples from a non-treated animal (control animal) were used as references for determination of the basal non-heme iron level.

## **2.9. *Transfection/transduction experiments of Jurkat T cells and hUC-MSCs using magnetofection***

### **2.9.1. Standard magnetofection of suspension cells**

For magnetofection of the suspension-type Jurkat T cells (scheme shown in Figure 5), 150  $\mu$ l of the cell suspension in complete medium containing 20,000 cells was placed in the wells of a 96-well U-bottom plate. The plate was centrifuged at 1400 rpm on a Heraeus Megafuge 2.0 for 5 min to sediment the cells. Then, 50  $\mu$ l of the freshly prepared transfection complexes was carefully added to the cells in each well to avoid pellet dispersion, and the plate was immediately placed on a 96-well magnetic plate for 30 min, followed by incubation for 48 h at 37°C, 5% CO<sub>2</sub>, until gene expression analysis. Transfections were performed in triplicate wells. The data were represented as the mean  $\pm$  standard deviation.

### **2.9.2. Magnetofection combined with glycerol shock**

For magnetofection combined with a glycerol shock, after adding the magnetic transfection complexes, the cells were incubated at the magnet for 30 min, 150  $\mu$ l of the supernatant was carefully removed, and 150  $\mu$ l of the complete medium containing 1.2 M glycerol was added and the cells were incubated for 4 h. Afterwards, cells were centrifuged and 150  $\mu$ l of the supernatant was carefully removed, and the cells were further cultivated until gene expression analysis.

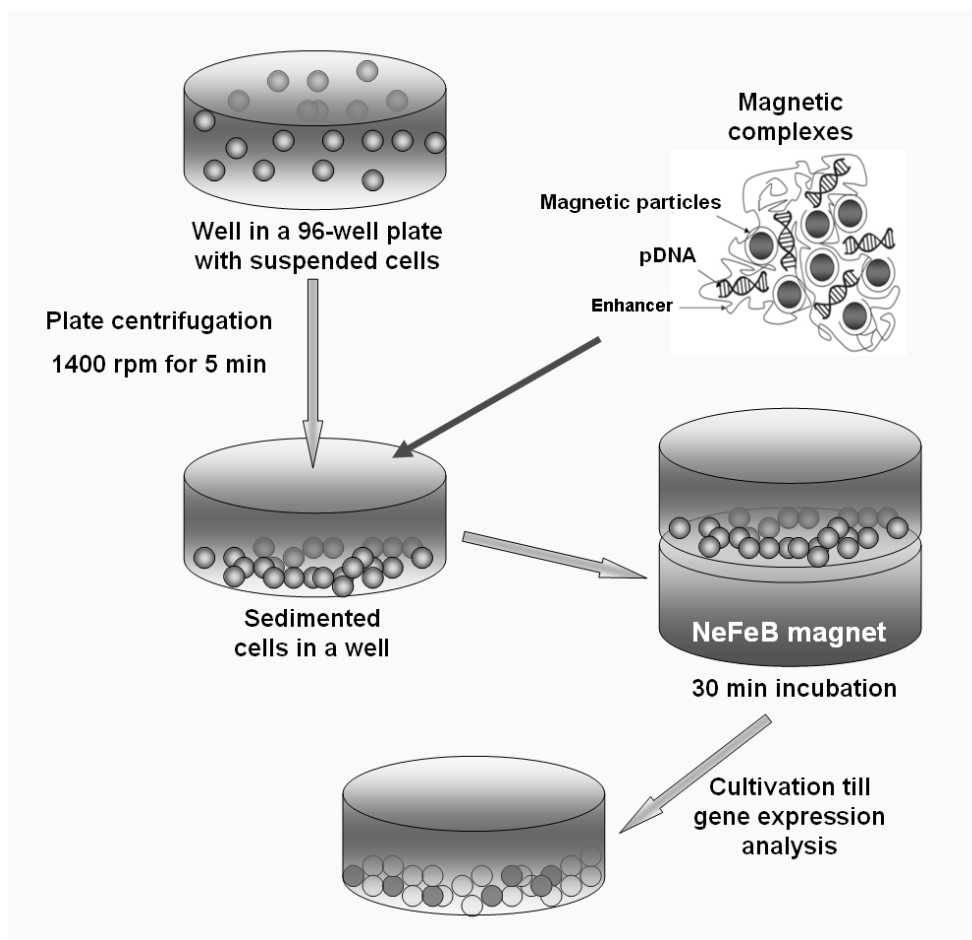


**Figure 5. Scheme of a magnetofection of suspension type cells.** Suspended cells are filled into the wells of the 96-well plate and (1) the plate is centrifuged to sediment the cells at the well bottom followed by (2) adding transfection complexes to the wells, afterwards (3) the cell culture plate is exposed to gradient magnetic field at 96-well Magnetic plate for 30 min and (4) cells are further cultivated till gene expression analysis.

### 2.9.3. Magnetofection using lentivirus and adenovirus vectors

For lentivirus infection using magnetofection, hUC-MSCs were seeded at the 24-well plate at a density of 50,000 cells per well 24 h prior infection. On the day of infection, the medium was aspirated, the cells were washed with complete cell culture medium and the medium was removed. Then, magnetic virus complexes were added to the cells in a final volume of 100 $\mu$ l and the plate was placed on the 24-well magnetic plate for 20 min. Afterwards, we added 1 mL complete culture medium per well and incubated for 3 days till analysis of the percentage of eGFP expressing cells by FACS.

For adenovirus infection by magnetofection,  $1.3 \times 10^6$  hUC-MSC were seeded in a 10 cm dish in 10 mL complete cell culture medium 24 h prior infection. On the next day, medium was aspirated and 1.5 mL of complexes magnetic virus complexes prepared

in OptiMEM® medium was added to the cells. Dish was incubated under magnetic field at 37°C in 5% CO<sub>2</sub> incubator for 20 min. Afterwards, magnetic plate was removed, the infection medium was aspirated, the cells were washed once with PBS, 10 mL of complete culture medium was added to the cells and the cells were incubated for about 72 h till gene expression analysis by FACS.

#### **2.9.4. Standard infection protocols for lenti- and adenovirus**

For standard lentivirus infection, virus stock containing desired MOI was mixed with 8 µg/mL polybrene and added to the cells in a well of 24-well plate in a final volume of 1 mL.

Cells were incubated up to 72h post-magnetofection till gene expression analysis was done by FACS.

For standard adenovirus infection, virus suspension was prepared in OptiMEM® medium in a final volume of 1.5 mL. Culture medium was aspirated from the dish and the virus suspension was added to the cells and incubated for 30 min at 37°C in 5% CO<sub>2</sub> incubator. Afterwards, infection medium was aspirated and the cells were washed with PBS and 10 mL of complete culture medium was added to the cells in a 10 cm dish. The cells were cultured until gene expression analysis (normally 48h post-magnetofection) by FACS.

#### ***2.10. Modification of the Miltenyi LS separation column with magnetic complexes***

Two different protocols to modify LS columns with the magnetic complexes prior transfection were developed. These protocols were called standard and freeze-drying protocols.

##### **2.10.1. Standard protocol**

To modify the cell separation column with magnetic transfection/transduction complexes, complex suspension was added to the LS Miltenyi column in a volume, corresponding to the dead column volume. After distribution of the fluid within the column volume, the column was placed at the MidiMACS™ Separator magnet. The column loaded with the magnetic complex can be optionally incubated at the Separator for maximal 30 min at room temperature till cell loading. To ensure



maximal complex association with the cells and maximal transfection efficiency longer incubation time between complex loading and cell loading should be avoided.

### **2.10.2. Freeze-drying protocol**

In this protocol, LS Miltenyi column modified with magnetic transfection/transduction complexes according to the standard protocol described in p. 2.10.1, was freeze-dried in liquid nitrogen, placed into a vacuum chamber of lyophilization device and then the surrounding pressure was reduced to allow the frozen water in the column to sublime directly from the solid phase to gas. After overnight freeze-drying, the column was stored at room temperature until usage.

## ***2.11. Genetic modification of magnetically labelled cells by viral and non-viral magselectofection***

### **2.11.1. Magnetic labeling of the cells before magselectofection**

Just before magselectofection in parallel to the assembling of the magnetic transfection/transduction complexes, the cell suspension was treated with specific magnetic Microbeads from Miltenyi® Biotec, to label target cells magnetically as is routinely performed for cell separation according to the modified protocol from Miltenyi® Biotec. CD45 MicroBeads were used to label Jurkat T cells and PBMCs, whereas CD105 and CD34 MicroBeads were used to label hUC-MSCs and hCB-HSCs, respectively. Briefly, 10 µl of the specific MicroBeads suspension was added to cell suspension containing about  $10^6$  hCB-HSCs or  $2.5 \times 10^6$  Jurkat or hUC-MSCs in 100 µl complete RPMI medium, and mixed with a pipette. The suspension was incubated for 15 min at 4 - 6°C and the cells were washed with complete cell culture medium by centrifugation at 1200 rpm for 3-5 min and resuspended in a total 2 mL of the complete RPMI medium. To notice is that the magnetic labelling should be performed just before magselectofection or cell sorting, as magnetization of the cell was lost gradually during incubation.

### **2.11.2. Magselectofection general protocol**

When adopting the 2-column cell separation protocol for achieving increased purity of target cells, magnetically labeled cells or cell mixtures were first passed through an unmodified LS column according to the instructions of the manufacturer. This was

applied for mixtures of Jurkat T and K562 cells or upon isolation of the CD34-positive HSC from the cord blood mononuclear cells (CBMC) Ficoll gradient fraction from the UC blood or for Sca-1<sup>+</sup> mouse hematopoietic stem cells isolated from bone marrow. After the first positive selection, the cells were applied to vector-modified column. Using magselectofection to transfect/transduce cell monoculture of UC-MSCs or Jurkat T cells, the 1-column cell separation protocol was used (Figure 6).

After vector loading, the modified LS columns remained positioned within the magnet. Cells suspended in 2 mL complete culture medium, were loaded and allowed to infiltrate into the column. When applying mixtures of cells, we washed the column using 3x3 mL of cell culture medium. The magnetically-labeled cells were retained in the column and the unlabeled cells passed through. We incubated the column within the magnet for 30 min at room temperature. Then, we removed the column from the MidiMACS magnet, placed it over a 15 mL test tube, loaded 2 mL of complete RPMI medium into the column reservoir and flushed the cells from the column by firmly pushing the plunger supplied with the column. Subsequently the cells were transferred to cell culture plates for further cultivation at 37°C in a humidified atmosphere containing 5% CO<sub>2</sub> until evaluation of cell separation and/or gene transfer efficiency.

Forty-eight hours after magselectofection with the non-viral and adenoviral vectors and seventy-two hours after infection with the lentiviral vectors, reporter eGFP or luciferase gene expression was evaluated by FACS analysis or using a luciferase assay.

### **2.11.3. Analysis of the magnetic cell separation and gene transfer efficiency**

To clarify whether modification of the separation column altered the cell separation efficiency, we tested the purity of the selected cell population after separation with two unmodified LS columns against separation using an unmodified column and a vector-modified column (with viral or non-viral vectors) sequentially. Before the experiment, the CD2<sup>+</sup>/CD3<sup>+</sup> status of the Jurkat T cells and the CD2<sup>-</sup>/CD3<sup>-</sup> status of the K562 cells was confirmed by FACS analysis. Vector-modified columns were prepared as described above with complexes comprising 20 µg plasmid DNA in magnetic DF-Gold formulation (DNA/DF-Gold/MNP = 1:4:1 (w/v/w)) or using SO-Mag2/LV.eGFP complexes with 20 fg Fe/VP at various MOIs with respect to the

target cell (Jurkat) numbers. We labeled Jurkat T cells with CD2 MicroBeads from Miltenyi Biotec as described above for labeling with CD45 MicroBeads. The cells were washed with cell culture medium to eliminate unbound beads according to the standard labeling protocol from Miltenyi. We then prepared 1:1 mixtures of labeled Jurkat T cells and unlabeled K562 cells in RPMI. For the non-viral experiment, we subjected two portions comprising  $2.5 \times 10^6$  cells of each species to a first round of selection on unmodified LS columns according to the instructions of the manufacturer. Retained cells were eluted by pressure enforced elution with 2 mL medium. Then one portion was passed through a second unmodified column, while the other portion was applied to a vector modified column as described above. For the lentiviral experiment, we proceeded in the same manner but applied cell mixtures comprising  $5 \times 10^5$  cell of each species. Aliquots of the positively selected cells were treated with an anti-CD3-PE antibody (AbD Serotec, Düsseldorf, Germany) immediately after magselectofection and the purity of the  $CD2^+/CD3^+$  cell population (Jurkat T cells) was determined by FACS analysis. The residual selected and non-target cells were cultivated until evaluation of reporter gene expression by FACS analysis or luciferase assay at the time points.

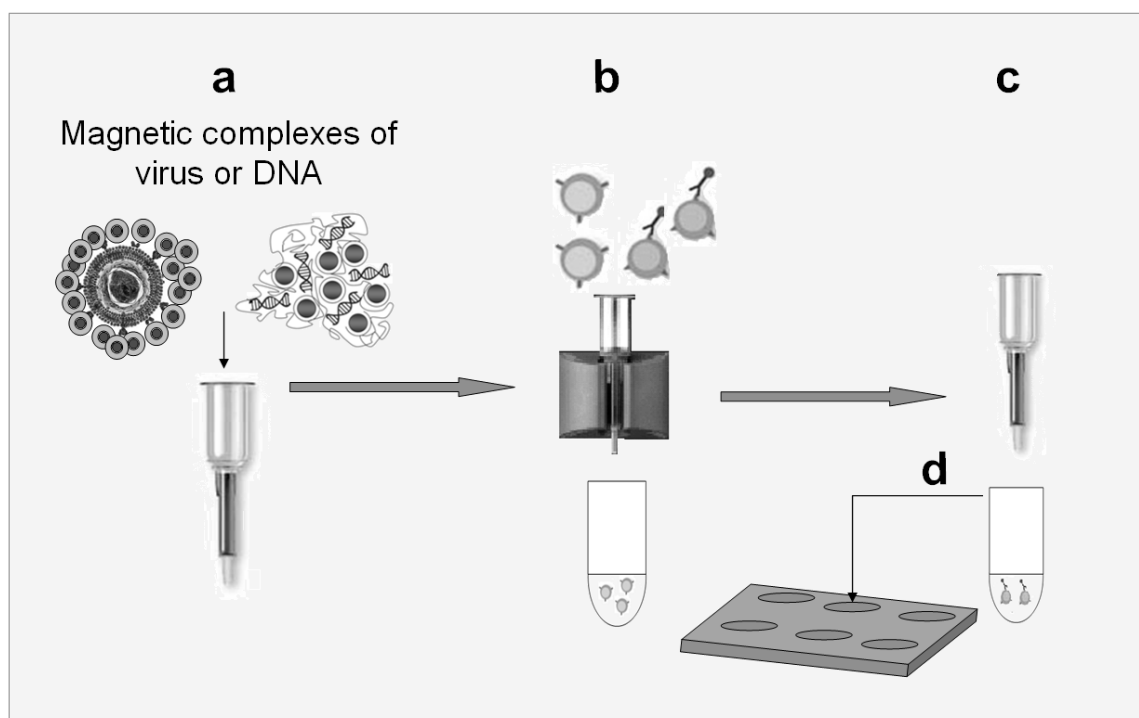


**Figure 6. Schematic representation of the magselectofection.** (a) modification of the LS Miltenyi separation column with transfection complexes prior-transfection, (b) loading of the cell mixture into the modified column and incubation for 30 min at the magnet, (c) elution of the retained cells from the column, (d) incubation in a plate for 48 h till gene expression analysis.

#### **2.11.4. Magselectofection experiments using XS columns**

For upscale of magselectofection from LS columns to XS columns and CliniMACS,  $2.5 \times 10^7$  CD45 MicroBead-labelled Jurkat T cells were resuspended in 10 mL of CliniMACS buffer containing 2% human AB serum and placed in a sample application bag. This was connected to the prototype CliniMACS tubing sets and the cells were separated using the CD34 Selection Program. Towards the end of the third cell wash step, the program was paused, the 3-way taps opened and magnetic transfection complexes containing 80  $\mu\text{g}$  pCMV-kk or peGFP, 80  $\mu\text{g}$  SO-Mag2 magnetic beads and 320  $\mu\text{L}$  DreamFect-Gold were added. After flushing an additional 8 mL buffer through the tubing, the 3-way taps were closed and the complexes incubated with the cells for 30 minutes at room temperature. At this point the program was resumed and the cells eluted and taken into culture.

#### **2.11.5. Lentiviral magselectofection versus standard infection of hCB-HSCs**

These experiments were carried out together with Prof. Wagemaker's group (Department of Hematology, Erasmus Medical Center, Rotterdam, The Netherlands). The third generation self-inactivating lentiviral vector backbone pRRL.PPT.eGFP.WPRE (LV.eGFP2) containing the spleen focus forming virus (SF) promoter was used (Prof. Wagemaker lab). The viral vector stock was concentrated by ultracentrifugation and contained  $9 \times 10^{12}$  p24 VP/mL with a biological titer of  $1.9 \times 10^9$  TU/mL (as determined by transducing HeLa cells with a serial dilution of the virus).

For the separation, infection and magselectofection of CD34<sup>+</sup> cells from cord blood (hCB-HSCs),  $1.4 \times 10^8$  CBMC cells that had been freshly isolated using a Ficoll gradient (as described above) were pooled with  $5.7 \times 10^8$  of freshly thawed CBMCs in a total volume of 2.1 mL of PBS solution containing 2 mM EDTA. To label the CD34<sup>+</sup> hUC-HSCs magnetically, 400  $\mu\text{L}$  of FcR Blocking Reagent (to avoid unspecific labeling of the cells via Fc receptors) and 400  $\mu\text{L}$  CD34+ MicroBeads were added to the CBMC suspension. This was then mixed well and incubated at 4 - 6°C for 30 min. 10 mL of PBS buffer containing 2 mM EDTA was added, the cells were centrifuged at 300 x g for 10 min, the supernatant was aspirated and the cells were resuspended to a total volume of 1 mL in a serum free modified Dulbecco's medium as described (Guilbert and Iscove, 1976), (Merchav and Wagemaker, 1984). The resulting  $7.1 \times 10^8$

CBMCs treated with CD34+ MicroBeads were loaded into the LS column positioned in a MidiMACS™ Separator magnet. The positively-selected hCB-HSCs were eluted in a volume of 2 mL of serum free modified Dulbecco's without growth factors. To increase the purity of the cell fraction, the resulting suspension of the positively-selected cells can be optionally passed through a second LS column and be eluted in 3 mL of the medium supplemented with 50 ng/mL Flt3, 100 ng/mL TPO and 100 ng/mL SCF.

For magselectofection, SO-Mag2/LV.eGFP2 magnetic complexes with SO-Mag2 magnetic particles were formulated. 4.3 µl of the LV.eGFP2 stock were mixed with 5.6 or 56 µl of a SO-Mag2 stock solution containing 14 µg Fe/µl and the volume was adjusted to 400 µl with RPMI medium without additives. This resulted in magnetic particle:VP ratios of 2 and 20 fg Fe/VP, respectively. Two LS columns were modified with the complexes and 150.000 pre-selected hUC-HSCs were loaded per modified LS column positioned at the MidiMACS™ Separator magnet. The column was incubated for 30 minutes. Then, the column was removed from the magnet and the cells were eluted with growth factor supplemented medium. The samples were transferred into individual wells of a 24-well plate and incubated for 2 days until the expression of eGFP was analyzed using FACS.

For a standard infection, 150.000 positively-selected cells were loaded on an unmodified LS column positioned at the MidiMACS™ Separator and were incubated for 30 min. The column was removed from the magnet and the cells were eluted with 1 mL of growth factor supplemented medium into one well of a 24-well plate. 4.3 µl of the LV.eGFP2 virus stock were added, resulting in an MOI of 40 TU/cell, and the plate was incubated for 2 days until the expression of eGFP was analyzed using FACS.

### **2.11.6. Testing of immobilization of the magnetic complexes at the Miltenyi® column and association with cells upon magnetic field application**

#### **2.11.6.1. Using non-viral complexes**

The magnetic transfection complexes were prepared as described above using radioactively labelled plasmid DNA (20 µg plasmid per column, 250.000 CPM/column). Then, LS Miltenyi® columns were modified using the standard (“fresh”) or freeze drying protocols as described above. Jurkat T cells were magnetically labeled as described above and loaded into the modified column placed at the MidiMACS™ magnet in 4 fractions of 0.5 mL. Unlabeled cells or non-magnetically labeled DNA passed through and fractions were collected in Eppendorf tubes, centrifuged at 1200 rcf for 5 min, and the radioactivity was measured in both pellets and supernatants. Column was incubated for 30 min at room temperature at the MidiMACS™ magnet to achieve gene delivery complex association with the cells. After that, the column was removed from the magnet and magnetically retained cells were flushed out by firmly applying the plunger supplied with the column using 8 times 0.5 mL RPMI media culture media. The eluted fractions were collected in Eppendorf tubes, centrifuged at 1200 rcf for 5 min and the radioactivity was measured in parallel both in pellets and supernatants.

#### **2.11.6.2. Using viral complexes**

To analyse efficacy of magnetic lentivirus immobilization within the LS column upon magnetic field application, magnetic viral complexes were prepared as described above using in each case MOI of 0.5 and 1 and 20 fg Fe/LVP. Then, magselectofection was performed as explained above using  $10^6$  CD45 magnetically labelled Jurkat T cells. The elution volume received when the column was placed at the MidiMACS magnet was collected and frozen for further p24 HIV associated protein ELISA analysis. The percentage of LVPs immobilized within the LS column was calculated with account for the number of the applied LVPs and LVPs detected in elute.

### **2.11.7. Analysis of cell association and internalization efficiency of the non-viral transfection complexes by flow cytometry**

To evaluate the percentage of the cells that associated with and internalized the complexes, we used a FACS method previously described by Ogris et al. (Ogris et al., 2000) with slight modifications. Briefly, 360  $\mu$ l of the transfection complexes carrying the luciferase plasmid was prepared as described above, and 0.5  $\mu$ l of the DNA-intercalating dye YOYO-1 (1 mM in DMSO; corresponding to one dye molecule per every 11 bp) was added, resulting in green fluorescence of the plasmid DNA. The magnetofection of the Jurkat T cells was performed as described. Cell suspensions for FACS analysis were prepared as described above at 48 h post-transfection. FACS analysis was performed with fluorescence excitation using an argon laser with an excitation maximum of 488 nm, and analysis was performed using both a 530/30-nm bandpass filter (green fluorescence from the cells associated with YOYO-1-labelled transfection complexes) and a 575/26-nm bandpass filter for red fluorescence. A minimum of 5000 events per sample were analysed. The percentage of cells associated with transfection complexes was determined as the percentage of gated fluorescent events, using untreated cells as a reference. Additionally, the YOYO-1 fluorescence from the complexes that are associated with cells but are not internalized into cells was quenched by the cell-impermeable nucleic acid stain propidium iodide (PI). Briefly, 1  $\mu$ l of PI stock solution was added to 1 mL of the cell suspension for FACS analysis (a final PI concentration of 1  $\mu$ g/mL), followed by FACS with the 575/26-nm bandpass filter (red fluorescence of PI-positive cells). The cells exhibiting green fluorescence in the presence of PI were identified as those that have internalized the transfection complexes. Only living cells were taken into account, whereas the cells incorporating high levels of PI and showing a reduction in forward scattering as a measure of cell size were excluded from further analysis.

### **2.11.8. Analysis of pDNA internalization using radioactively labeled pDNA**

pDNA labelled with  $^{125}$ I-isotope was used to evaluate the amount of DNA taken up by the cells. For this purpose, the magnetic transfection complexes were assembled using radioactively labelled DNA and applied for magselectofection. Cells were analyzed for internalized DNA at 0, 0.5, 3, 6, 24 and 48 h post-transfection. To remove the magnetic complexes associated with the cell membrane, cells were

treated with a solution containing heparin and DNase and washed with PBS. Then, cells were centrifuged and radioactivity was measured in both cell pellet and supernatants.

### ***2.12. Immunocharacterization of cells***

Jurkat T cells, K562 and hUC-MSC cells were characterized by FACS for several haematopoietic and non-hematopoietic markers such as CD2, CD3, CD34, CD45, CD90 and CD105, each one labelled with PE. Briefly, a single cell suspension ( $1 \times 10^6$  cells each) of Jurkat T cells, K562 or hUC-MSCs were suspended in complete RPMI media and incubated with 5  $\mu$ l of antibody at room temperature in the dark for 30 min. After incubation time, cells were washed twice with FACS buffer at 1200 rpm for 5 min and resuspended in a final volume of 0.5 mL of FACS buffer. An isotype control was included in each experiment. Cell fluorescence was evaluated by FACS.

### ***2.13. Reporter gene expression analysis***

#### **2.13.1. Luciferin & luciferase assay**

48 h after transfection, cell suspension from the 6-well plate was resuspended in a 15 mL tube and centrifuged at 1200 rpm for 5 min, supernatant was discarded, the cells were washed with 1 mL PBS, and the cell pellets were resuspended in 200  $\mu$ l of lysis buffer (0.1% Triton X-100 in 250 mM Tris pH 7.8) per tube and incubated for 10-15 min at room temperature. The cell lysate (100  $\mu$ l per well) was transferred to the wells of a black 96-well plate and mixed with 200  $\mu$ l of luciferin buffer containing 35 mM D-luciferin, 60 mM DTT, 10 mM magnesium sulphate, 1 mM ATP and 25 mM glycyl-glycine-NaOH buffer, pH 7.8. Chemiluminescence was recorded using a TopCount instrument (Canberra Packard, Groningen, The Netherlands).

#### **2.13.2. eGFP expression analysis**

##### **2.13.2.1. Fluorescence microscopy**

To quantify eGFP<sup>+</sup> cells, fluorescence microscopy images were taken at 490/509 nm 48h or 72h after non-viral or viral magselectofection, respectively. In some cases, to quantify percentage of eGFP<sup>+</sup> cells more precisely, digital analysis of the bright field and fluorescence images was performed by S.CO-lifescience Company (Garching,



Germany): total number of cells in the brightfield image were counted and compared to the number of eGFP<sup>+</sup> cells counted in the fluorescence image.

#### **2.13.2.2. Analysis of transfection/transduction efficiency by fluorescence-activated cell sorting (FACS)**

To evaluate the transfection efficiency, 48 h post-transfection the cells were washed twice with PBS supplemented with 1% FCS (further referred to as FACS buffer). For analysis of transduction efficiency, 72h post-transduction (if not other indicated) the cells were fixed using Cytofix<sup>TM</sup> Fixation Buffer (Becton Dickinson), washed and resuspended in 0.5 mL of the FACS buffer for FACS analysis. FACS analysis was performed in FACS vantage (Becton Dickinson) with fluorescence excitation with a maximum at 488 nm using an argon laser. Cell fluorescence was registered using a 530/30-nm bandpass filter (green fluorescence from the cells expressing eGFP). A minimum of 20000 events per sample were analysed. The gated (viable) eGFP<sup>+</sup> cells were evaluated as a dot displaying FL-1 (eGFP) on the X-axis and FL-2 on the Y-axis. To correct the results for weak fluorescence of the enhancer and to avoid overestimating the percentage of eGFP-expressing cells post-transfection with magnetic lipoplexes, untransfected cells and those transfected using magnetic triplexes of DF-Gold, luciferase plasmid and magnetic MNPs were used as the controls. Data were analyzed by using FlowJo software.

### **2.14. Cell viability**

#### **2.14.1. Trypan blue dye exclusion test**

The trypan blue dye exclusion test was used to determine the number of viable cells present in the cell suspension. It is based on the principle that live cells possess intact cell membranes that exclude certain dyes, such as trypan blue, whereas dead cells do not. 48 h post-magselectofection procedure 100 µl of cell suspension was mixed with 100 µl of trypan blue solution and 10 µl of the mixture was loaded in a Neubauer chamber and then visually examined under microscope to determine whether cells have taken up or excluded the dye. Viable cells had a clear cytoplasm whereas nonviable cells presented blue cytoplasm. The results were expressed in percentage of living cells.

### **2.14.2. MTT assay**

The MTT assay, based on reduction of the MTT reagent into formazan by superoxide anions produced in the mitochondrial respiratory chain, was carried out to assess the cytotoxicity of the complexes. 48 h post-transfection the cells were washed once with PBS, the supernatant was discarded, and the cells were incubated for 2-3 h in 100  $\mu$ l of 1 mg/mL MTT solution prepared in Hank's balanced salt solution with 5 mg/mL glucose. Afterwards, 100  $\mu$ l solubilisation solution (10% Triton X-100 in 0.1 N HCL in anhydrous isopropanol) was added and incubated at 37°C with shaking overnight to dissolve the formazan. The optical density was measured at 590 nm. Untreated cells were used as a reference.

### **2.15. Differentiation assay**

#### **2.15.1. Colony-forming cell (CFC)**

CFC assays were performed just post-magselectofection in a well-defined methylcellulose-based culture media using MethoCult<sup>®</sup> reagent (StemCell technologies). The majority of CFCs consist of lineage-restricted colonies: erythroid restricted burst-forming units-erythroid (BFU-E), which are more immature than the colony-forming units erythroid (CFU-E); megakaryocyte-restricted CFU-Mk; colony-forming units-granulocytes (CFU-G), colony-forming units-monocytes/macrophages (CFU-M); and colony forming units-granulocytes/macrophages (CFU-GM). The most immature (multipotent) CFC measurable contains granulocytes, erythrocytes, macrophages, and often megakaryocytes (CFU-GEMM) and is usually measured at day 12 after culture initiation. This CFC is also often called CFU-mixed, as it may not always contain megakaryocytes but does contain erythroid and granulocyte/macrophage cells. Just after magselectofection,  $2 \times 10^3$  hCB-HSCs were seeded in a well from a 24-well plate with methylcellulose-based culture media and colonies were counted 6 days post-magselectofection for GM, BFU-E or mixed colonies.

#### **2.15.2. Osteogenesis**

To analyse whether the UC-MSCs have maintained the potential to differentiate into other cell types post-magselectofection procedure, the in vitro osteogenic assay

using hUC-MSCs was carried out. After transfection/transduction using magselectofection technology, the cells were seeded in a 6-well plate at a density of 70.000-100.000 cells/well and incubated for 48 h in a complete DMEM cell culture medium without antibiotics. Afterwards, the medium was changed for osteogenic induction medium and the cells were incubated in this medium for the next 18 days in a humidified atmosphere at 37°C. The osteogenic medium contained low glucose DMEM (1g glucose/L) medium supplemented with 10% heat-inactivated FCS, 100 U mL<sup>-1</sup> penicillin, 100 mg mL<sup>-1</sup> streptomycin, 100µL of 1mM dexamethasone, 5 mL of 10mM ascorbate-2-phosphate, 10 mL of 1M β-glycerol phosphate, sterile filtered through 0.22 µm filter. The cells cultivated in a complete DMEM high glucose medium without antibiotics and without osteogenic induction components were used as a reference. After 18 days of osteogenic differentiation, the cells were stained with alizarin red for calcium depositions/mineralization, which are considered a functional in vitro endpoint reflecting advanced cell differentiation. Briefly, the medium was aspirated and cells were washed twice with PBS. After that, the cells were fixated using 1 mL 70% ice cold ethanol at RT for 5 min. Then, the cells were washed using incubation with 1 mL of H<sub>2</sub>O at RT for 5min. Afterwards, 500µl 2 % Alizarin Red solution (0.4g of Alizarin is dissolved in 20 mL ddH<sub>2</sub>O and the pH is adjusted to 4.3 - 4.5 pH with ammonium hydroxide filtered through a Whatman-filter) were added and incubated at RT for 3 min. Then, wells were washed with 5x1 mL of H<sub>2</sub>O. Bright field images were taken immediately after staining. The principle of the alizarin red staining is that calcium forms an alizarin red S-calcium complex in a chelation process. The reaction is birefringent.

### ***2.16. In vivo biodistribution analysis of magselectofected hUC-MSCs and magnetic labeled hCB-HSCs***

hUC-MSCs (10<sup>6</sup> cells) and hCB-HSCs (10<sup>6</sup> cells) were transduced by magselectofection procedure using a MOI of 0.2. Then, the cells were magnetically labelled with SO-Mag2 nanoparticles at a dose of 50 pg Fe/cell of magnetic nanoparticles. Two days post-magselectofection hUC-MSCs were trypsinised and resuspended in 500 µl PBS. 5 x 10<sup>5</sup> hCB-HSCs were also resuspended in 500 µl PBS one day after labelling with MNPs. SCID mice were injected. For each cell type, 5 x 10<sup>5</sup> cells suspended in 500 µl were injected via the lateral tail vein SCID mice were injected with 500µl of cells. After 24 h the mice were sacrificed by cervical

dislocation and the liver, spleen, lungs, kidney, muscle, heart and brain were removed. The entire harvested organs were weighed, transferred to a cryovial with tissue-freezing medium (Jung) and immersed in liquid nitrogen for fast freezing. The cryovials were stored at  $-80^{\circ}\text{C}$  until analysis. Frozen tissues were sectioned and histological sections were analysed under fluorescence microscope for biodistribution of eGFP expressing hUC-MSCs.

Prussian blue staining of the histological section was done to identify and analyse the biodistribution of iron associated with magnetically labeled cells. For Prussian Blue staining (PB), histological sections were transferred to glass slides and fixed with 4% paraformaldehyde. Prussian blue cellular staining was performed by incubating the fixed cells in a mixture of 4% potassium ferrocyanide and 3.7% HCl for 30 minutes. Slides were washed in distilled water, 3 changes followed by counterstain with nuclear fast red for 5 minutes. Then, slides were rinse twice in distilled water and dehydrate through 95% and 2 changes of 100% alcohol, clear in xylene (2 changes, 3 minutes each). Finally, slides were mounted with a coverslip with resinous mounting medium.

### ***2.17. Statistics***

All values are expressed as the mean  $\pm$  standard deviation.

### 3. RESULTS

In this chapter the characteristics of the magnetic particles and magnetic transfection/transduction complexes used are shown. The results of selection of magnetic vector for magselectofection using 2D transfections (magnetofection) in Jurkat T cells are illustrated in this chapter. The results of experiments which examined the binding of DNA to magnetic beads are presented. The results of the vector loading Miltenyi column strategy, association/internalization of magnetic complexes with/into the target cells, cell separation efficiency, cell recovery and transfection/transduction efficiency in the target cells after magselectofection are here described. The validation of magselectofection in therapeutically relevant cells and within other established technologies (magnetofection and standard lentivirus infection) is proven. A first pilot study of the applicability of magselectofection *in vivo* is presented.

#### 3.1. *Magnetic nanoparticles used in this study and their characteristics*

Core-shell-type magnetic nanoparticles (MNPs) were selected for self-assembly with viral and non-viral vectors to be used for magnetofection in 2D-cell arrays and for magselectofection. Size, electrokinetic potential, saturation magnetization, iron content and surface composition was analysed in order to characterize the selected MNPs.

Table 1 summarises some essential characteristics of the commercially available and synthesised magnetic nanoparticles that were used in this work. All particles are iron-oxide-based core-shell nanoparticles. For our custom nanoparticles, data of phase composition based on X-ray diffraction patterns collected from the dry powder of MNPs (data not shown) suggest a magnetite composition of the core with a mean crystallite size in the range of 8-12 nm. Empirically, magnetite nanoparticles with a magnetite crystallite size of 9–11 nm were found to be superior to smaller particles for use as components of the magnetic transfection vectors for magnetofection. The saturation magnetization of our synthesised MNPs is lower than the saturation magnetization of bulk magnetite and typical for rather well-stabilised magnetite nanocrystals of this size. The iron content of the magnetic nanoparticles used during this work varies from 0.21 to 0.68 g iron per g dry weight. The hydrodynamic diameter in aqueous suspension varied from 17 nm for PEI-Mag3, corresponding

---

mainly to individual particles, to 400 nm for aggregates of the SO-Mag2 nanoparticles. The electrokinetic potential ( $\zeta$ ) is highly positive for the CombiMag, PolyMag, SO-Mag2 and PEI-Mag particles and negative for the PL-Mag2, NDT-Mag1 and PalD1-Mag1 particles, as shown in Table 1, depending on the coating material used. The surface composition for selected nanoparticles (PEI-Mag2, NDT-Mag2 and PL-Mag1) was analysed by XPS spectra. The XPS data showed that both PEI and NDT assembled with the fluorosurfactant at the surface of the nanoparticles in the course of the synthesis. The resulting self-assembled mixed layers were stable and remain bound to the surface after extensive dialysis used to purify the particles. Surprisingly, the XPS spectra of the PL-Mag1 nanoparticles indicate that ~100% of the carbon atoms should be attributed to the fluorosurfactant, i.e., the Pluronic F-127 was fully eliminated after dialysis.

Table 1. Characteristics of magnetic nanoparticles

Magnetic nanoparticles	Core composition	Coating	Mean magnetite crystallite size $\langle d \rangle$ (nm)	Saturation magnetization of the core $M_s$ (emu/g iron)	Mean hydrodynamic diameter $D$ (nm)	Electrokinetic potential $\xi$ (mV)	Iron content (g Fe / g dry weight)
CombiMag <sup>#</sup>	Iron oxide		No data	No data	96 ± 1	+ 57.2 ± 1.7	0.64
PolyMag-41/1 <sup>#</sup>	Iron oxide		No data	No data	230 ± 2*	+ 59.4 ± 0.6	0.60
ViroMag R/L <sup>#</sup>	Iron oxide		12	No data	542 ± 115*	+ 38.4 ± 1.6	0.47
PEI-Mag2	magnetite	25KDa branched Polyehylenimin	9	62	28 ± 2	+ 55.4 ± 1.6	0.56
PEI-Mag3	magnetite	Polyehylenimin	8	46	17 ± 4	+ 53.4 ± 0.7	0.21
PL-Mag2	magnetite	Pluronic F127	10.6	99	101 ± 20*	- 18.3 ± 1.6	0.47
NDT-Mag1	magnetite	1-9 Nonanedithiol	11.6	74	43 ± 6	- 16.6 ± 2.0	0.68
SO-Mag2	Magnetite	condensation of tetraethyl orthosilicate and 3-(trihydroxysilyl)propylmethylphosphate	11	118	427 ± 90*	+ 37.4 ± 1.6	0.50
PalD1-Mag1	magnetite	Palmitoyl dextran	8.5	63	55 ± 10	- 15.6 ± 1.6	0.53

<sup>#</sup>commercially available nanoparticles; \*assemblies of the particle

### 3.2. *Magnetic vectors and their characteristics*

Magnetic non-viral and viral vectors were assembled and characterized. The mean hydrodynamic diameter and the  $\xi$ -potential of the magnetic vectors were determined by photon correlation spectroscopy as described in *Material and Methods*. The binding efficiency, sedimentation stability and magnetophoretic mobility were analysed. Sedimentation stability and magnetophoretic mobility were analysed using a turbidity measurement both without magnetic field application and when subjected to inhomogeneous magnetic fields, respectively, as recently described by Mykhaylyk et al. (Mykhaylyk et al., 2008) (Mykhaylyk et al., 2009a) and in *Material and Methods*.

#### **3.2.1. Efficient association of nucleic acids with magnetic particles after complex formation**

##### **3.2.1.1. Non-viral magnetic lipoplexes**

To assess pDNA association with magnetic nanoparticles and magnetic sedimentation of the resulting magnetic lipoplexes, the complexes were prepared using  $^{125}\text{I}$ -labelled pDNA, DF-Gold and magnetic nanoparticles at iron-to-plasmid w/w ratios ranging from 0.125 to 10. After 30 min of incubation at the 96 magnetic plate, creating an average magnetic field of 70–250 mT and a field gradient of 50–130 T/m in the vicinity of the cells, the radioactivity was measured in the supernatant and the percentage of DNA associated and magnetically sedimented with magnetic nanoparticles was quantified as described in the *Material and Methods*. The data presented in Figure 7, for magnetic lipoplexes prepared for magnetofection, show that more than 90% of the DNA was magnetically sedimented when associated with each of the four selected nanoparticles in the presence of DF-Gold at iron-to-DNA w/w ratios higher than 0.2.

In the case of magnetic lipoplexes prepared for magselectofection, 65%, 85% and 100% of the DNA was magnetically sedimented when associated with each of the selected nanoparticles SO-Mag2, PEI-Mag2 and PEI-Mag3, respectively.



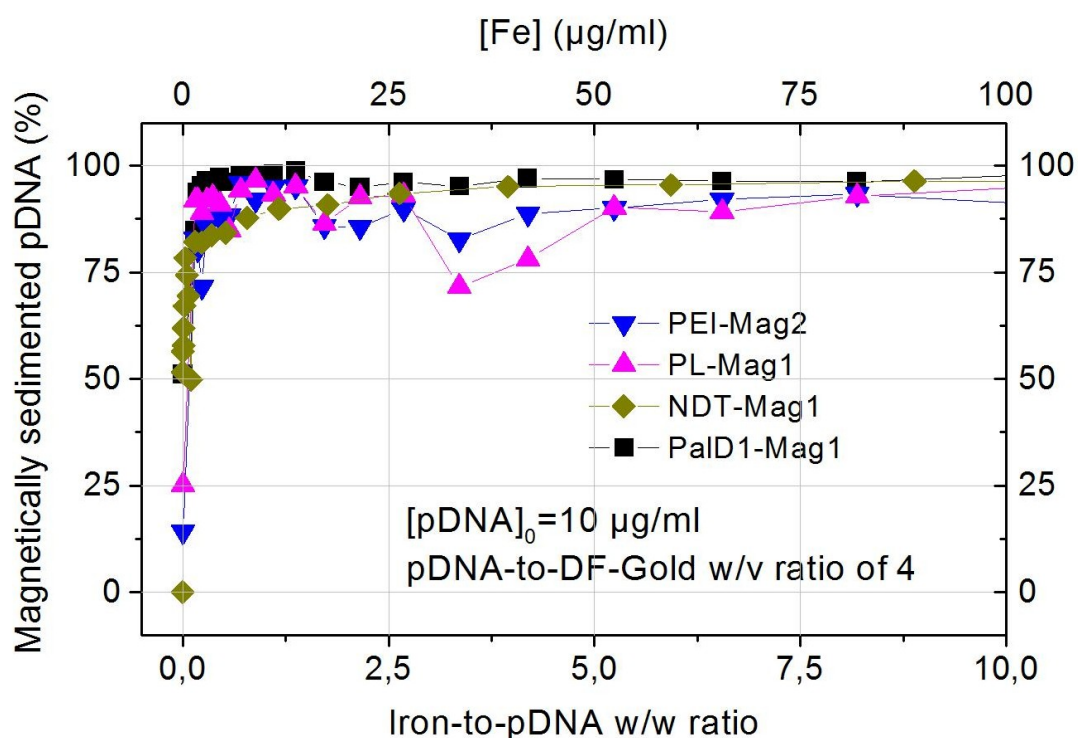


**Figure 7. Magnetic sedimentation of nucleic acid associated with magnetic nanoparticles.** The figure shows plasmid DNA associated and magnetically sedimented with magnetic nanoparticles after incubation at the magnetic plate for 20 min in the presence of DF-Gold lipid transfection reagent as an enhancer at a DF-Gold-to-pDNA v/w ratio of 4 and a starting pDNA concentration of 10 µg/ml plotted against nanoparticle concentrations in terms of iron-to-nucleic acid weight/weight ratios after complex formation.

### 3.2.1.2. Viral magnetic complexes

Experiments carried out together with Arzu Cengizeroglu, M.Sc. (Cengizeroglu, 2008). We were interested to evaluate the binding efficiency between LVPs and MNPs using three different virus concentration at seven different serial dilutions of fg Fe magnetic nanoparticles per LVPs. For that purpose viral magnetic complexes were assembled and magnetically sedimentated as described in *Material and Methods*. The vector fraction remaining in the supernatants was determined using a p24-specific ELISA kit. Virus detected in the supernatant after 30 min magnetic sedimentation was defined as unbound.

The results from the binding capacity assay indicated that up to 94% bound with MNPs. Moreover, the percentage of bound LVPs in complexes remains nearly constant throughout all fg Fe/LVP ratios and for every virus concentration used.

### 3.2.2. Characteristics of non-viral magnetic lipoplexes

Table 2 summarizes data on the mean hydrodynamic diameters and electrokinetic potentials of the lipoplexes and magnetic lipoplexes prepared to be used for magnetofection. Data on the mean hydrodynamic diameters, electrokinetic potentials, magnetic moments, magnetophoretic mobilities and number of nanoparticles per complex for magnetic lipoplexes synthesized for magselectofection are summarized in Table 3. Most of the complexes had a positive net charge when suspended in medium without FCS. In contrast, the complexes possess a negative net charge when suspended in medium with serum. The results indicate that under transfection conditions, i.e. complete culture medium with 10% FCS, complexes are negatively charged and aggregated.

**Table 2. Characteristics of the lipoplexes and selected magnetic lipoplexes at iron-to-DNA w/w ratio of 0.5-to-1\***

Complex	Luciferase plasmid		GFP plasmid	
	Mean hydrodynamic diameter D (nm)	$\xi$ -potential (mV)	Mean hydrodynamic diameter D (nm)	$\xi$ -potential (mV)
DF-Gold /pDNA	742 $\pm$ 340	+ 16.9 $\pm$ 4.7	693 $\pm$ 391	+ 27.1 $\pm$ 1.3
PL-Mag1/DF-Gold/ pDNA	1509 $\pm$ 715	- 2.5 $\pm$ 3.3	1807 $\pm$ 982	- 4.8 $\pm$ 2.7
PEI-Mag2/DF-Gold/ pDNA	1616 $\pm$ 798	+ 19.2 $\pm$ 3.0	790 $\pm$ 432	+ 25.8 $\pm$ 0.9
NDT-Mag1/DF-Gold/ pDNA	1730 $\pm$ 879	+ 16.5 $\pm$ 3.2	1953 $\pm$ 1104	+ 21.3 $\pm$ 2.5
PalD1-Mag1/DF-Gold/pBLuc	544 $\pm$ 11.5	+ 28.4 $\pm$ 1.5	2462 $\pm$ 154	+ 27.5 $\pm$ 3.5

\*in RPMI medium without additives

We found major differences regarding the mean hydrodynamic diameters. The average size of the magnetic transfection complexes with both transfection lipids varied from about 450 nm to almost 3300 nm. The results show a tendency of complex aggregation when suspended in medium with serum resulting in an increase of the mean hydrodynamic diameter. Li *et al.* (Li et al., 2005) found size, and not

surface charge, to be a major determinant of the *in vitro* lipofection efficiency of a TFL-3 cationic lipid composed of lipid components in a pDNA/TFL-3 complex. We found that bigger complexes yielded higher transfection efficiency than smaller complexes using magselectofection (see page 78; Figure 25).

**Table 3. Characteristics of the magnetic transfection complexes for magselectofection**

Complex	RPMI medium containing 7.3% FCS		RPMI medium without FCS					
	Mean hydrated diameter <i>D</i> (nm)	$\xi$ -Potential (mV)	Mean hydrated diameter <i>D</i> (nm)	$\xi$ -Potential (mV)	Magnetophoretic Velocity* (m/s)	Magnetic moment* <i>M</i> (A <sup>2</sup> m <sup>2</sup> )	<i>M</i> <sub>eff</sub> * (A <sup>2</sup> m <sup>2</sup> )	<i>N</i> nanoparticles / complex ( <i>M</i> / <i>m</i> <sub>eff</sub> )
PEI-Mag2/DF-Gold/pBLuc	3142	-9.6 ± 2.1	1052	+22.6 ± 1.6	2.3*10 <sup>-5</sup>	5.1*10 <sup>-14</sup>	1.2*10 <sup>-19</sup>	4.3 *10 <sup>5</sup>
PEI-Mag3/DF-Gold/pBLuc	2442	-12.1 ± 3.4	282	+18.8 ± 2.3	3.6*10 <sup>-5</sup>	2.2*10 <sup>-14</sup>	6.2*10 <sup>-20</sup>	3.4 *10 <sup>5</sup>
SO-Mag2/DF-Gold/pBLuc	1920	-8.5 ± 1.3	2108	+16.6 ± 1.0	3.4*10 <sup>-5</sup>	1.5*10 <sup>-13</sup>	4.1*10 <sup>-19</sup>	3.6 *10 <sup>5</sup>
PEI-Mag2/SM4-31/pBLuc	2768	-10 ± 1.9	450	+20.2 ± 1.6	3.2*10 <sup>-5</sup>	3.0*10 <sup>-14</sup>	1.2*10 <sup>-19</sup>	2.5 *10 <sup>5</sup>
PEI-Mag3/SM4-31/pBLuc	2112	-7.1 ± 2.7	745	+16.5 ± 2.2	2.4*10 <sup>-6</sup>	3.7*10 <sup>-15</sup>	6.2*10 <sup>-20</sup>	5.9 *10 <sup>4</sup>
SO-Mag2/SM4-31/pBLuc	3311	-17.4 ± 1.6	3000	+12.9 ± 1.4	3.4*10 <sup>-6</sup>	2.1*10 <sup>-14</sup>	4.1*10 <sup>-19</sup>	5.2 *10 <sup>4</sup>

Magnetophoretic mobility analysis was used in order to determine the magnetic moments and sedimentation velocities of the synthesized magnetic vectors. The time course of the turbidity of the magnetic lipoplexes PEI-Mag2/DF-Gold/pBLuc, plotted in Figure 8, shows that 90% of the complexes are sedimented within 13.1 min in the applied magnetic field. The magnetic field was equal to the magnetic field generated from the 96 magnetic plate used for *in vitro* transfection experiments. The derived magnetophoretic mobilities of the complexes of 1.3  $\mu\text{m s}^{-1}$  and the average hydrodynamic diameters of the complexes of 1616 nm allow one to estimate the average magnetic moment of the complexes and the number of magnetic nanoparticles associated with each complex, as shown in Figure 8.

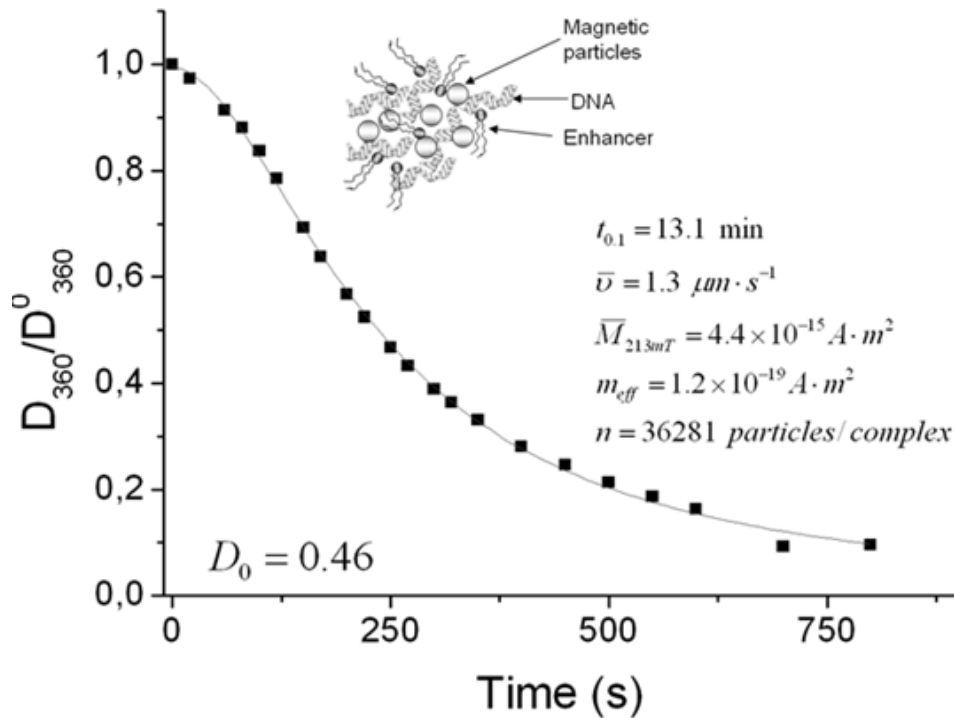


**Figure 8. Magnetophoretic mobility of selected magnetic lipoplexes.** Time course of the normalised turbidity of the magnetic lipoplexes of PEI-Mag2/DF-Gold/pBluc (iron-to-plasmid ratio of 0.5:1) upon application of a gradient magnetic field (average field and field gradient of 213 mT and 4 Tm<sup>-1</sup>) and derived magnetic responsiveness  $\bar{v}$ , average magnetic moment of the complex  $\bar{M}_{213\text{mT}}$  in the applied field and average number of magnetic nanoparticles  $n$  associated with each complex, accounting for the effective magnetic moment of the core of the insulated particle  $m_{\text{eff}}$ , as described in the Materials and Methods.

Figure 9 shows that 90% of the complexes were sedimented within 20-40 sec in the applied magnetic field, which is similar to the magnetic field created within the MidiMACS magnet used for magselectofection experiments. The derived magnetophoretic mobilities of the complexes varied between 2.3-3.6  $\mu\text{m s}^{-1}$  and the average hydrodynamic diameters of the complexes was around 300-2000 nm depending of the magnetic nanoparticle used. This allows one to estimate the average magnetic moments of the complexes and the number of magnetic nanoparticles associated with each complex, as shown in Table 3.

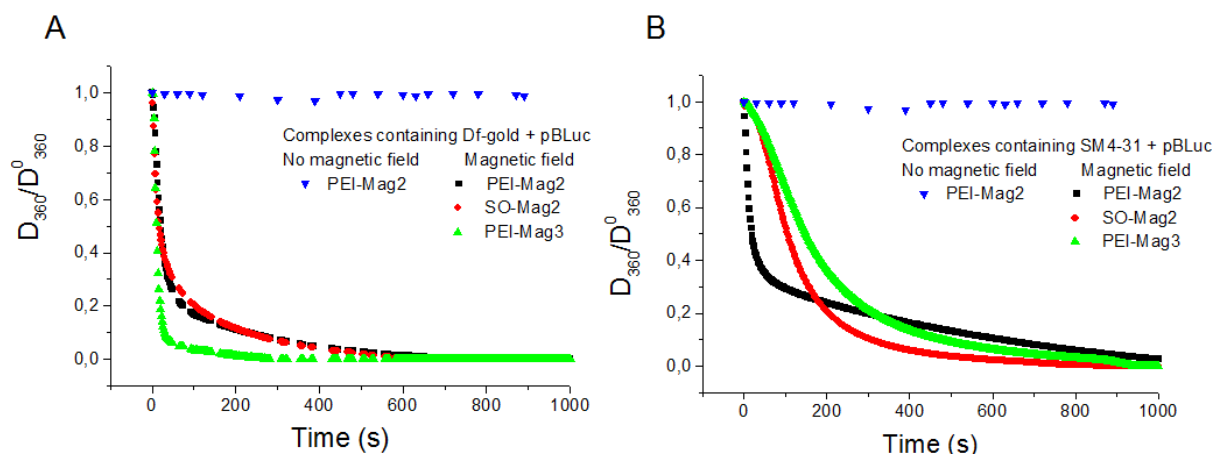


**Figure 9. Magnetophoretic mobility of selected magnetic lipoplexes.** Time course of the normalised turbidity of the magnetic lipoplexes (iron-to-plasmid ratio of 1:1) upon application of the gradient magnetic fields (average field and field gradient of 213 mT and  $4 \text{ Tm}^{-1}$ ). (A) Lipoplexes comprising DF-Gold as enhancer; (B) Lipoplexes comprising SM4-31 as enhancer.

### 3.2.3. Characteristics of viral complexes used for transfection using magnetofection

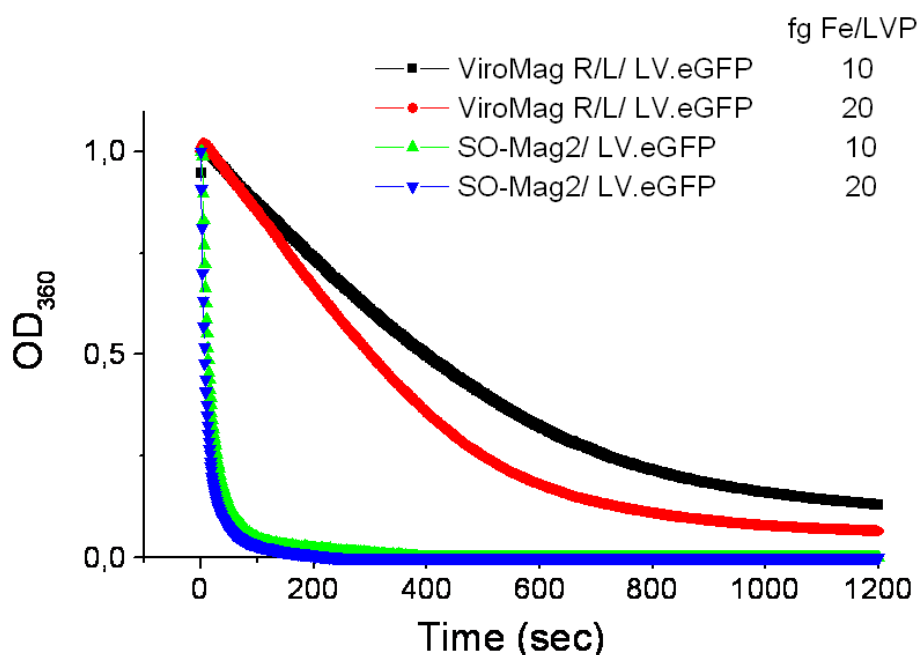
Data on the mean hydrodynamic diameters, electrokinetic potentials and magnetophoretic mobilities of viral complexes measured immediately after preparing the complex in DMEM medium with additives are given in Table 4. The average sizes of the viral complexes were between 340-400 nm for complexes comprising ViroMag nanoparticles and between 250-3100 nm the SO-Mag2/LV.eGFP complexes, indicating aggregation of these complexes. The complexes had negative net charges because they were prepared in medium with serum.

Table 4. Characteristics of the magnetic viral complexes for magselectofection

<b>Nanoparticle-to-VP ratio (fg Fe/VP)</b>	<b>Mean hydrated diameter D (nm)</b>	<b>Electrokinetic potential <math>\xi</math> (mV)</b>	<b>Magnetophoretic Mobility<sup>#</sup> (<math>\mu\text{m/s}</math>)</b>
<b>ViroMag R-L/LV.eGFP complexes</b>			
10	340 $\pm$ 94	-8.1 $\pm$ 1.6	0.8
20	396 $\pm$ 97	-10.2 $\pm$ 1.7	1.2
<b>SO-Mag2/LV.eGFP complexes</b>			
10	2368 $\pm$ 407 (65%)* 432 $\pm$ 58 (35%)	-10.6 $\pm$ 2.0	23.5
20	3090 $\pm$ 414 (53%)* 247 $\pm$ 32 (47%)	-10.1 $\pm$ 2.0	34.7

\*% intensity

The time course of the turbidity of the magnetic viral complexes plotted in Figure 10 shows that 90% of the complexes were sedimented within 20-50 sec for the SO-Mag2/LV.eGFP complexes and the magnetic moment increases with higher amounts of fg Fe/LVP. We found complexes formed using SO-Mag2 MNPs are faster magnetically sedimented than complexes comprising the commercially available ViroMag R/L particles (OZ Biosciences), indicating that the magnetic moment of SO-Mag2/LV.eGFP complexes is higher than that of ViroMag R/L/LV.eGFP complexes. An explanation could be that SO-Mag2/LV.eGFP complexes have a tendency to aggregate.



**Figure 10. Magnetic responsiveness of the viral vectors.** Time course of the normalized turbidity for the suspensions of the magnetic viral complexes SO-Mag2/LV.eGFP and ViroMag R/L / LV.eGFP prepared at 10 or 20 fg Fe/LVP and upon application of the inhomogeneous magnetic field ( $\langle B \rangle = 213$  mT and average gradient of the field of 4 T/m).

Summarizing, the analysis of the magnetophoretic mobility of the magnetic viral and non-viral complexes is a simple experimental approach that could be useful for experimental estimations of the kinetics of magnetic sedimentation of magnetic vector. The results of magnetophoretic mobility indicate that the average magnetic moment of these magnetic lipoplexes and magnetic viral complexes was high enough to fully immobilize and associate the complexes in the column after 30 min of incubation at MidiMACS magnet (see page 69; figure 19).

### 3.3. Selection of magnetic vectors for magselectofection (results from 2D transfection)

In order to find the most efficient magnetic vectors to be use for magselectofection, the transfection efficiencies of different magnetic vectors was analysed in Jurkat T cells using magnetofection in a 2D system.

### **3.3.1. Correction for the autofluorescence of the transfection reagent is needed for true percentage of eGFP-positive Jurkat T cells**

In this study, FACS analysis was used to quantify the percentage of Jurkat T cells expressing eGFP protein after transfection. The gated viable Jurkat T cells were evaluated as a dot plot displaying FL-1 (eGFP) on the X-axis (Figure 11 A). It is known that some lipid transfection reagents exhibit weak fluorescence that can be seen in both the green and red FACS channels. To correct the results for the weak fluorescence that cannot be attributed to fluorescence of eGFP, (I) untransfected cells, (II) cells transfected with duplexes of magnetic nanoparticles with luciferase plasmid or (III) with DF-Gold and (IV) those transfected with magnetic triplexes of the luciferase plasmid combined with DF-Gold and MNPs were used as references.

Figure 11 A shows that neither the untransfected cells nor the cells transfected with duplexes of the luciferase plasmid with magnetic NDTMag1/pBluc nanoparticles gave rise to fluorescence in FL1. In contrast, a high percentage of the cells transfected with luciferase plasmid lipoplexes and magnetic lipoplexes exhibited weak fluorescence (histograms for DF-Gold/pBLuc and NDT-Mag1/DF-Gold/pBLuc complexes are shown in Figure 11 A) that could reasonably be attributed to fluorescence of the lipid. Of note, the percentage of cells showing this weak fluorescence was dependent on the type of MNPs used to formulate the complex. Thus, to quantify the “true” percentage of eGFP-expressing cells, it is necessary to correct the percentage of FL1-positive cells for the weak fluorescence of the lipid, taking the cells transfected with analogous magnetic complexes formulated with the luciferase plasmid as a reference. Examples of the results are shown in Figure 11 B for non-magnetic and magnetic lipoplexes with PL-Mag1 and NDT-Mag1 nanoparticles. Comparison with the data calculated using untransfected cells as a reference (compact symbols in Figure 11 B) unambiguously leads to an overestimation of the percentage of eGFP-expressing cells.

All eGFP expression data given in this thesis were corrected for the autofluorescence of the applied lipid transfection reagent and thus represent the true percentages of eGFP-positive cells.



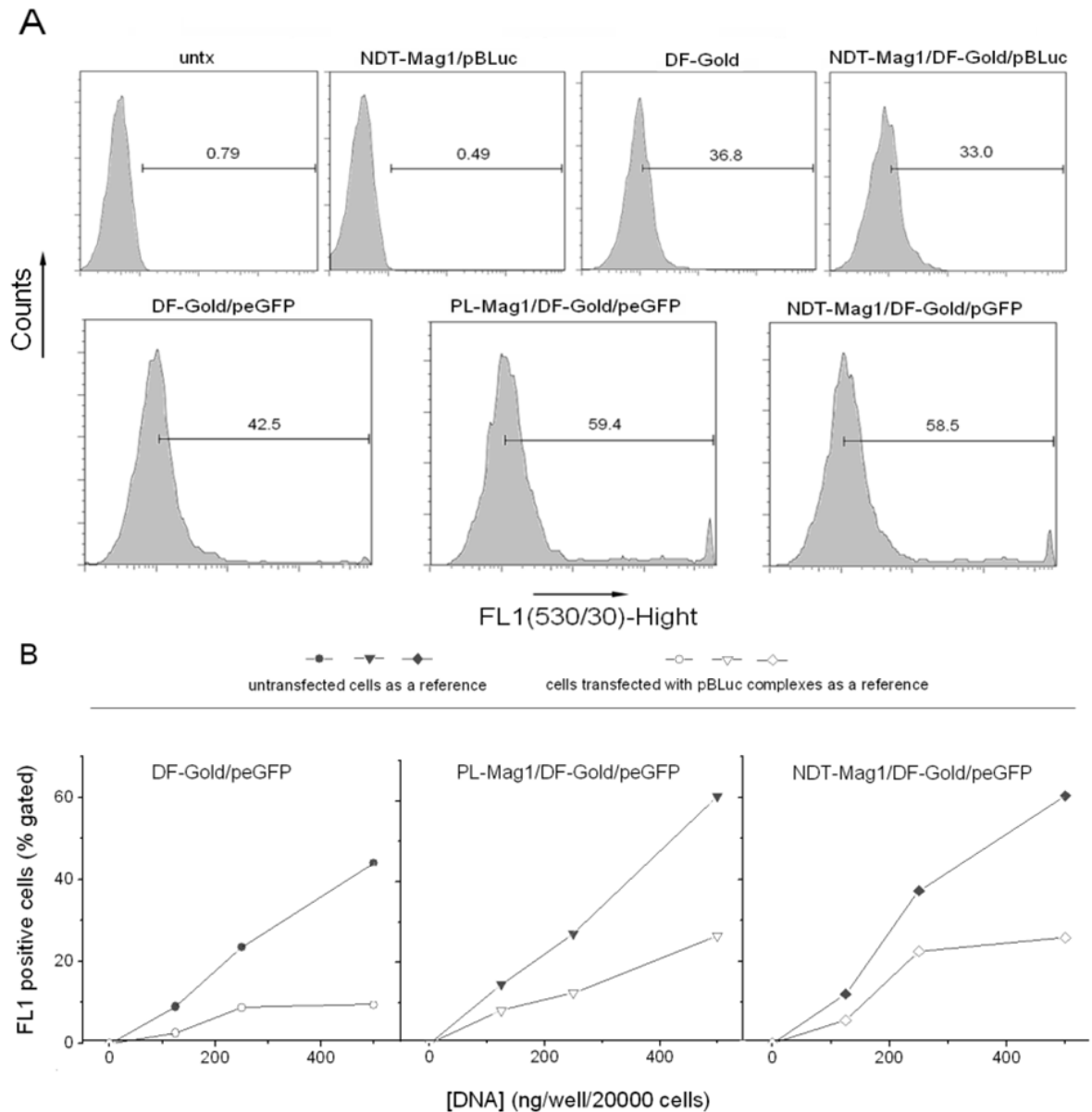


**Figure 11. Quantification of eGFP<sup>+</sup> Jurkat cells after (magneto)lipofection by flow cytometry.** (A) Histogram plots of untransfected Jurkat cells (untx); cells transfected with duplexes of NDT-Mag1/pBLuc or liposomal transfection reagent alone (DF-Gold) or lipoplexes of DF-Gold/peGFP, triplexes of NDT-Mag1/DF-Gold/pBLuc, PL-Mag1/DF-Gold/peGFP and NDT-Mag1/DF-Gold/peGFP for eGFP gene expression analysis. The DNA dose was 500 ng per 20000 cells. The percentage of the gated FL1-positive cells is shown on the histogram plots; (B) The percentage of the FL1-positive cells versus DNA dose, calculated using untransfected cells as a reference (compact symbols) and cells transfected with the corresponding luciferase plasmid triplexes as a reference (open symbols).

### 3.3.2. Magnetic lipoplexes transfect Jurkat T cells more efficiently than magnetic polyplexes

Polyplexes and lipoplexes comprising targeting molecules have previously been used to transfect Jurkat T cells (Guillem et al., 2002), (Uduehi et al., 2003), (Puls and Minchin, 1999). A maximum of 19% cells expressing the transgene was observed

using cell stimulation with phorbol 12-myristate 13-acetate (PMA) prior to transfection. We have searched for magnetic vectors to transfect Jurkat cells more efficiently without any stimulation of the cells. With this aim in mind, we compared the transfection efficiency of several complexes of the luciferase plasmid with branched polyethylenimin 25 kD at an N/P ratio of 10 ( $\text{PEI}_{\text{Br}}/\text{pBLuc}$ ), lipoplexes with Lipofectamine2000 (Lipofectamine2000/pBLuc) and DF-Gold (DF-Gold/pBLuc) and similar magnetic vectors associated with magnetic PEI-Mag2 nanoparticles at an iron-to-DNA ratio of 0.5:1 in Jurkat T cells. The results given in Figure 12 indicate that the lipoplexes formulated with DF-Gold showed significantly higher transfection efficiency in terms of the level of luciferase reporter expression, as compared to lipoplexes with Lipofectamine2000 and polyplexes with  $\text{PEI}_{\text{Br}}$  and the magnetic complexes thereof. Magnetic lipoplexes of PEI-Mag2/DF-Gold/pBLuc were significantly more efficient than non-magnetic lipoplexes of DF-Gold/pBLuc at the highest DNA concentration. For this reason, further screening of the magnetic particles and the formulation of magnetic vectors for Jurkat T cell magnetofection was performed with complexes consisting of DF-Gold as a lipid enhancer.

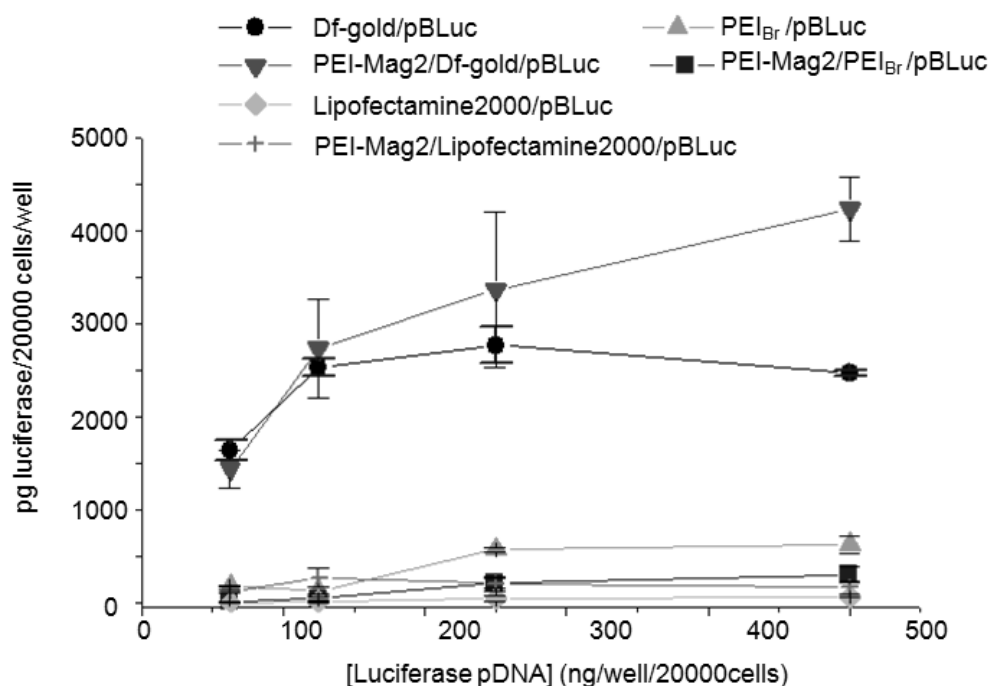


**Figure 12. Reporter gene expression in Jurkat T cells after lipo-, poly- and magnetofection using different enhancers.** Jurkat T cells were transfected using Luciferase plasmid lipoplexes with DF-Gold or Lipofectamine 2000 (enhancer-to-plasmid v/w ratio of 4), polyplexes with PEI<sub>Br</sub> (at N/P=10) or with magnetic lipo- and polyplexes comprising PEI-Mag2 magnetic nanoparticles at iron-to DNA ratio of 0.5-to-1. 48 h post-transfection luciferase activity was measured in cell lysate vs. applied plasmid doses.

### 3.3.3. Reporter gene expression in Jurkat T cells is increased by magnetofection without causing cell toxicity

To find the most efficient formulations for transfecting Jurkat T cells, we have tested DF-Gold-plasmid duplexes and magnetic triplexes consisting of pDNA, DF-Gold and the magnetic nanoparticles NDT-Mag1, PL-Mag1, PalD1-Mag1 or PEI-Mag2 or commercially available CombiMag and PolyMag nanoparticles.

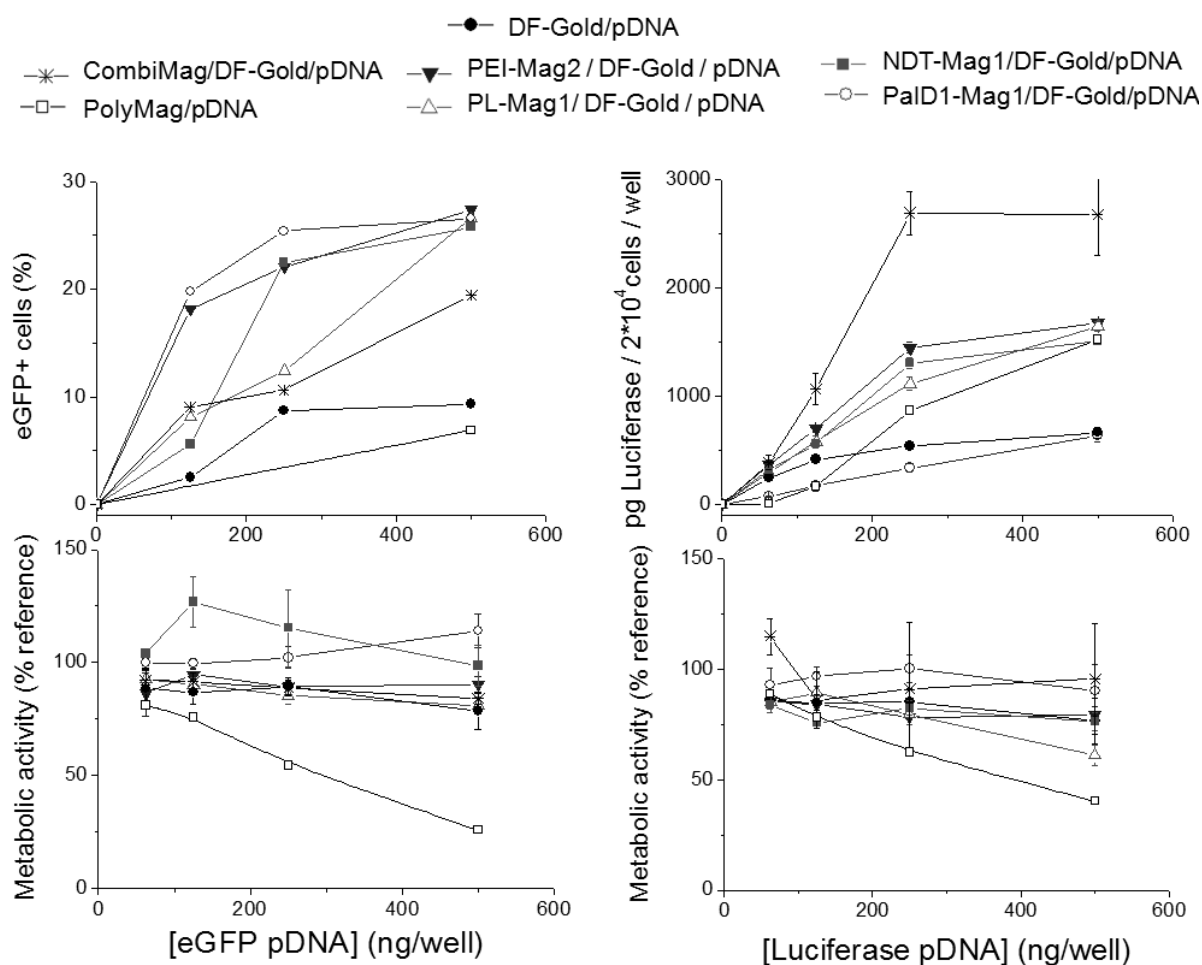


**Figure 13. Percentage of eGFP-positive cells, luciferase reporter expression and MTT-based toxicity data from Jurkat cells 48 h post-lipo- and magnetofection.** Jurkat T cells were transfected with eGFP or luciferase plasmid lipoplexes of DF-Gold/pDNA or with magnetic lipoplexes prepared with the magnetic nanoparticles NDT-Mag1, PL-Mag1, PalD1-Mag1, PEI-Mag2 or commercially available CombiMag and PolyMag, as described in the Materials and Methods. The Figures show (top panels) the percentage of eGFP<sup>+</sup> cells and luciferase expression (pg luciferase per 20000 cells) and (bottom panels) cell respiration activity versus applied plasmid concentration.

All magnetic vectors were formulated at an iron-to-plasmid w/w ratio of 0.5, which was previously found to result in high transfection efficiency with minimum toxicity (Mykhaylyk et al., 2007a), (Mykhaylyk et al., 2007b). A DF-Gold-to-DNA v/w ratio of

4:1 was used, as recommended by the manufacturer, and was also found to be the optimal ratio in our own numerous experiments.

All of the tested particles, except for PolyMag, increased the transfection efficiency in terms of the percentage of transfected cells, as compared to the DF-Gold lipoplexes (Figure 13). The vectors combined with the PalD1-Mag1, PEI-Mag2 and NDT-Mag1 particles transfected up to 27% of the cells at the highest plasmid dosage of 500 ng per 20,000 cells, followed by the PL-Mag1 and CombiMag particles. Non-magnetic DF-Gold lipoplexes transfected up to 9% of the cells. The data given in Figure 13 represent the true percentage of eGFP-positive Jurkat T cells after correction for the autofluorescence of the lipid discussed in more detail in paragraph 3.3.1. Figure 14 shows bright-field and fluorescence microscopy images of the Jurkat T cells taken 48 h post-lipofection and post-magnetofection with NDT-Nag1/DF-Gold/peGFP lipoplexes.

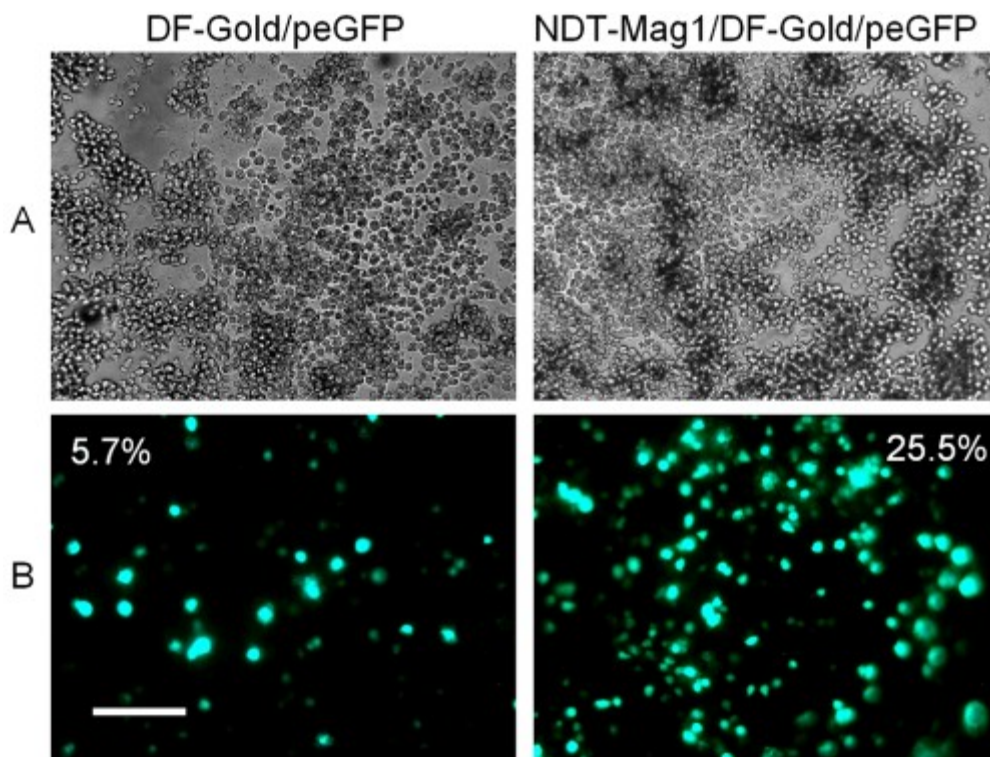


**Figure 14. Enhanced GFP (eGFP) reporter gene expression in Jurkat cells detected by microscopy.** Jurkat cells were incubated for 30 min at the magnetic plate with lipoplexes of DF-Gold/peGFP or magnetic lipoplexes of NDT-Mag1/DF-Gold/peGFP at a DNA concentration of 500 ng/20,000 cells/well and observed 48 h post-transfection with a fluorescence microscope. The Figures show (A) bright field and (B) fluorescence images taken at 490/509 nm for eGFP+ cell green fluorescence. Images were obtained at an original magnification of 10X, scale bar = 200  $\mu$ m.

In terms of luciferase reporter gene expression levels, the CombiMag nanoparticles demonstrated the highest and the PalD1 lipoplexes the lowest luciferase expression levels measured after 48 h (Figure 13). Magnetofection using the optimal vector formulations resulted in a significant (3-4.5-fold) enhancement of luciferase transfection, as compared to lipofection at high (500 ng per 20,000 cells) and low (125 ng per 20,000 cells) plasmid doses, respectively.

We also found that the cell passage number plays an important role in the transfectivity of Jurkat T cells. At a cell passage higher than 15, the transfection efficiency decreased considerably. The results shown in this work were obtained with cell passage numbers between 6 and 10.

The results shown in Figure 15 reveal lentiviral magnetofection of NIH 3T3 fibroblasts (Experiments carried out together with Arzu Cengizeroglu, M.Sc. (Cengizeroglu, 2008).

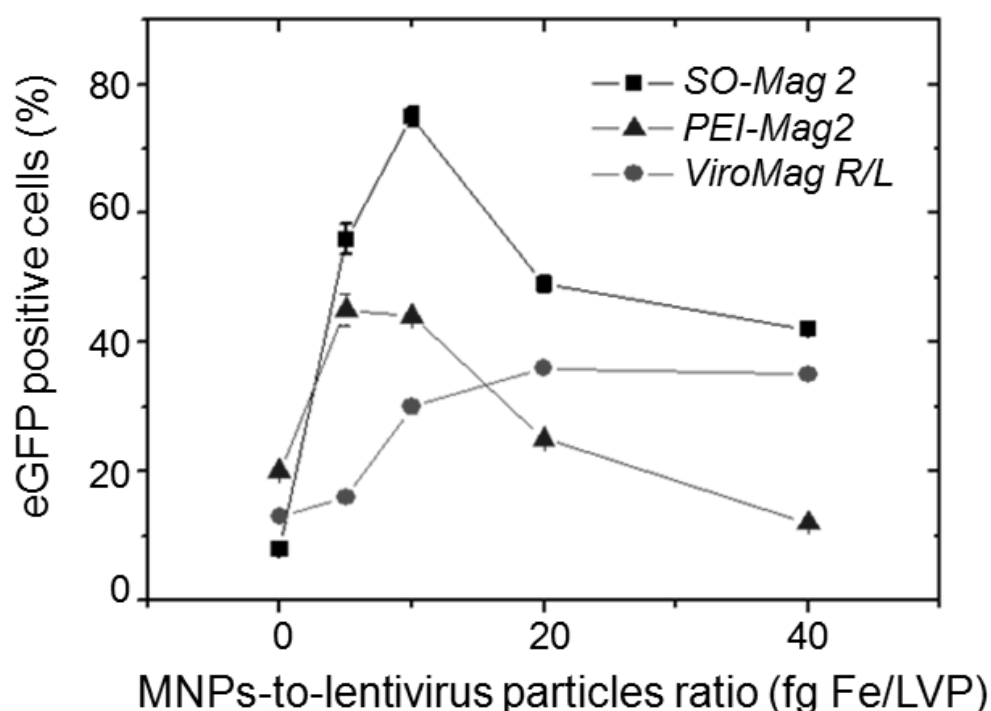


**Figure 15.** Transduction efficiency in 3T3 NIH mouse fibroblasts by magnetofection in a 2D-cell array using the complexes with SO-Mag2, PEI-Mag2 and ViroMag R/L (OZ Biosciences) MNPs. eGFP-positive 48 h after transduction by magnetofection using LV.eGFP magnetic complexes with different magnetic nanoparticles at an MOI of 2 versus the nanoparticle:virus particle ratios applied to formulate the complex.

The results of the MTT assay shown in Figure 13 suggest that there was no additional toxicity associated with the particles, as compared to the non-magnetic lipoplexes, within the tested concentration range, except for the highly toxic PolyMag complexes. Triplexes containing the eGFP plasmid were less toxic than those with the pCMV-Luc plasmid. MTT assay of the selected SO-Mag2/LV.eGFP viral complex resulted in no toxicity neither in Jurkat T cells, hPBMCs nor hUC-MSCs (for more information, see Master thesis of Arzu Cengizeroglu (Cengizeroglu, 2008)).

Summarizing, the magnetic lipoplexes with PEI-Mag2, NDT-Mag1 and PL-Mag1 MNPs and magnetic viral complexes with SO-Mag2 MNPs resulted in a high percentage of cells transfected with the eGFP plasmid as well as high luciferase reporter gene expression without toxicity.

#### **3.3.4. Transfection efficiency of Jurkat T cells is not increased by combination of magnetofection with glycerol or DMSO shocks**

Some compounds that destabilise cell membranes, such as glycerol, have been reported to increase the transfection efficiency of ligand-coupled polyplexes in different cell lines as well as in some primary human fibroblasts under specific conditions (Zauner et al., 1996). We have tested whether treatment with 0.9 M glycerol for 4 h, resulting in a 100-fold increase in luciferase expression in H225 human melanoma cells (Zauner et al., 1996), can further increase the magnetofection efficiency achieved in Jurkat T cells using magnetic lipoplexes comprising PEI-Mag2 nanoparticles. The data given in Figure 16 demonstrate a dramatic (about 4.5-fold) decrease in the luciferase reporter expression post-magnetofection with PEI-Mag2 lipoplexes with cationic lipid DF-Gold under glycerol shock. These data are in agreement with the findings of Zauner et al., who observed no positive effect of glycerol shock on the transfection efficiency with the lipid transfection reagent DOTAP or the cationic lipopolyamine Transfectam<sup>®</sup> (Zauner et al., 1996).

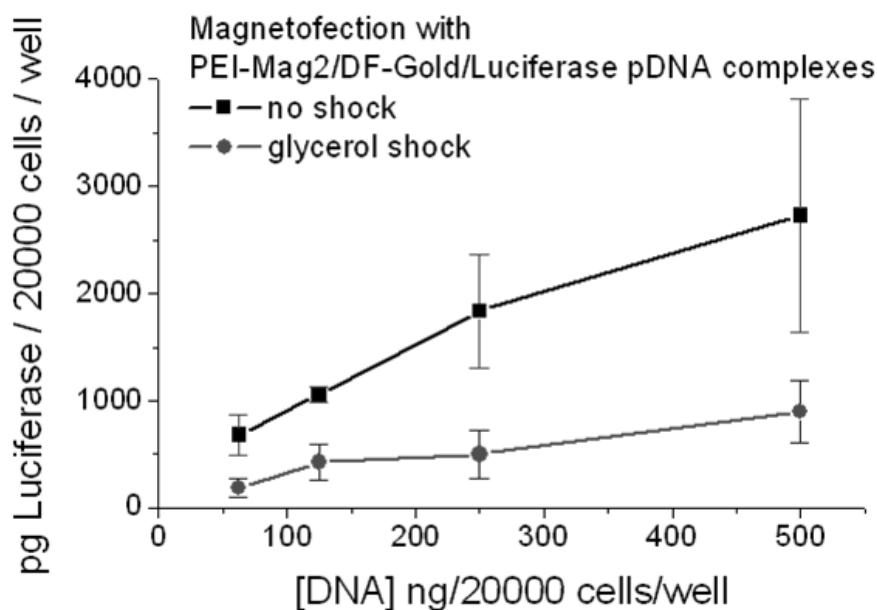


**Figure 16. Effect of glycerol shock on luciferase gene expression in Jurkat T cells post-magnetofection.** Cells were transfected with PEI-Mag2/DF-Gold/pBLuc magnetic triplexes at different plasmid concentrations. After incubation with transfection complexes at a magnetic plate for 30 min, the cells were centrifuged, the medium was replaced with complete RPMI containing 0.9 M glycerol and incubated for 4 h, the cells were washed with PBS and further incubated in complete RPMI media for 48 h, and gene expression analysis was performed.

In a study by Lopata et al. (Lopata et al., 1984), mouse L cells were first transfected with DEAE-dextran polyplexes of the reporter gene followed by a short, 2-min shock with 10% DMSO 4-20 h after transfection (Lopata et al., 1984). This treatment resulted in a 50-fold improvement of transgene expression. We have tested the effect of a 2-min shock with 0.5% DMSO on luciferase expression post-magnetofection with the magnetic PEI-Mag2 lipoplexes. The treatment resulted in high toxicity, and no luciferase expression was observed.

### 3.3.5. Magnetic lipoplexes are better internalized in Jurkat T cells upon gradient magnetic field application, as compared to non-magnetic lipoplexes

In order to examine the mechanisms behind the observed improvement in Jurkat T cell transfection using magnetofection, cell association and internalization into Jurkat T cells were quantified using the approach of Ogris et al. (Ogris et al., 2000) described in detail in Materials and Methods. Figure 17 A shows a superposition of the phase contrast, green fluorescence (490/509 nm) from the internalized complexes and red/yellow fluorescence (510/650 nm) from the complexes associated with the cell membrane. Almost 100% of the cells were associated with the

---

transfection complexes and few of them have also internalized pDNA 5 h after magnetofection. An example of the FACS data for NDT-Mag1/DF-Gold/pBLuc/YOYO-1 magnetic lipoplexes is shown in Figure 17 B. The data given in Figure 17 C for two magnetic lipoplexes formulated with the NDT-Mag1 and PL-Mag1 magnetic nanoparticles show that 100% of the Jurkat T cells were associated with both non-magnetic and magnetic lipoplexes. However, the magnetic lipoplexes were internalized into the cells 1.5-fold more efficiently, as compared to the non-magnetic lipoplexes.

Thus, the observed improvement in transfection efficiency for magnetofection, as compared to lipofection of the Jurkat T cells, can be partially attributed, but not limited to, the increase in internalization of the selected magnetic lipoplexes under magnetofection conditions, as compared to non-magnetic lipoplexes.



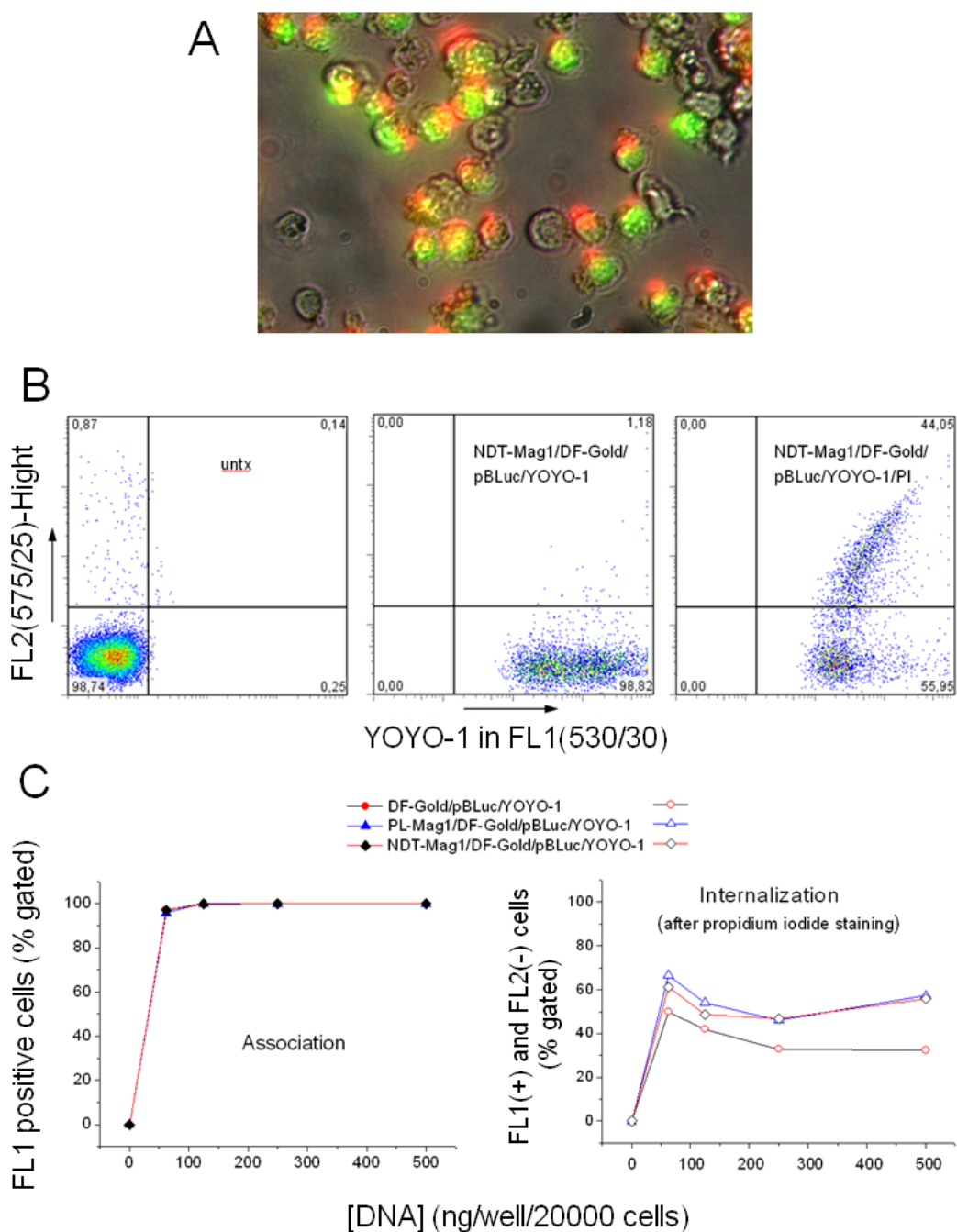


**Figure 17. Association/internalization of lipoplexes in Jurkat T cells characterised by microscopy and flow cytometry.** Jurkat T cells were transfected in a 96-well plate with luciferase plasmid complexes labelled with the cell-impermeable intercalating nucleic acid stain YOYO-1 iodide. For vector internalization analysis, cells were additionally incubated with propidium iodide (PI) at a final concentration of 1  $\mu\text{g/ml}$  to quench the complexes associated with the cells but not those internalized into cells (A) Five hours post-transfection with NDT-Mag1/DF-Gold/pBLuc/YOYO-1 complexes, the cells were incubated with PI. The image shows a superposition of the phase contrast, green fluorescence from the internalized complexes measured at a wavelength of 490/509 nm and red and yellow fluorescence from the complexes associated with cell membranes measured at a wavelength of 510/650 nm. (B) Forty-eight hours post-transfection, the cells were washed with PBS and resuspended in 1% FCS in PBS. Cell association and internalization of complexes was analysed using a FACS Vantage microflow cytometer. The Figure shows density plots of untransfected Jurkat cells (untx), cells transfected with magnetic triplexes of NDT-Mag1/DF-Gold/pBLuc/YOYO-1 at a plasmid dose of 500 ng per well and those incubated with propidium iodide at a final PI concentration of 1  $\mu\text{g/ml}$  to stain the complexes of NDT-Mag1/DF-Gold/pBLuc/YOYO-1/PI associated with the cells but not internalized. (C) Percentage of YOYO-1-positive Jurkat cells (*Association*) and of Jurkat cells that have internalized complexes (*Internalization*) for lipoplexes of Df-Gold/pBLuc/YOYO-1 and magnetic triplexes containing PL-Mag1 and NDT-Mag1 magnetic nanoparticles are plotted against the applied DNA concentration, respectively.

### **3.4. Establishing magselectofection**

Establishing the system described herein involved characterizing vector retention and elution, characterizing the association/internalization of the vector with target cells, analyzing of the cell separation efficiency with the Jurkat/K562 model mixture and the efficiency of gene delivery in Jurkat T cells or mixtures of Jurkat T and K562 erythroleukemic cells or primary and stem cells. Finally optimization of vector loading onto columns and cell loading onto modified column was analyzed.

#### **3.4.1. Reversible immobilization of transfection complexes and association with the cells at the Miltenyi® column**

To test whether magnetic transfection complexes can be immobilized and associated with the cells after magselectofection, LS Miltenyi® columns were prepared following the two protocols (standard or freeze-drying protocol) described in *Material and methods* using a radioactively <sup>125</sup>I labelled plasmid.

Miltenyi cell separation columns are filled with iron beads. We assumed that these might quench radiation and thus give rise to false results when quantifying radioactive material immobilized on the column. In fact we obtained a linear calibration curve when measuring equal amounts of radiolabeled complexes in aqueous suspension in Eppendorf tubes versus those immobilized on the column. The quenching factor was 13.6 (Figure 18).

Upon magnetoselectofection procedure, the cells to be separated and transfected were given to the magnetized modified column and incubated for 30 min to achieve association of the cells with magnetic vector. After that, the columns were removed from the magnetic field and the cells were eluted using so-called pressure enforced elution according to Miltenyi® protocol.

The results show that the retention of vectors on the columns and their association with cells is dependent on the protocol followed to prepare the vector loaded LS separation columns.

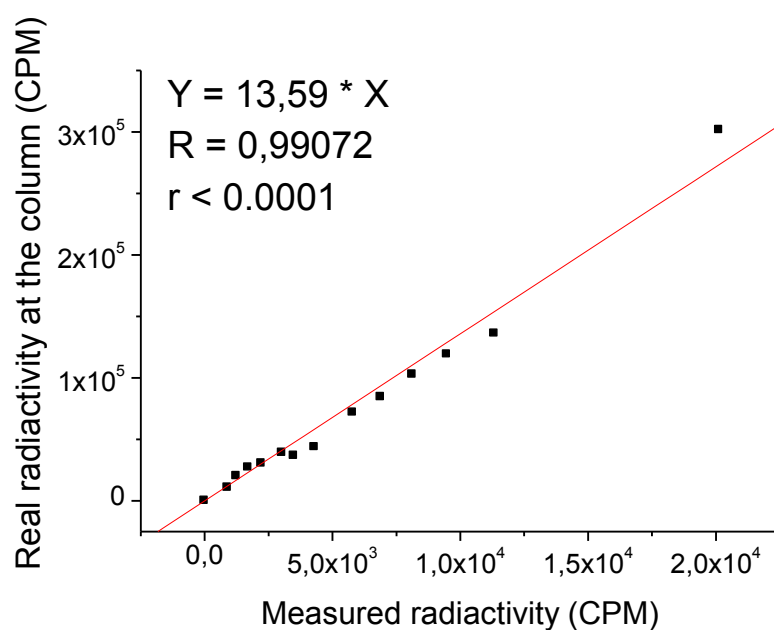
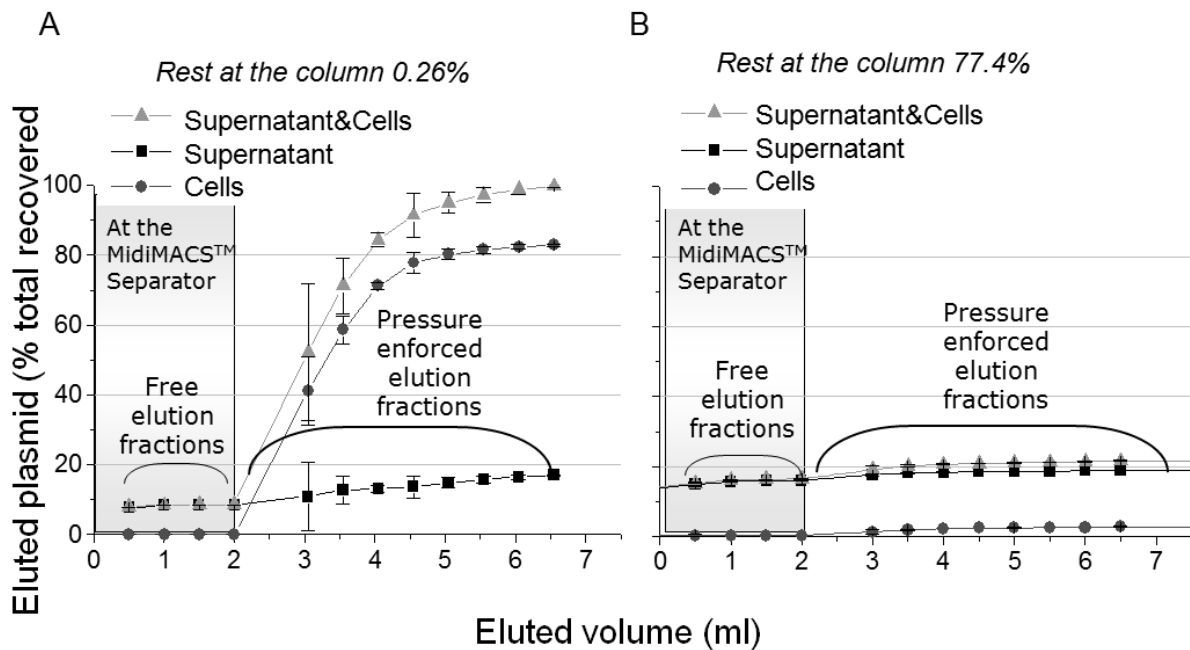


Figure 18. Real  $^{125}\text{I}$  radioactivity immobilized at the column versus measured radioactivity.

Figures 19 A and B show that when the column was placed at the MidiMACS magnet about 10% of plasmid was eluted for both, fresh (standard) and freeze-drying (lyophilized) columns. In parallel to this experiment, we measured the binding efficiency between DNA and magnetic particles and the results showed that approximately 90% of DNA was bound with the PEI-Mag2 magnetic particles (data shown in Figure 7 and paragraph 3.2.2) meaning that the eluted pDNA is non-magnetically labelled pDNA. The amount of eluted plasmid was increased when the column was removed from the MidiMACS™ Separator and washed using pressure enforced procedure. Using freshly prepared columns (Figure 19 A), about 83% of the eluted plasmid was associated with the cells and 16.95% of the eluted plasmid was found in supernatants. The total plasmid recovery was 99.74% indicating that the immobilization of the complex in the column was reversible. In contrast, using the lyophilised columns (Figure 19 B) only about a 10% of the plasmid was associated with the cells. Only 25% of the total applied plasmid was recovered from the column and a 75% of the plasmid remained on the column, indicating that the immobilization of the complex in the column was not reversible using the applied lyophilization procedure. Hence, protocols without lyophilisation appeared more appropriate for subsequent experiments.



**Figure 19. Immobilization of magnetic transfection complexes on the Miltenyi column and association of the complexes with the target cells after the magselectofection procedure. A** Magnetic transfection complex (PEI-Mag2/DF-Gold/125I-pBLuc) containing 20  $\mu\text{g}$  plasmid labelled with 125I isotope was loaded to the column. The column was placed into the MidiMACS<sup>TM</sup> Separator and Jurkat T-cells magnetically labelled with CD45 Microbeads were loaded onto the column in 4 portions of 0.5 ml RPMI media each and *free elution fractions* were collected. After 30 minutes incubation the column was removed from the Separator and the retained cells were flush out by firmly applying the plunger supplied with the column using 8 portions of 0.5 ml RPMI media each (*Pressure enforced elution fractions*). The fractions were centrifuged and the radioactivity was measured in supernatants and in the pellets to recalculate the DNA fractions associated with the cells, unbound DNA in supernatants and the total DNA recovered from the column (Supernatant&Cells). (A) Columns were prepared following the Standard procedure; (B) Columns were prepared following the Freeze-drying procedure.

To explain why the magnetic transfection complexes and magnetically labeled cells are retained in the columns upon magnetic field application, the stability and magnetically induced velocity of both, magnetic transfection complexes and magnetic cells were measured.

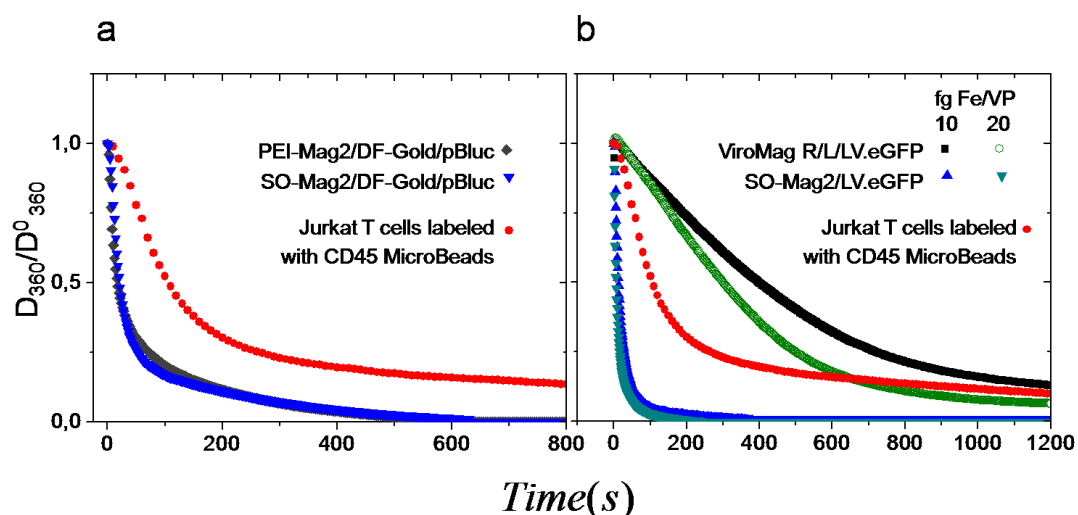


**Figure 20. Magnetic responsiveness of magnetic viral vectors and Jurkat T-cells labeled with CD45 magnetic beads.** Time course of the normalized turbidity for the suspensions of the magnetic viral complexes and magnetically labelled Jurkat T-cells with CD45 Microbeads upon application of the inhomogeneous magnetic field ( $\langle B \rangle = 213$  mT and average gradient of the field of 4 T/m).

We observed that magnetic lipoplexes and magnetic lentiviral complexes comprising in-house synthesized MNPs display higher magnetophoretic mobility than target cells labelled with Miltenyi microbeads (Figure 20). We also found that magnetic lentiviral complexes comprising the commercial MNPs have lower magnetophoretic mobility than the magnetically labeled cells.

### 3.4.2. Efficient association and internalization of magnetic lipoplexes in Jurkat T cells after magselectofection

In order to examine whether the complexes that have been associated with the cells can be also internalized, cell association and internalization into Jurkat T cells were quantified using the approach of Ogris et al. (Ogris et al., 2000), as described before. Figure 21 C shows a superposition of the phase contrast, green fluorescence from the internalized pDNA complexes measured at a wavelength of 490/509 nm and red and yellow fluorescence from the complexes associated with the cell membrane measured at a wavelength of 510/650 nm 5 h post-magselectofection. We can see that almost 100% of the cells were associated with the transfection complexes and that some of them have also internalized pDNA at this time point. An example of the FACS data for PEI-Mag2/DF-Gold/pBLuc/YOYO-1 magnetic lipoplexes is shown in Figure 21A. The data given in Figure 21 B show that 100% of the Jurkat T cells were associated with magnetic lipoplexes and approximately 15% of the cells have

internalized the transfection complexes just after 30 min incubation time at the MidiMACS separator. Time course experiments show that the percentage of the cells associated with the transfection complexes was maintained during the time, while the percentage of the cells that have internalized the transfection complexes was increased. Up to 50% of the cells had internalized the magnetic complexes by 48 h after magselectofection. The major fraction (40-45%) had been taken up within 6 h.

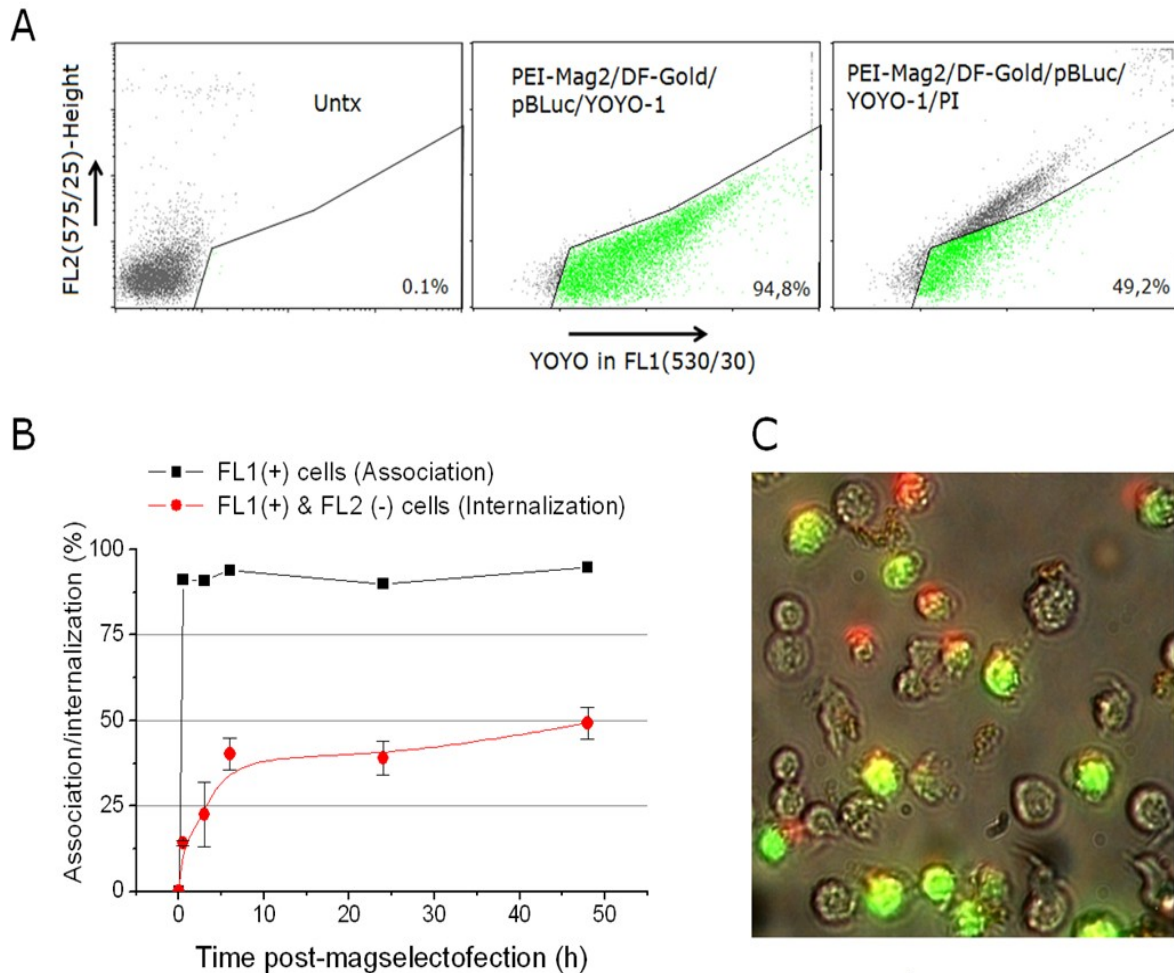


**Figure 21. Percentage of the Jurkat T cells that are associated with or have internalized DNA post magselectofection characterized by flow cytometry.** Jurkat T cells were transfected using magselectofection procedure with PEI-Mag2/DF-Gold/pBLuc complexes labelled with the cell-impermeable intercalating nucleic acid stain YOYO-1 iodide (DNA association). For vector internalization analysis, cells were additionally incubated with propidium iodide (PI) at a final concentration of 1  $\mu\text{g/ml}$  to quench the complexes associated with the cells but not those internalized into cells (PEI-Mag2/DF-Gold/pBLuc/YOYO-1/PI). (A) Density plots of untransfected Jurkat T cells (untx) and cells transfected with the magnetic triplexes (PEI-Mag2/DF-Gold/pBLuc-YOYO-1). (B) Percentage of YOYO-1 positive Jurkat T cells (*Association*) and of Jurkat T cells have internalized complexes (*Internalization*) versus time post-magselectofection. (C) Superposition of phase contrast, green fluorescence from the internalized pDNA complexes measured at a wavelength of 490/509 and red and yellow fluorescence from the complexes associated with cell membrane measured at a wavelength of 510/650 nm 24 hours after magselectofection with PEI-Mag2/DF-Gold/pBLuc-YOYO-1 complexes and after staining with PI.

### **3.4.3. Modification of the LS column yields gene delivery specific to the target cell population without compromising the cell separation efficiency**

Magnetic cell separation efficiency can be influenced by a number of variables such as the quality of the cell preparation and the frequency of the target cell population in the sample. To increase the purity of target cells, especially in the case of cells present at low frequencies such as hematopoietic stem cells, the magnetically isolated fraction can be further enriched by passing the cells over a second separation column. Therefore we first decided to assess the effectiveness of magselectofection in a model system using a 2 column separation strategy. For this purpose we labeled magnetically CD2<sup>+</sup>/CD3<sup>+</sup> Jurkat T cells using CD2 MicroBeads and mixed the magnetically labeled cells with non-magnetically labeled CD2<sup>-</sup>/CD3<sup>-</sup> K562 cells. We separated the cells using one unmodified LS column, and carried out magselectofection of the positively-selected cells using the second LS column, which was modified either with magnetic lipoplexes SO-Mag2/DF-Gold/pDNA or with magnetic lentiviral complexes SO-Mag2/LV.eGFP. As a reference procedure, we used the standard two column magnetic cell separation protocol from Miltenyi by passing the cells through two unmodified LS columns (MACS). We analyzed the purity of the positively-selected cells (CD2<sup>+</sup>/CD3<sup>+</sup>) using CD3-PE Ab treatment. We expected that the magnetically-retained cells would be close to 100% CD3<sup>+</sup> (i.e., Jurkat T cells) and that the cells that were not retained in the column would be 100% CD3<sup>-</sup> (i.e., K562 cells). FACS analysis showed that 97±1.7% and 96±0.4% of the CD3<sup>+</sup> Jurkat T cells were positively selected after standard MACS (Figure 22 A) and non-viral magselectofection (Figure 22 B), respectively. A similarly high separation efficiency of CD3<sup>+</sup> Jurkat T cells was observed after viral magselectofection (see Figures 23 A and B). The results clearly suggest that the cell separation efficiency was not disturbed by modification of the Miltenyi<sup>®</sup> LS column with the non-viral or viral magnetic complexes.



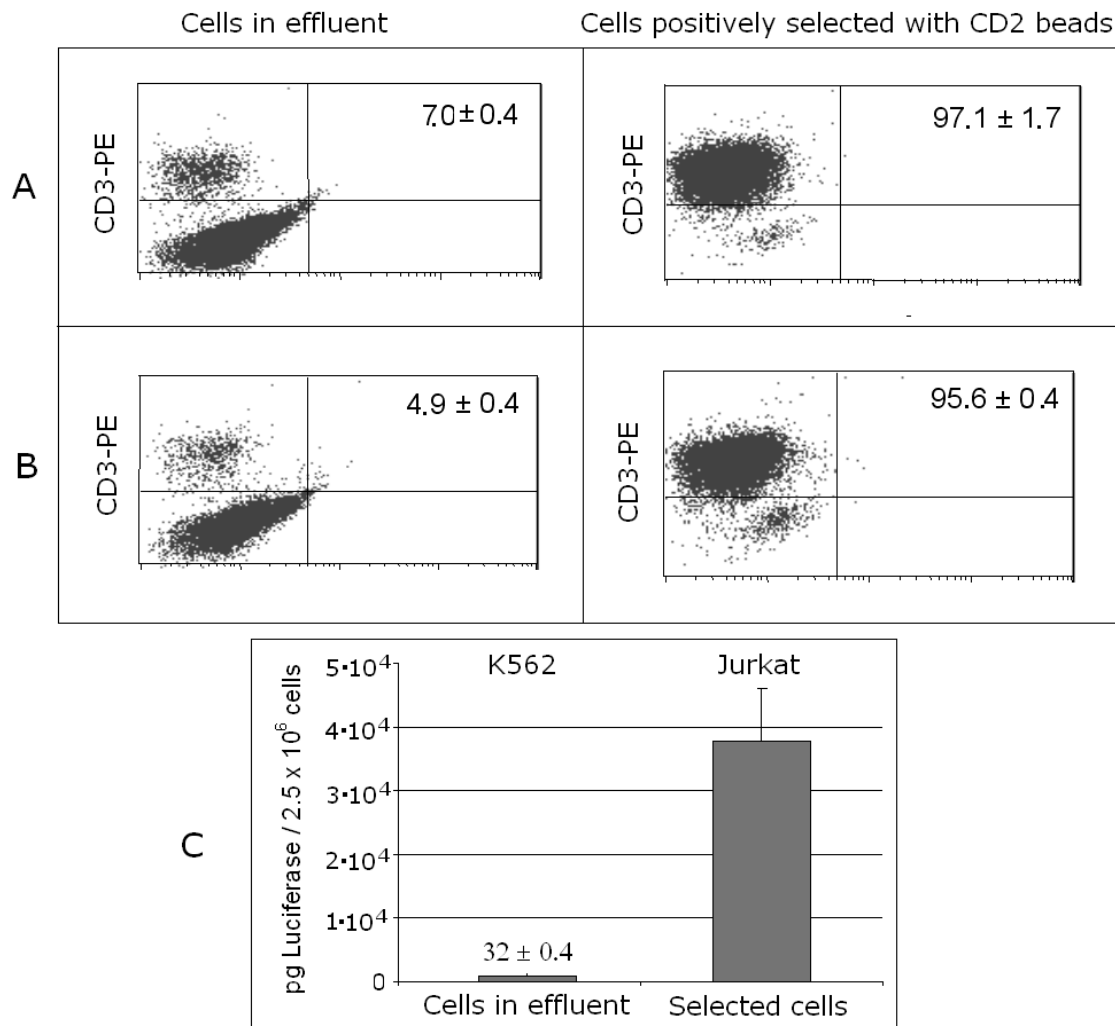


**Figure 22. Cell separation efficiency and specific transfection of the Jurkat T-cell using non-viral magselectofection.** A mixture of the  $2.5 \times 10^6$  Jurkat T cells and  $2.5 \times 10^6$  K562 cells was treated with CD2 microbeads and passed (A) sequentially through two LS columns (MACS procedure) or (B) through one LS column followed by magselectofection at the second LS column modified with PEI-Mag2/DF-Gold/pBLuc magnetic lipoplexes. CD2<sup>-</sup> cell fraction in effluent (K562 cells) and the CD2<sup>+</sup> cells positively selected at the column (Jurkat T cells) were treated with CD3-PE antibody and analyzed for percentage of the CD3-PE positive cells by FACS analysis. (C) Luciferase expression in effluent (CD3<sup>-</sup>/CD2<sup>-</sup> cells) and in cell fraction magnetically selected with CD2 beads (CD3<sup>+</sup>/CD2<sup>+</sup> cells).

We also analyzed the specificity of magselectofection for the target cell population (Jurkat T cells) in a mixture with non-labeled K562 cells. Forty-eight hours post-magselectofection, a high level of luciferase expression was found in the positively-selected cell fraction of the target Jurkat T cells. This compared to negligible luciferase expression in the eluate containing the non-target K562 cells (Figure 22C). Magselectofection of Jurkat T cells with magnetic lipoplexes of the plasmid coding for eGFP resulted in  $25.5 \pm 3.9$  % eGFP<sup>+</sup> cells measured by FACS. After lentiviral magselectofection, we detected up to 50% eGFP positive cells in the positively-



selected fraction (Jurkat T cells) compared to a very low percentage (0.2%) of the transduced cells in the eluate containing predominantly non-target K562 cells (Figure 23D). The data clearly demonstrate that gene delivery using both the viral and non-viral magselectofection procedures is specific for the target cell line.

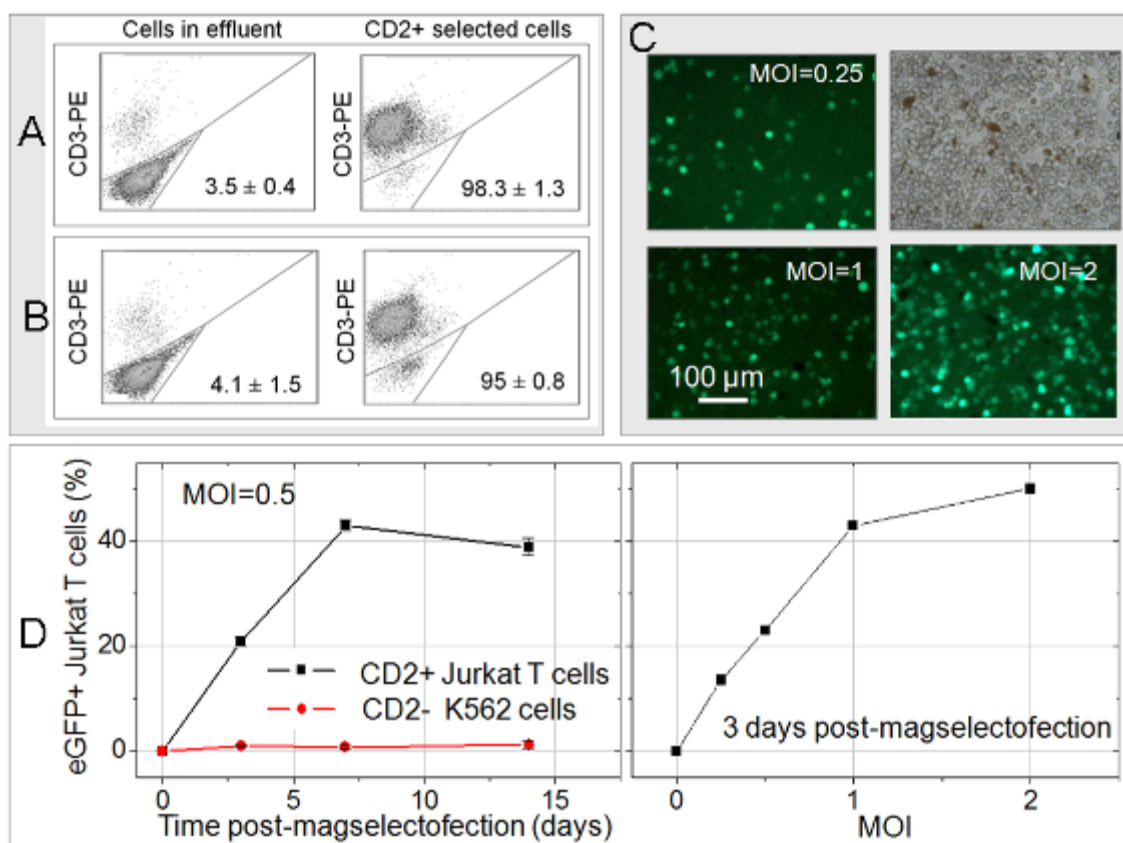


**Figure 23. Cell separation efficiency and specific transfection of the Jurkat T-cell using viral magselectofection.** A mixture of the  $10^6$  Jurkat T cells and  $10^6$  K562 cells was treated with CD2 microbeads and passed (A) sequentially through two LS columns (MACS procedure) and (B) through one LS column followed by magselectofection at the second LS column modified with SO-Mag6-5/LV.eGFP magnetic lentivirus complexes. The CD2<sup>-</sup> cell fraction in effluent (K562 cells) and the CD2<sup>+</sup> cells positively selected at the column (Jurkat T cells) were treated with CD3-PE antibody and analyzed for percentage of the CD3-PE positive cells by FACS analysis. (C) bright field and fluorescence (490/509 nm) microscopy of the Jurkat T cells at day 3 post-magselectofection using with SO-Mag2/LV.eGFP magnetic lentivirus complexes at different MOI. (D) eGFP positive cells at different time points post-magselectofection transduced using MOI of 0.5 (left graph) or at different MOI 3 days post-magselectofection (right graph).

#### 3.4.4. Optimal parameters for the magselectofection procedure yielding the highest transfection efficiency

A series of experiments were performed in order to optimize the efficiency of the magselectofection procedure. Target gene expression 48 h after magselectofection

---

of Jurkat T cells was determined depending on the applied plasmid DNA dosage, the number of cells applied per LS column and the time of the column exposure at the MidiMACS magnet (Figures 24 A-C). We found that at cell loading of  $10^7$  cells per column, a complex loading equivalent to 20  $\mu$ g plasmid per LS column resulted in high luciferase expression and viability of transfected cells (Figure 24 A). We have learned that incubation of the magnetically labelled cells at the modified column at the magnet for 30-60 min was enough to achieve maximum cell association with transfection complexes and gene expression, while a further increase of the incubation time until 90 min resulted in a more than two-fold decrease in reporter gene expression (Figure 24 B). We loaded  $2.5 \times 10^6$  or  $5 \times 10^6$  cells per LS column and tested magselectofection efficiency for the case we applied the cells to the modified column (Complex first) or for the case the cells were loaded to the column positioned at the MidiMACS magnet followed by loading the magnetic transfection complex (Cells first). We discovered that for both cell densities, the modification of the column prior to cell loading results in higher transfection efficiency. Hence, this sequence of magselectofection was adopted (Figure 24 D). We also found that the optimal cell density that yielded the highest luciferase activity was  $2.5 \times 10^6$  Jurkat T cells per column (Figures 24 C and D). Transfection efficiency was higher using the standard protocol for column preparation than using the freeze-drying protocol (Figure 24 E). The explanation for this result is that the association efficiency of transfection complexes with the cells is higher using the standard protocol for column preparation (see Figure 19).

Hence, the standard protocol for column modification loading first the complexes comprising 20  $\mu$ g plasmid and then between  $1-2.5 \times 10^6$  cells and 30 min incubation time at the magnet turned out most appropriate for subsequent experiments.

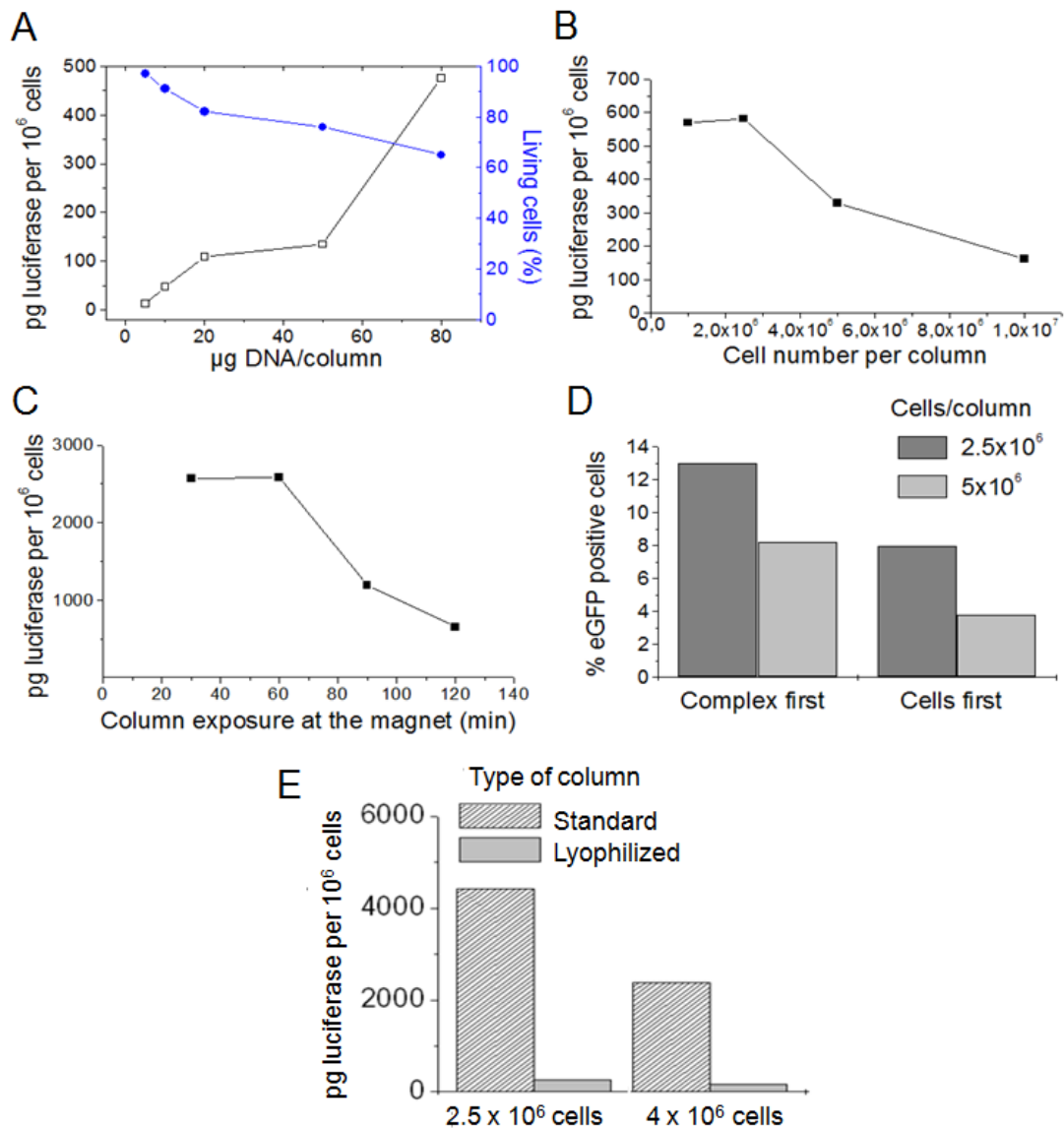


**Figure 24. Optimization of magselectofection procedure in Jurkat T cells.** (A) Luciferase expression (open squares) and cell viability evaluated using Trypan-blue based test (blue circles) versus plasmid DNA dosage per column at cell loading of 107 cells per column. (B) Luciferase expression versus column exposure time at the MidiMACS magnet at DNA dosage of 20 µg and cell loading of 2.5x10<sup>6</sup> cells per column. (C) Relative Luciferase expression versus cell loading per column at DNA dosage of 20 µg per column using as a reference value the expression at 2.5x10<sup>6</sup> cells per column. (D) percentage of the eGFP positive cells post-magselectofection at 2.5x10<sup>6</sup> and 5x10<sup>6</sup> cells per column loaded into the column modified with magnetic transfection complexes (Complex first) or cell loaded to the column followed by loading the magnetic transfection complexes to the column (Cells first). (E) Luciferase expression at 2.5x10<sup>6</sup> and 4 x10<sup>6</sup> cells loaded to the column modified with magnetic transfection complexes just prior magselectofection (Standard) or column modified with magnetic transfection complexes and lyophilized as described in Materials and Methods. Gene expression analysis was performed 48 h post-magselectofection. Magnetic transfection complexes PEI-Mag2/DF-Gold/pBLuc ((A-C,E) ) and (D) SO-Mag2/DF-Gold/pBLuc were prepared at iron-to-DNA (wt/wt) ratio of 1-to-1 and DF-Gold-to-DNA (v/wt) ratio of 4-to-1.

### **3.4.5. Magselectofection results in high transfection efficiency in Jurkat T cells.**

For screening magnetic vector compositions, magnetic lipoplexes were prepared with the commercial reagents Dreamfect-gold, SM4-31 and Ecotransfect. A magnetic polyplex was prepared with PEI-transferrin. All magnetic vectors were formulated at an iron-to-plasmid w/w ratio of 1. A lipid v/w ratio of 4:1 was used as recommended by the manufacturer.

Transfection with magnetic complexes comprising PEI-transferrin or Ecotransfect resulted in no genetically modified Jurkat T cells.

FACS analysis was used to quantify the percentage of Jurkat T cells expressing eGFP protein. A correction for the background of the lipidic transfection reagent was carried out as described in paragraph 3.3.1 (see also Figure 11). Up to 30% of positive transfected Jurkat T cells (Figure 25 A) were obtained upon transfection with complexes comprising SO-Mag2/DF-Gold/eGFP.

In terms of luciferase gene expression, the highest transfection efficiency was achieved with SO-Mag2/DF-Gold/eGFP or SO-Mag2/SM4-31/eGFP magnetic complexes (Figure 25 B). Therefore, we decided that SO-Mag2/DF-Gold/eGFP or SO-Mag2/SM4-31/eGFP transfection complexes will be used for the further transfection experiments.

We evaluated the uptake of magnetic complexes into cells in order to determine whether uptake alone accounts for transfection efficiency. Uptake was quantified using radioactive labelled DNA. Data showed in Figure 25 C indicates that no significant differences in uptake were found for the three tested magnetic complexes (PEI-Mag2/DF-Gold/eGFP, PEI-Mag3/DF-Gold/eGFP and SO-Mag2/DF-Gold/eGFP). Hence, uptake alone does not account for the observed differences.

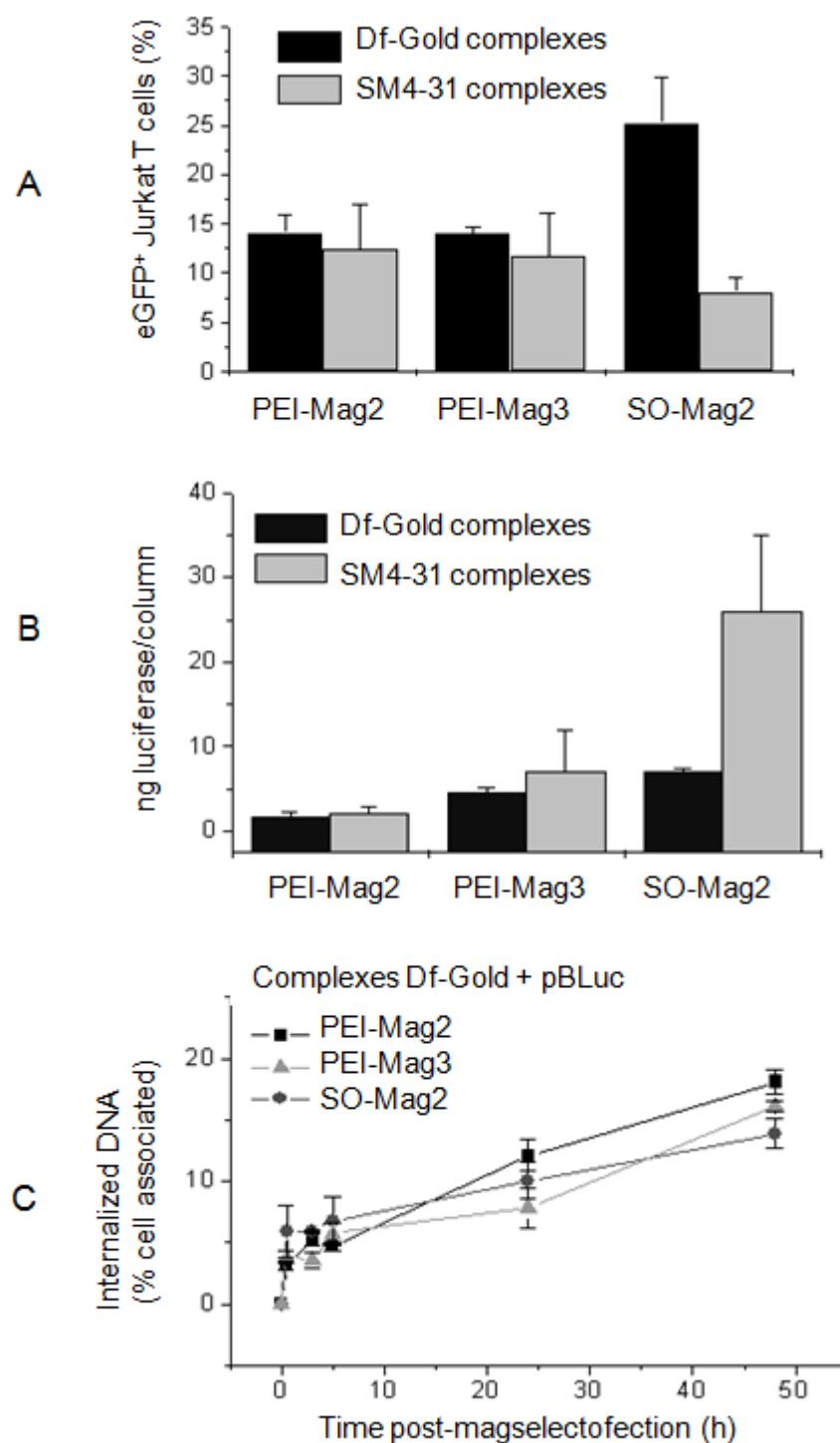


**Figure 25. Reporter gene expression and kinetics of DNA internalization in Jurkat T cells post-magselectofection.** Jurkat cells were transfected with magnetic triplexes comprising magnetic nanoparticles PEI-Mag2, PEI-Mag3 or SO-Mag2 and DF-Gold or SM4-31 lipids as enhancers and pBLuc. The Figures show (A) percentage of GFP+ Jurkat T cells according to microscopy analysis and (B) luciferase expression (pg luciferase/column/ $2 \times 10^6$  cells) 48 h post magselectofection and (C) kinetics of DNA internalization post-magselectofection with selected magnetic complexes.

### **3.5. *Magselectofection of therapeutically relevant cells***

Once the magselectofection procedure was established in Jurkat T cells we were interested to validate the technology in cells with therapeutically relevant U-MSCs, hCB-HSCs and PBMCs.

#### **3.5.1. Human umbilical cord mesenchymal stem cells (hUC-MSCs)**

Magselectofection of hUC-MSCs was performed using SO-Mag2/DF-Gold/peGFP magnetic lipoplexes and the percentage of hUC-MSCs expressing eGFP was analyzed by FACS at 3-18 days post-magselectofection. Figure 26 A indicate that about 30% of the cells expressed the eGFP reporter 3-7 days after non-viral magselectofection (see also Figure 26 B). This was followed by a decrease in the percentage of the eGFP-positive cells to 9% and 6% at days 11 and 18, respectively. We also tested the potential of the transfected hUC-MSCs to differentiate into osteoblasts when cultured in osteogenic differentiation media. Alizarin red staining performed 20 days post-magselectofection and after 18 days (see Figure 26 C) indicate that the stimulated cells differentiated into osteoblasts. Furthermore, the differentiation capacity of both the stimulated magselectofected cells and the stimulated untreated cells (Untx) was comparable (Figure 26 C, right and left images, respectively).

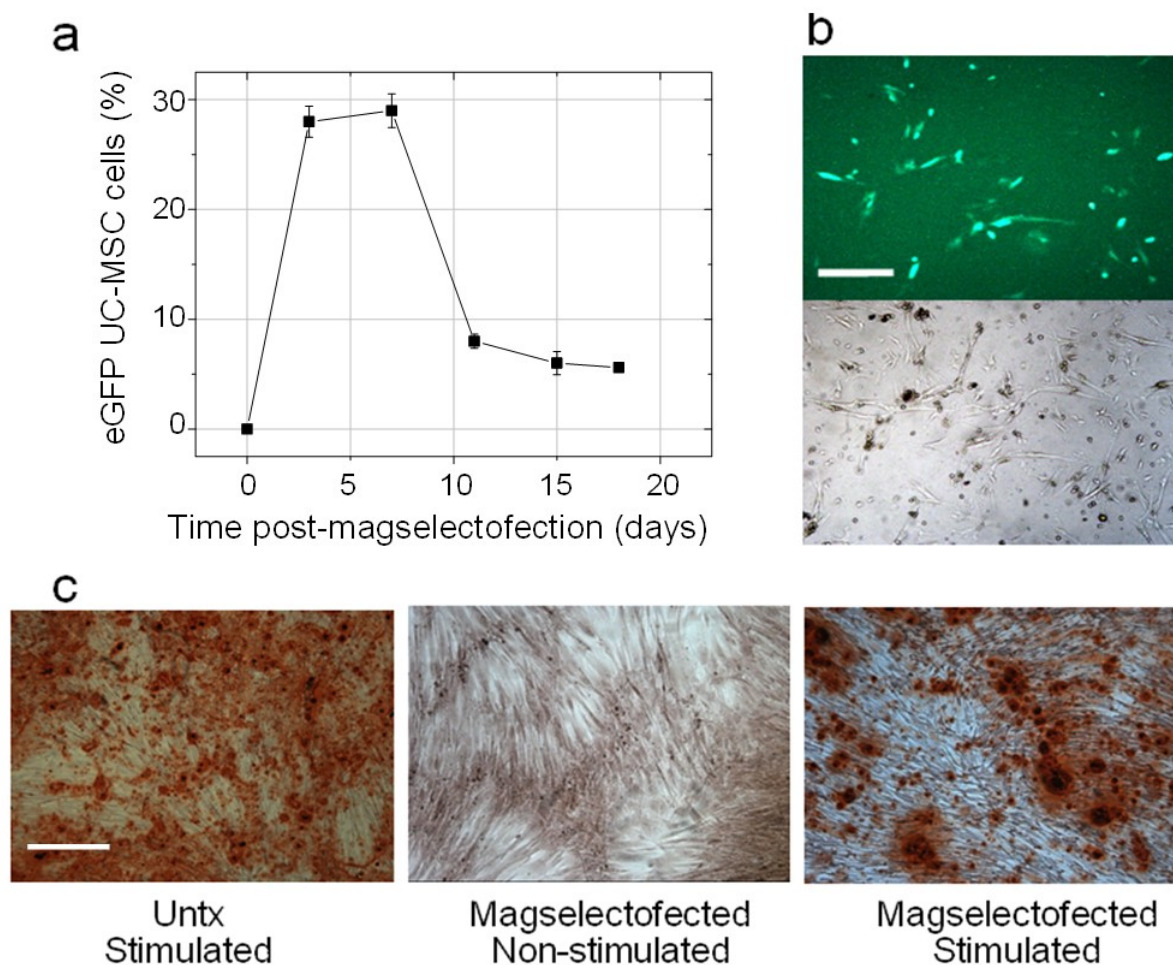


**Figure 26. eGFP reporter gene expression and differentiation potential of hUC-MSCs post non-viral magselectofection.**  $2.5 \times 10^6$  hUC-MSCs were labelled using CD105 microbeads and transfected with magnetic lipoplexes SO-Mag2/DF-Gold/eGFP. 2 days post-magselectofection the cells were stimulated using an osteogenic medium and 18 days post-stimulation the cells were analysed using alizarin red staining. (a) FACS data on the percentage of the eGFP positive cells at different time points post-magselectofection. (b) Bright field and fluorescence (490/509 nm) microscopy images of hUC-MSCs 7 days post-magselectofection; bar=500  $\mu$ m. (c) Microscopy images of the untreated (untx) stimulated hUC-MSCs and non-stimulated and stimulated hUC-MSCs 20 days post-magselectofection; bar=200  $\mu$ m.

Additionally, the results indicated that approximately 100%, 75-80% and 60% of magselectofected hUC-MSCs were expressing the stem cell marker CD105 at 3, 7 and 15 days post magselectofection, respectively (Table 5).



**Table 5. FACS data on eGFP+ CD105+ hUC-MSCs.**

Days post-magselectofection	eGFP + hUC-MSC		CD105+ hUC-MSCs	
	Mean	SD	Mean	SD
3	26,3	0,4	99,4	0,2
7	28,8	1,5	71,7	1,2
15	7,6	0,7	57,3	5,9

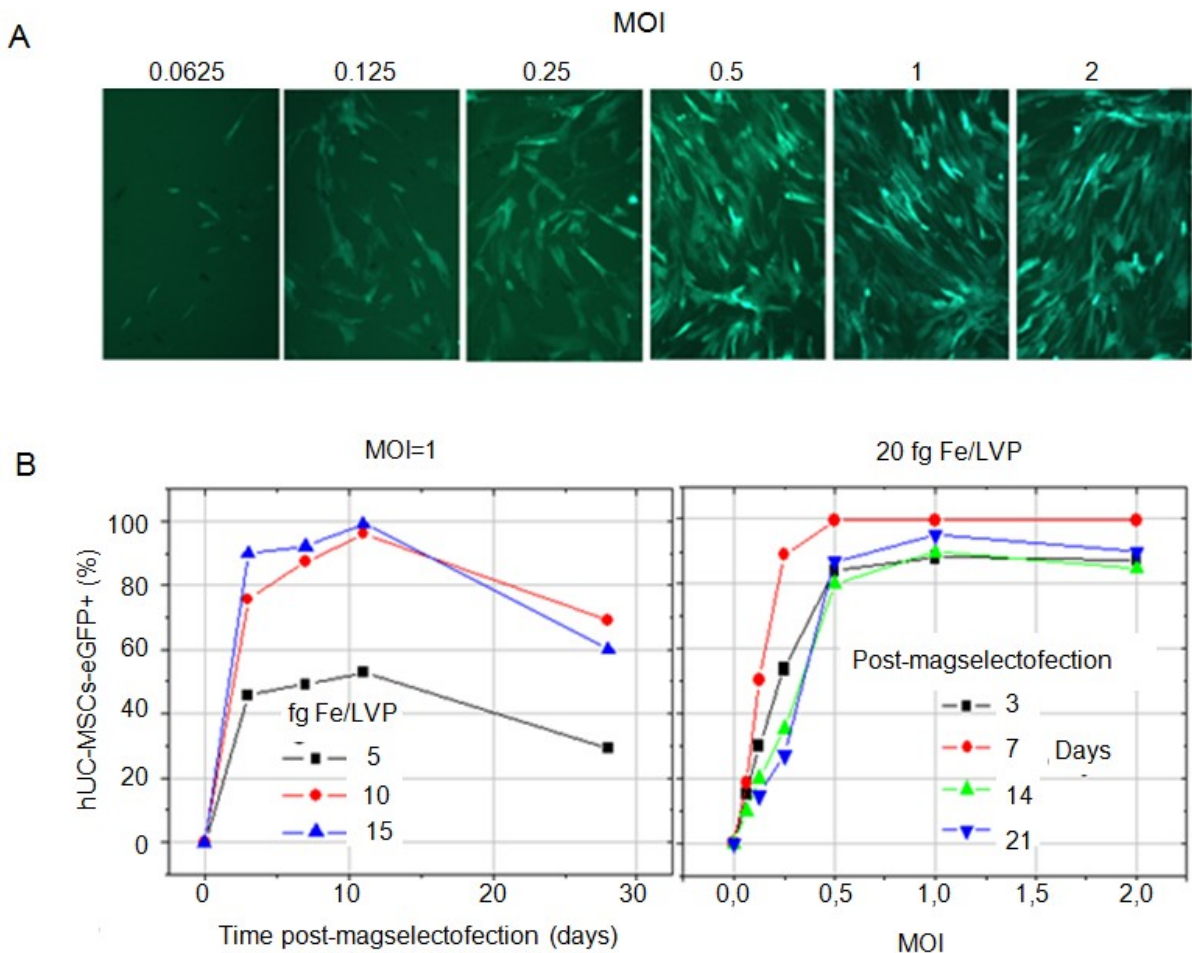


**Figure 27. eGFP reporter gene expression and differentiation potential of hUC-MSCs post viral magselectofection.**  $10^6$  hUC-MSCs were labelled using CD105 microbeads and transduced with viral magnetic complexes SO-Mag2/LV.eGFP. 2 days post-magselectofection the cells were stimulated using an osteogenic medium and 18 days post-stimulation cells were analysed using alizarin red staining. (a) Fluorescence microscopy (490/509 nm) images of hUC-MSCs 7 days post-magselectofection with different MOI at 20 fg Fe/LVP. (b) FACS data on the percentage of eGFP positive hUC-MSCs: (left graph) versus time post-transduction at different iron-to-lentivirus particles ratio in terms of fg Fe/VP with MOI of 1 and (right graph) versus MOI using the ratio of 20 fg Fe/VP.



We transduced the hUC-MSCs by magselectofection using complexes of lentiviral particles with magnetic SO-Mag2 nanoparticles at low MOIs and at different magnetic particle:virus particle ratios. The FACS results and microscopy data shown in Figure 27 reveal up to 100% of eGFP-positive hUC-MSCs 7 days post-magselectofection at MOIs of 0.5 to 2 TU/cell using the complexes formulated at 20 fg Fe/VP. We found that maximum transduction efficiency was achieved using the complexes formulated at 10 and 20 fg Fe/VP (Figure 27 B). Follow-up testing during the 21 days after magselectofection showed that the high percentage of eGFP-positive cells was maintained.

The differentiation of the cells into osteocytes was undisturbed (See Figure 28), as for non-viral magselectofection, and was comparable to stimulated untreated cells (Figure 26 C, Untx).

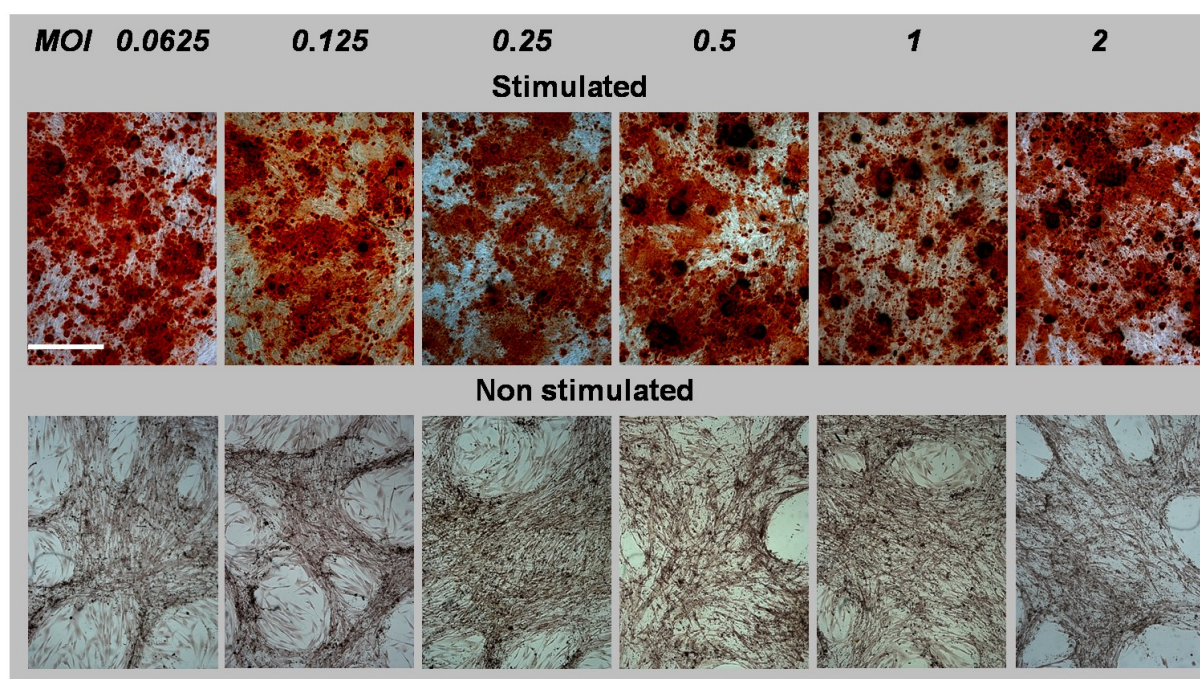


**Figure 28. Differentiation potential of hUC-MSCs post viral magselectofection.** Bright field microscopy images of magselectofected stimulated (differentiated) (up) and non-stimulated (down) hUC-MSCs 20 days post-magselectofection with different MOI at 20 fg Fe/LVP. Bar=200  $\mu$ m.

### 3.5.2. Human cord blood hematopoietic stem cells (hCB-HSCs)

Cells were isolated and cultured in Dulbecco's medium supplemented with 50 ng/mL Flt3, 100 ng/mL TPO and 100 ng/mL SCF for 48 h prior magselectofection. Then, magselectofection was carried out using transfection complexes comprising SO-Mag5-6/Df-Gold/peGFP. Fluorescence microscopy (Figure 29 A) shows that hCB-HSCs were transfected at low percentage. FACS analysis showed that approximately 1% of the hCB-HSCs expressed the eGFP reporter gene 48 h post-magselectofection.

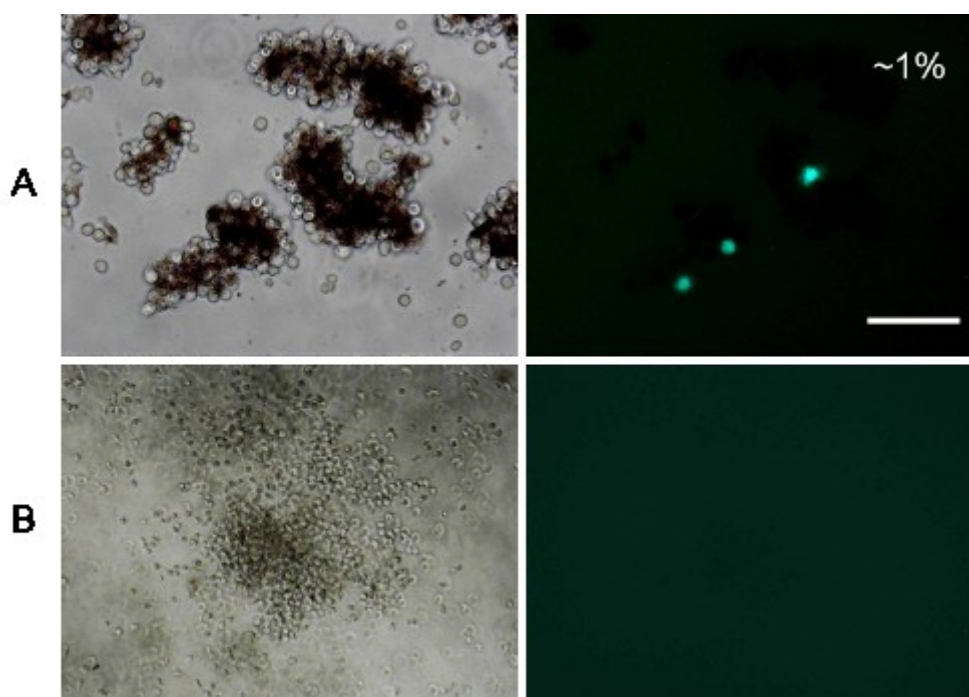


**Figure 29. Quantification of eGFP positive and differentiation potential of hCB-HSCs post viral magselectofection.**  $10^6$  hCB-HSCs were labelled using CD34 microbeads and transfected with viral magnetic complexes SO-Mag6-5/DF-Gold/eGFP. Just post-magselectofection,  $2 \times 10^3$  hCB-HSCs were seeded in a well from a 24-well plate with methylcellulose-based culture media and colonies were counted 6 days post-magselectofection. (a) fluorescence microscopy of transfected hCB-HSCs at 24h days post-magselectofection; (b) brightfield and fluorescence field (490/509 nm) microscopy images magselectofected differentiated hCB-HSCs at 6 days post-magselectofection. Scale bar equals 100  $\mu\text{m}$ .

Colony-forming cell (CFC) assays were performed just post-magselectofection in a well-defined methylcellulose-based culture medium. Figure 29 B shows that the CB-HSCs were differentiated into CFU-GM, BFU-E and CFU-GEMM 6 days post-magselectofection, but the colonies did not express the reporter gene (eGFP). There are two possible explanations for this result: 1) the eGFP positive transfected cells

are losing the potential to differentiate into cell progenitors; 2) the genetic modification is not stable and the expression of the eGFP is lost. This is indeed the case, as was observed with magselectofected hCB-HSCs that were not subjected to the CFC assay.

Efficient gene delivery to hUC-HSCs and Sca-1+ Lin- mouse cells was achieved using lentiviral magselectofection, and the differentiation potential of the transduced cells was undisturbed. We treated the CBMC Ficoll gradient fraction from human UC blood with CD34+ MicroBeads, passed the cells through two LS columns and collected positively-selected human umbilical cord blood HSCs. We further transduced the collected cells by magselectofection. We also performed a standard infection of the cells as a reference procedure.

The cells were not stimulated (cultivated) before magselectofection or standard infection procedures. Forty-eight hours post-magselectofection, we observed approximately 22% and 6.5 % of eGFP<sup>+</sup> hCB-HSCs with complexes formulated at 2 and 20 fg Fe/VP, respectively (see the microscopy data and FACS shown in Figures 30 a and c). No eGFP<sup>+</sup> hCB-HSCs were found post-standard infection carried out at the low cell density of  $1.5 \times 10^5$  cells/ml.

We found that magselectofection of the Sca-1+ Lin- mouse cells at an MOI of 3 and complexes formulated at optimal MNP-to-VP ratio of 2 fg Fe/LVP resulted in a 45% transduction rate (Figures 30 d and e) 6 days post-magselectofection.

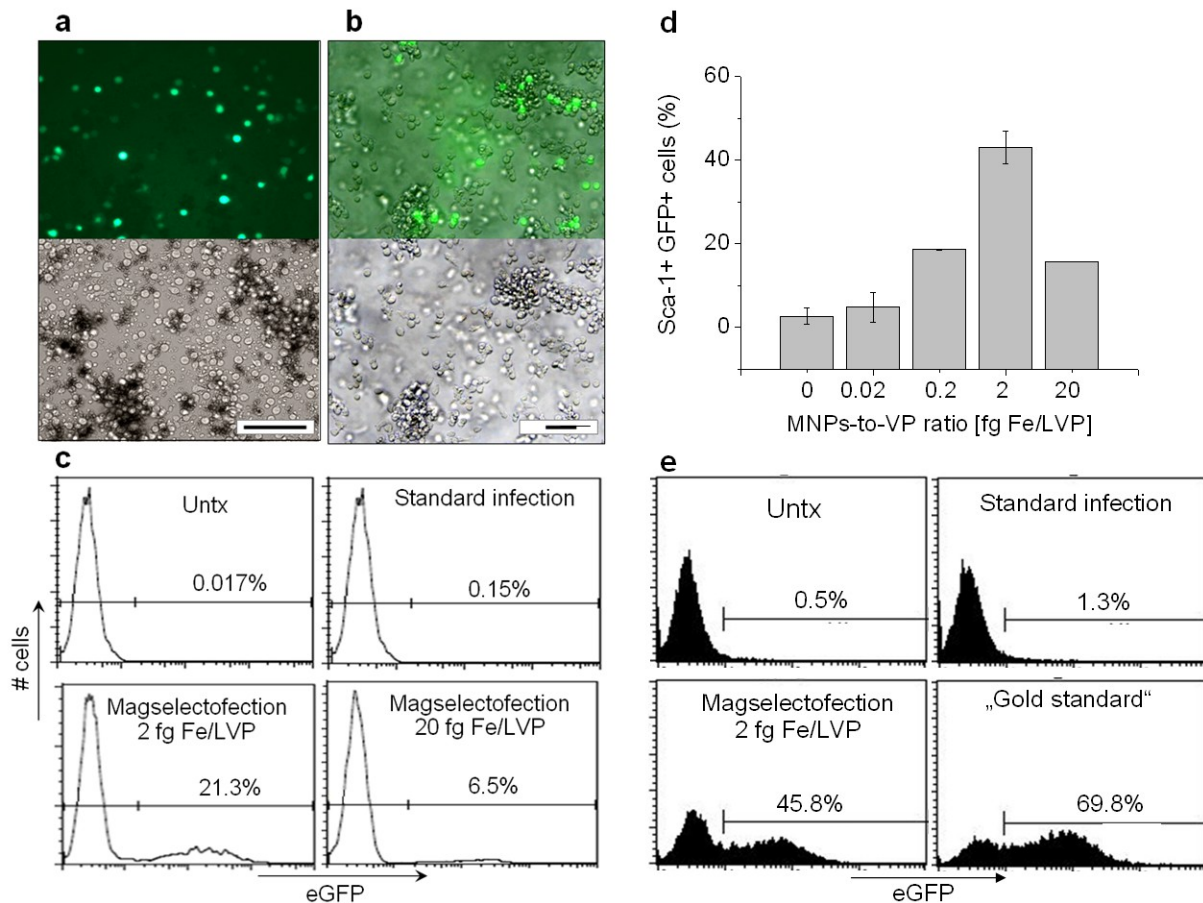


**Figure 30. Transduction efficiency of hCB-HSCs and Sca-1+ Lin- mouse cells, and the differentiation potential of the hCB-HSCs after lentiviral magelectofection.** hCB-HSCs were transduced at low cell density of  $1.5 \times 10^5$  cells/ml without cell stimulation before magelectofection. (a) Fluorescence (490/509 nm) and bright field microscopy images of the hCB-HSCs taken on day 3 after magelectofection with the magnetic complexes formulated at 2 fg Fe/VP. (b) (top) Overlay of the bright field and fluorescence (490/509 nm) microscopy images and (bottom) the bright field microscopy image of hCB-HSCs differentiated using a colony-forming assay taken 6 days after magelectofection with the magnetic complexes formulated at 20 fg Fe/VP. The bars represent 100  $\mu$ m. (c) Histogram plots of the untreated hCB-HSCs (untx), cells transduced using the standard infection protocol or viral magelectofection with the complexes formulated at 2 or 20 fg Fe/VP. Sca-1+ Lin- mouse cells were transduced at a cell density of  $5 \times 10^6$  cells/ml without cell stimulation before magelectofection. (d) Magelectofection efficiency of the Sca-1+ Lin- mouse cells versus MNP-to-VP ratio. (e) Histogram plots of the untreated Sca-1+ Lin- mouse cells (untx), cells transduced using the standard infection protocol or viral magelectofection with the complexes formulated at 2 fg Fe/VP or “Gold standard” infection (overnight incubation with non-magnetic lentivirus).

The results of the colony-forming assay for hUC-HSCs six days after magelectofection (shown in Figure 30 b) suggest that the cells were differentiated into multiple lineages and that the colonies expressed the reporter gene (i.e., eGFP). This indicates that the genetically-modified cells did not lose the capacity to differentiate into multiple lineages.



Moreover, we also found that the purity and recovery of the Sca-1+ selected cells after magselectofection were equal to those obtained after the standard MACS procedure (see Figure 31).

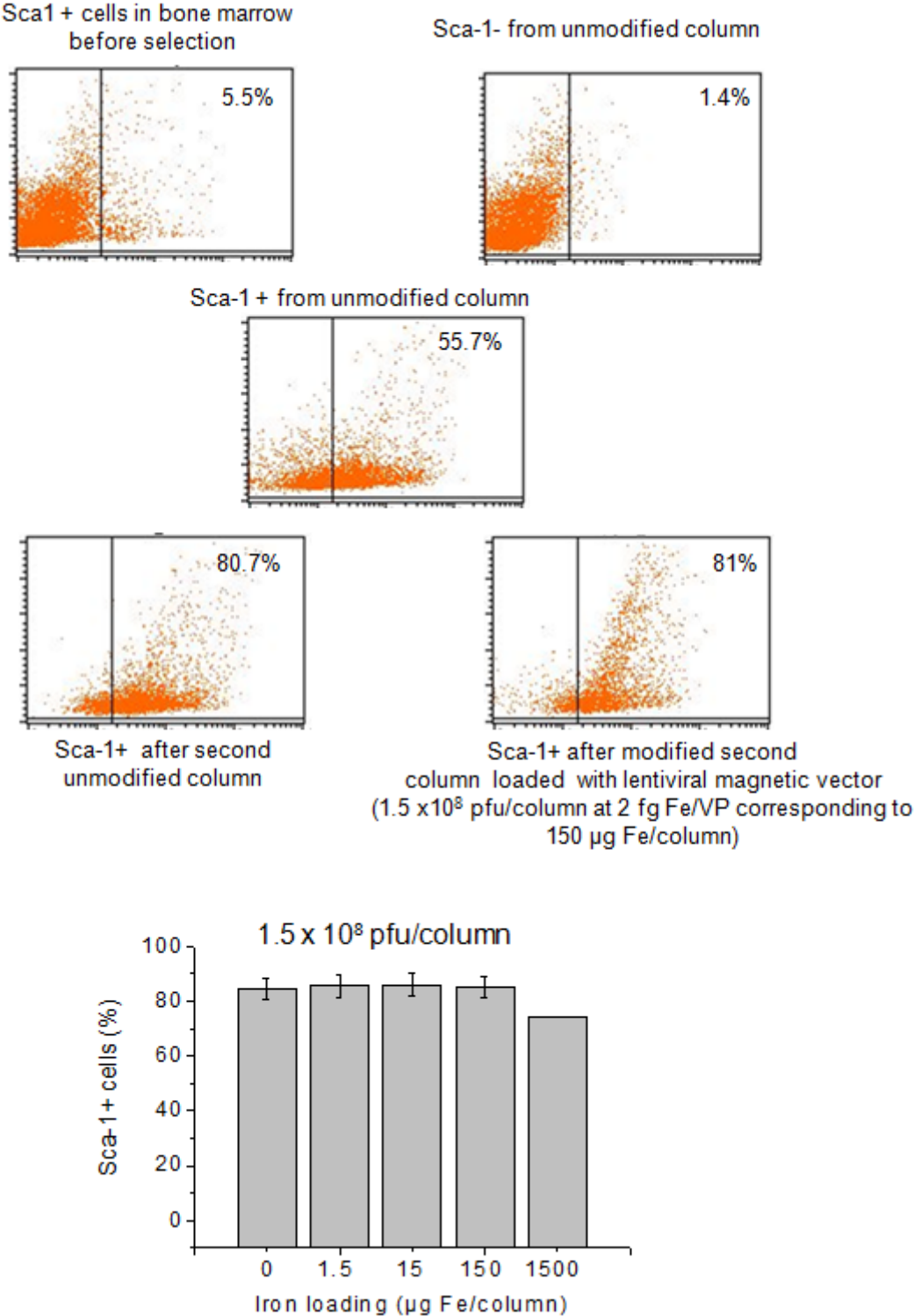
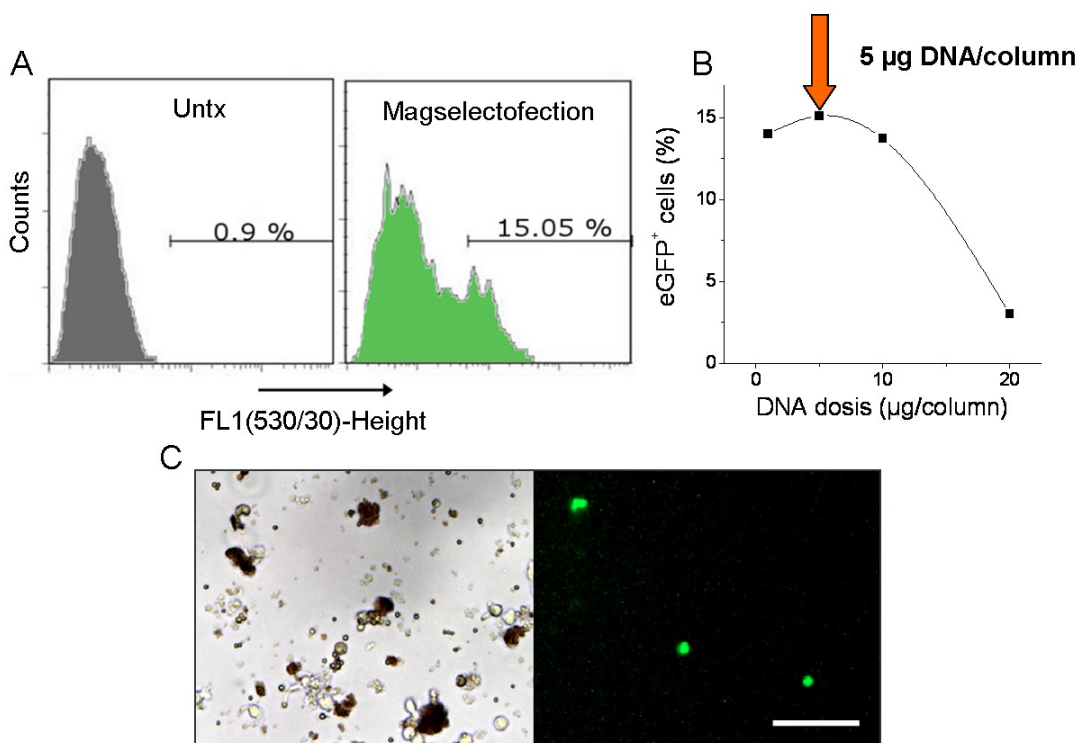


Figure 31. Purity of Sca-1+ cell fraction after MACS and Magselectofection procedures.

### 3.5.3. Human peripheral blood mononuclear cells (hPBMCs)

hPBMCs were isolated by Ficoll gradient and stimulated with Cytostim reagent 24h prior magselectofection. Then, magselectofection was performed using transfection complexes comprising peGFP/SO-Mag5-6/Df-Gold. The cells were re-stimulated just post-magselectofection using 5  $\mu$ l of the Cytostim solution. In Figure 22, the reporter gene expression in hPBMC analysed 24 h post-magselectofection by fluorescence microscopy and by FACS is plotted. The results show that approximately 15 % of the PBMC were transfected (Figure 32 A). The transfection efficiency was DNA dose-dependent (Figure 32 B). In contrast to Jurkat T cells or hUC-MSCs where 20  $\mu$ g DNA/column was found as optimal doses, we found that 5  $\mu$ g/column is yielding highest transfection efficiency (Figure 32 B). This indicates that it is necessary to find the optimal DNA dosage for every cell type.



**Figure 32. Quantification of eGFP positive hPBMC post-magselectofection by flow cytometry and by microscopy.** hPBMC were incubated for 30 min on the column with magnetic triplexes SO-Mag 2/DF-Gold/pBLuc at DNA dosage of 1-20 $\mu$ g DNA per column and analyzed 48 h post-magselectofection. (A) Histogram plots of untransfected hPBMC cells (untx) and cells post-magselectofection. (B) Percentage of eGFP-expressing hPBMCs versus DNA dosage. (C) Bright field (left) and fluorescence microscopy images (right) taken at 490/509 nm for eGFP+ cells green fluorescence for hPBMC, scale bar equals 100  $\mu$ m.

Transductions of hPBMCs were carried out using lentiviral complexes comprising SO-Mag MNPs. hPBMCs were labelled using CD45 microbeads. Figure 33 A shows that the hPBMCs were positively infected in the whole tested MOI range of virus. Serial titrations from MOI of 2 to 0.5 pfu/cell were performed in order to analyse the infection efficiency in hPBMCs using magselectofection procedure. FACS results (Figure 33 B) revealed that up to 20% of eGFP positive hPBMCs were found 3 days post-magselectofection at MOI of 2 pfu/cell and the percentage of eGFP<sup>+</sup> cells was maintained during more than 7 days. Moreover, FACS results (Figure 33 C) show that CD4<sup>+</sup> cells were expressing the reporter gene (eGFP).

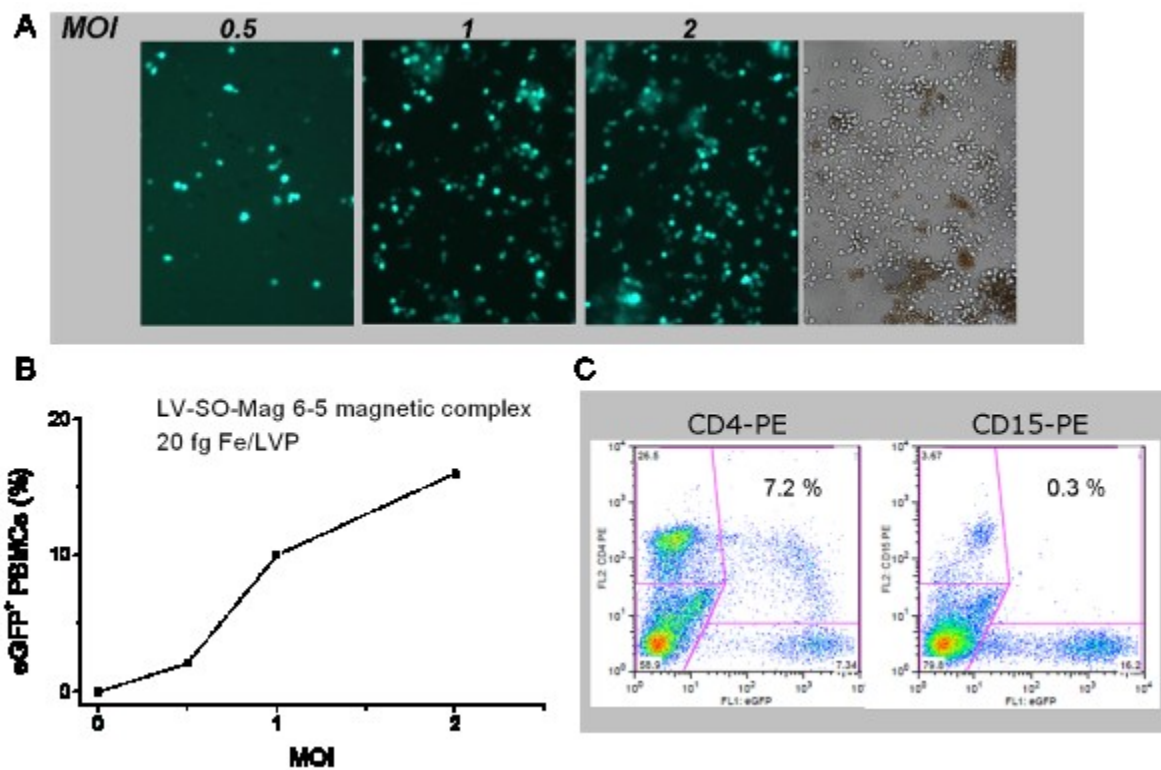


**Figure 33. Quantification of eGFP positive hPBMC post- viral magselectofection by flow cytometry and by microscopy.**  $2.5 \times 10^6$  hPBMCs were labelled using CD45 microbeads and transduced with viral magnetic complexes SO-Mag2/LV.eGFP. Cells were stimulated just post-magselectofection using the Cytostim reagent. (a) Bright field and Fluorescence microscopies (490/509 nm) images of hPBMCs 5 days post-magselectofection with different MOI at 20 fg Fe/LVP. (B) FACS data on the percentage of eGFP positive hPBMCs versus MOI using the ratio of 20 fg Fe/VP. (C) FACS data on the percentage of eGFP positive CD4<sup>+</sup> or CD15<sup>+</sup> cells.

The results suggest that higher MOI (pfu/cell) is needed to increase the number of positive infected cells. We suggest that FACS analysis should be done 7 days and

not 5 days post-magselectofection, as was found to be the optimal time point for FACS analysis in hUC-MSCs (see Figure 27).

### 3.5.4. Magselectofection in hUC-MSCs results in higher transduction efficiency compared to magnetofection and standard infection.

hUC-MSCs were infected at low MOIs using lenti- and adenoviral vectors by magselectofection, magnetofection and standard infection procedures.

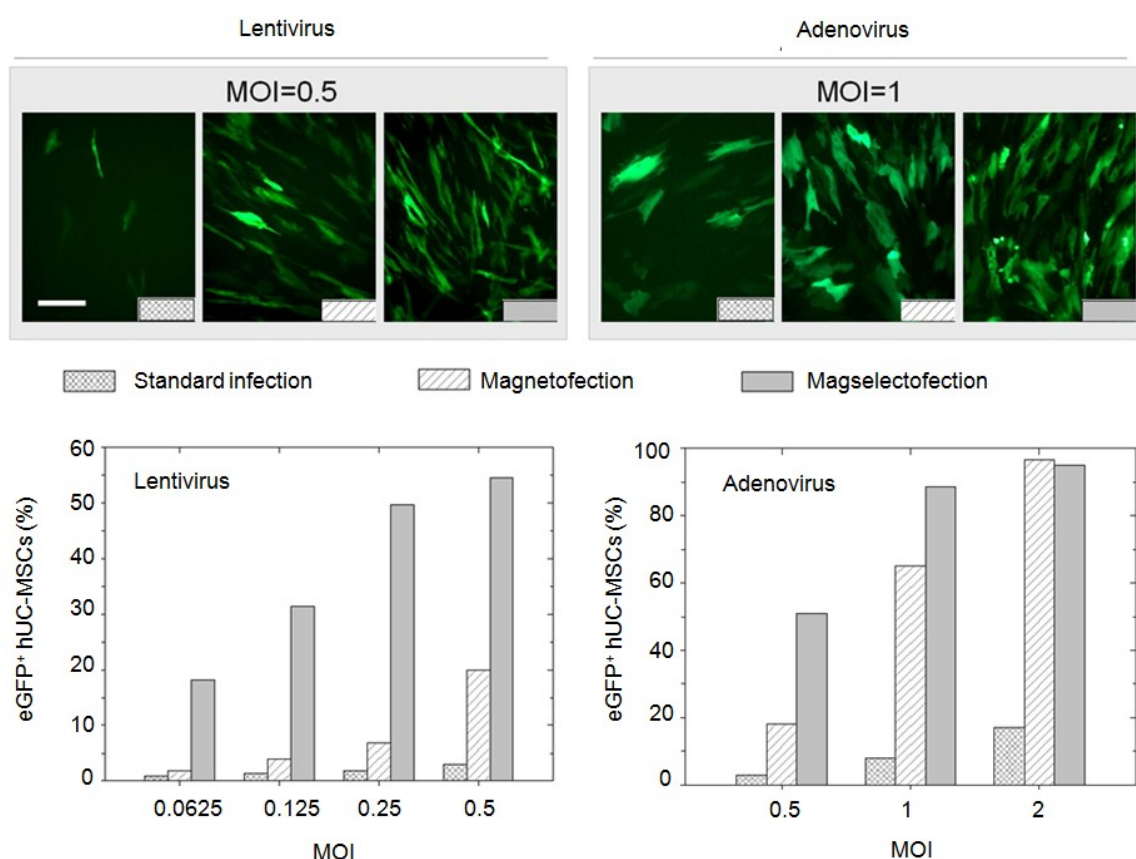


**Figure 34. Efficiency of the transduction of the hUC-MSCs using standard infection, magnetofection and magselectofection procedures with lenti- and adenoviral vectors coding for eGFP.** Fluorescence microscopy images of the transduced cells (at the top, bar=200  $\mu$ m) and FACS data on the percentage of eGFP positive cells transduced at different MOI at day 3 post-transduction (at the bottom). Magnetic viral complexes were formulated at nanoparticle-to-virus particle ratio of 5 and 20 fg Fe/VP for adeno- and lentivirus complexes, respectively.

FACS analysis and microscopy of the infected cells 3 days post-infection (Figure 34) shows that magselectofection resulted in a significant increase in the percentage of eGFP<sup>+</sup> cells compared to magnetofection and standard infection. At MOI of 0.25 pfu/cell, the infection efficiency was improved about 7 and 25-fold using lentiviral magselectofection compared to magnetofection and standard infection, respectively (data shown in Figure 34, left panel). At an MOI of 0.5 pfu/cell, the infection efficiency



was improved by approximately 3- and 17-fold when using adenoviral vectors compared to magnetofection and standard infection, respectively (Figure 34, right panel).

### 3.6. *Upscale from LS to XS and CliniMACS is possible*

These experiments were carried out together with Dr. Ian Johnston from Miltenyi Biotec.

The first step was to ensure that Magselectofection of Jurkat T cells can be efficiently upscaled to the large XS separation columns. To reduce reliance on the expression of the intracellular fluorescent protein, EGFP, transfections with a second expression system were established. For gene therapy, one goal is to express the IL-2 receptor common gamma chain (CD132) in stem cells of SCID patients, therefore we chose a molecule that is also expressed at the cell surface: the mouse H-2Kk MHC I molecule.  $2.5 \times 10^7$  Jurkat T cells were labelled with CD45 MicroBeads. Again, the order of complex loading was tested and transfection within the XS column was compared to a parallel transfection using the same magnetic transfection complexes, in LS columns containing  $2.5 \times 10^6$  immobilized Jurkat T cells.

As shown above, application of the magnetic transfection complex prior to cell loading in LS columns resulted in higher transfection efficiencies (Figures 35 A and D; 19.8% GFP+ cells) than adding the complex after the Jurkat T cells application (Figure 35 A; 9.5% GFP+ cells). This was also true using the murine histocompatibility antigen H-2Kk (Figures 35 A and C). Following Magselectofection in Jurkat T cells H-2Kk was similarly expressed to EGFP (Figure 35). An added advantage of the use of the H-2Kk system is that antibody conjugates can be used to stain the expressed molecule that are conjugated to different fluorescent dyes. This flexibility is especially relevant when working with SM4-31 and DreamFect Gold lipids which tend to show strong yellow and green background fluorescent signals. While the high transfection efficiencies seen in LS columns were not achieved in XS columns (Figure 35 E), no performance differences could be seen when alternative column loading protocols were used (Figure 35 A). It should be noted that while the cell number to be transfected in the XS columns has been increased by a factor 10, the amount of transfection complex has only been increased by a factor of 4 while the total column volume is in fact 18 times larger. These variables should be further investigated to see whether additional performance increases in XS columns are

possible. The current partial reagent upscale was chosen mainly to limit reagent consumption.

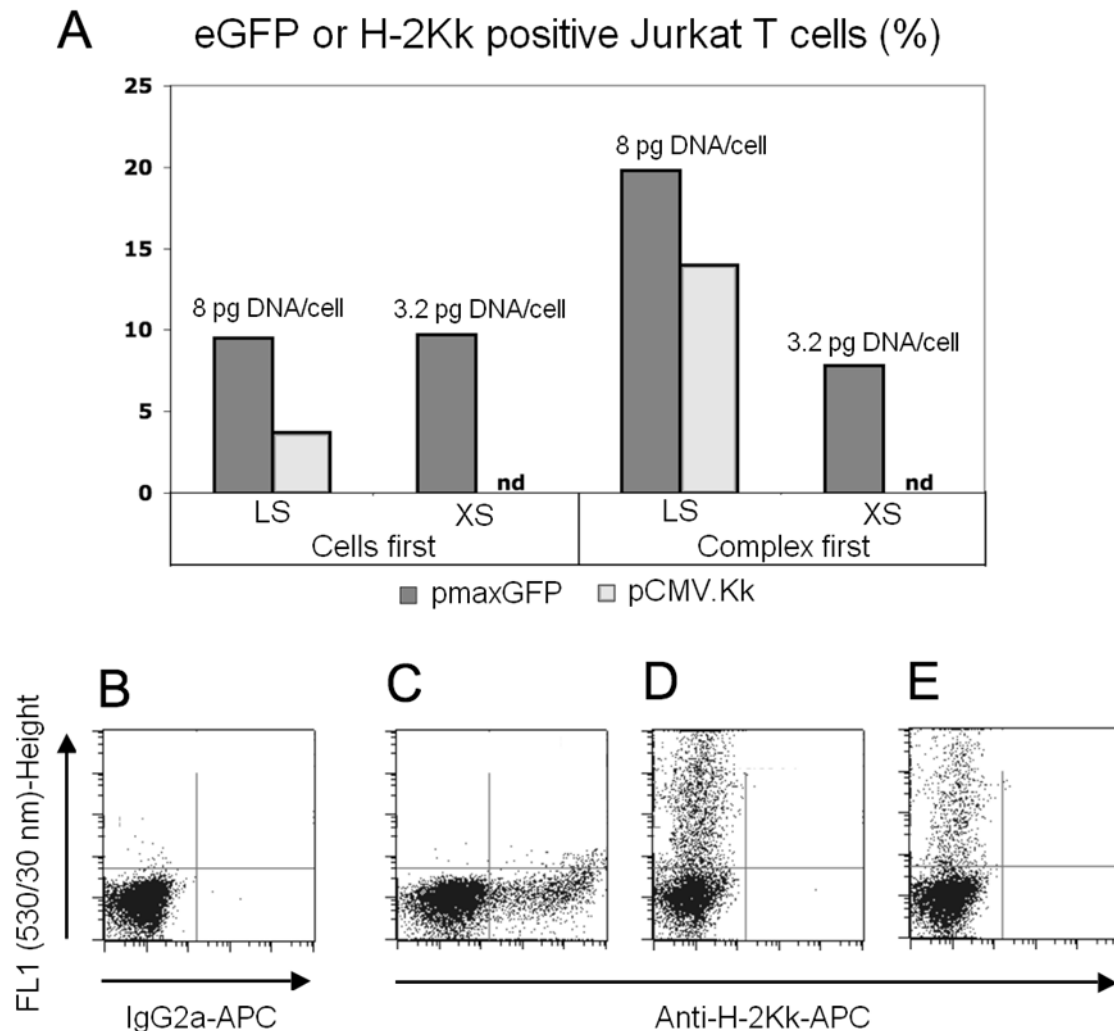


**Figure 35. Transfection of Jurkat cells can be successfully upscaled to XS columns.** Jurkat T cells were labelled with CD45 MicroBeads and  $2.5 \times 10^6$  (LS) or  $2.5 \times 10^7$  (XS) cells were added to a MACS separation column before (E) or after (B–D) loading the column with magnetic transfection complex. The transfection complex for XS columns consisted of 80  $\mu$ g pmaxGFP, 80  $\mu$ g S35 magnetic beads and 320  $\mu$ L DreamFect Gold. For LS columns, the complex consisted of 20  $\mu$ g pmaxGFP or pCMV.Kk plasmid, 20  $\mu$ g S35 magnetic beads and 80  $\mu$ L DreamFect Gold. After rinsing the columns with 0.5 mL (LS) or 3 mL (XS) RPMI, the cells were incubated for 30 minutes at room temperature. The cells were then eluted and cultivated for 48 hours. Transfected cells were stained with anti-H-2Kk-APC (C–E) or IgG2a-APC isotype control conjugate (B) and analysed using a MACSQuant flow cytometer. nd: not detectable

As XS columns are the columns used in the CliniMACS device, we were interested to know whether the Magselectofection procedure can be applied using CliniMACS. Separation of cells on the CliniMACS® plus instrument requires automated cell processing steps to be carried out in a closed system of tubes and bags (CliniMACS

Tubing set, Figure 36 A). To optimise the Magselectofection process, it is essential that the transfection complex can be administered to the separation column independently of the labelled cells – this was not possible in the earlier feasibility studies carried out with HEK-CD4 cells. To this end, Miltenyi Biotec generated a tubing set modification (Figure 36 B) which enables the transfection complex to be applied to the separation column via syringe and the column flow-through to be collected in a second syringe. During normal operation, the flow of buffers within the CliniMACS Tubing Set is directed by computer-operated valves. To add a new function to the tubing set, 3-way taps were welded to the tubing set above and below the separation column (Figure 36 C). After completion of the cell sorting process, the process can be paused, the taps opened and the transfection complex applied (Figure 36 D). The taps are then closed and the cells incubated on the column for 30 minutes before resumption of the separation program and elution of the cells (This work was performed with the collaboration partner Miltenyi Biotec).

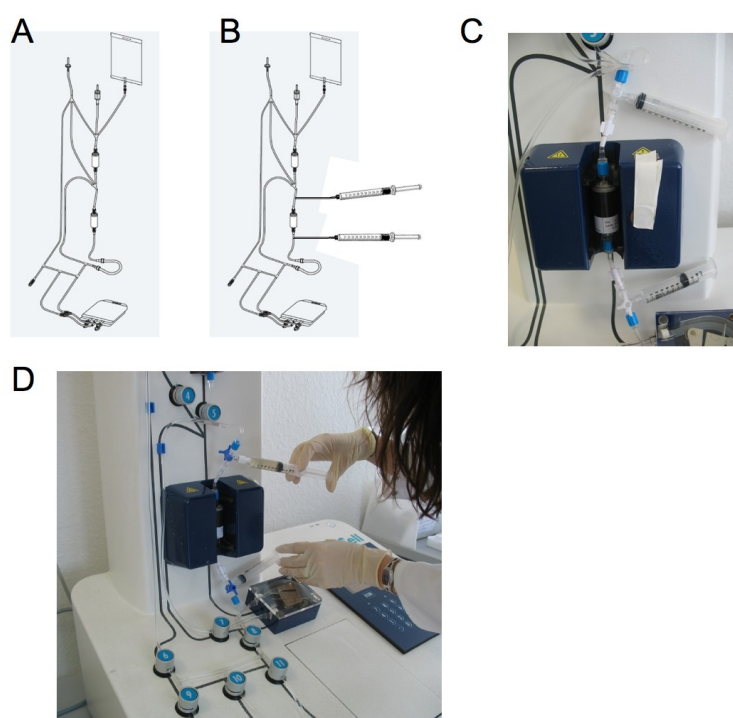


**Figure 36. CliniMACS Tubing Sets for Magselectofection: prototype 1.** (A) Standard CliniMACS Tubing Set. (B, C) CliniMACS Tubing Set modified with 3-way tap to allow in-process application of magnetic transfection complex. (D) Application of pmaxGFP, S35 magnetic particle, DreamFect Gold transfection complexes to  $2.5 \times 10^7$  CD45 MicroBead-immobilized Jurkat T cells.

The transfection efficiencies seen in the CliniMACS (Figure 37) were similar but significantly lower than those seen using XS columns. No significant differences in

transfection efficiencies could be seen using either of the prototype tubing sets or when using RPMI or PEB to generate the magnetic transfection complexes. The only protocol difference between the XS column process and the CliniMACS process is that a wash step occurs before the elution of the Magselectofected cells. If this wash step is too rigorous, it could account for the reduction in transfection efficiencies. This factor could be eliminated by suitable changes to the CliniMACS software.

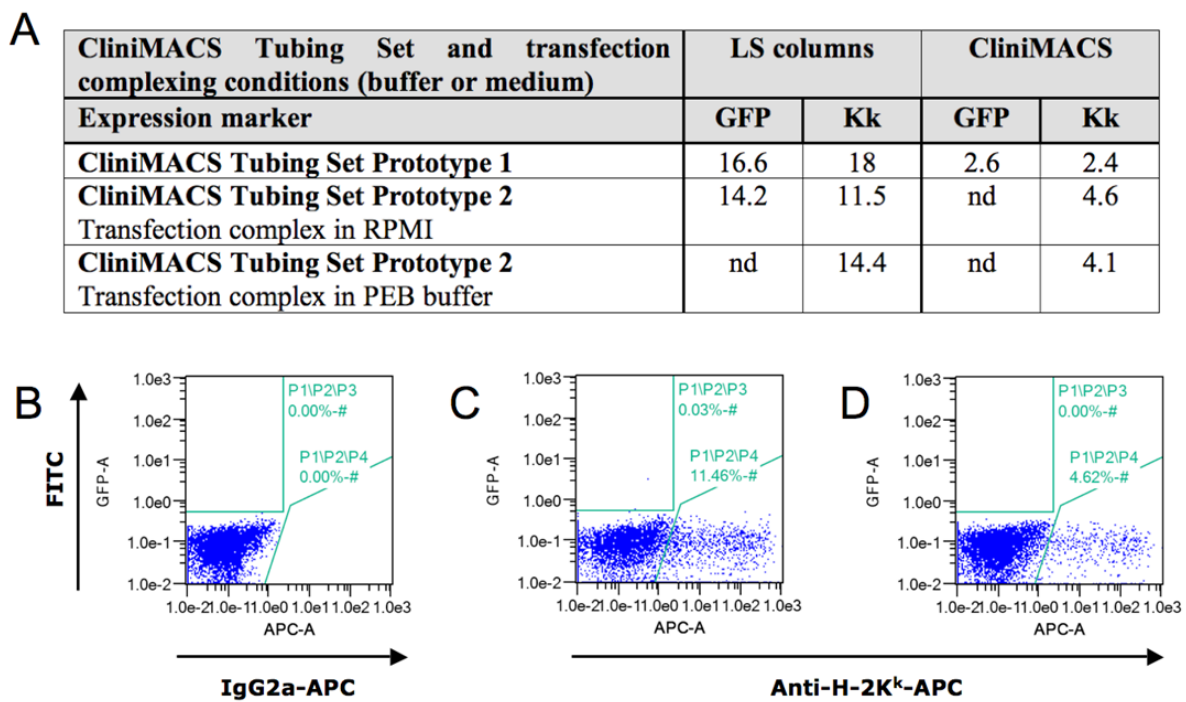


**Figure 37. Magselectofection of Jurkat cells in prototype CliniMACS Tubing Sets.** Jurkat T cells were labelled with CD45 MicroBeads.  $2.5 \times 10^6$  labelled cells were added to an LS separation column, and washed with 0.5 mL PEB before loading the column with magnetic transfection complex. For CliniMACS separations,  $2.5 \times 10^7$  cells were applied to a cell application bag, connected to the tubing set and separated using the CD34 Separation Program. During the third wash step, the separation was paused and the column was loaded with magnetic transfection complex. The transfection complex for CliniMACS columns consisted of 80  $\mu$ g pmaxGFP or pCMV-Kk, 80  $\mu$ g S35 magnetic beads and 320  $\mu$ L DreamFect Gold. For LS columns, the complex consisted of 20  $\mu$ g pmaxGFP or pCMV.KK plasmid, 20  $\mu$ g S35 magnetic beads and 80  $\mu$ L DreamFect Gold. After rinsing the columns with 0.5 mL (LS); 0 mL (Prototype 1) or 8 mL (Prototype 2) PBS/EDTA/BSA or RPMI, the cells were incubated for 30 minutes at room temperature. The cells were then eluted from the LS columns manually and from the CliniMACS Tubing Sets by resuming the separation program. The eluted cells were cultivated for 48 hours. Transfected cells were stained with anti-H-2Kk-APC (C, D), or IgG2a-APC isotype control conjugate (B) and analysed using a MACSQuant flow cytometer. Jurkat cells transfected with pCMV-Kk in CliniMACS Prototype Tubing Set 2 (B, D) or LS column (C) with the transfection complex prepared in RPMI. nd: not detectable.

### *3.7. Preliminary study of the in vivo biodistribution of the hUC-MSCs and hCB-HSCs: first pilot study*

#### **3.7.1. Biodistribution of the magnetically labeled hUC-MSCs after magselectofection**

hUC-MSCs were magnetically labelled using 50 pg Fe/cell of the SO-Mag2 magnetic nanoparticle 24 h prior magselectofection. For this purpose, the MNPs were added to the cells. Then, the cells were incubated for 20 min under magnetic field (96 well magnetic plate). Afterwards, the magnetic plate was removed and the cells were cultivated for 24 h. Viral magselectofection of hUC-MSCs was carried out as described above using a MOI of 0.2 pfu/cell and 20 fg Fe/LVP. Microscopy and FACS analysis revealed that SO-Mag2 magnetically labelled hUC-MSCs were more efficiently transduced than the non-magnetically labelled with SO-Mag2 (39.2% vs 19.1 %, respectively) (Figure 38). The non-magnetically labelled cells with SO-Mag2 nanoparticles were injected into mice 72 h post-magselectofection and 24 h post injection animals were sacrificed. The entire harvested organs were weighed, transferred to a cryovial with freeze tissue liquid and immersed in liquid nitrogen to allow fast freezing. Then, cryovials were stored at -80°C until analysis. These tissues were used for determination of iron content and histological examination.

Non-heme iron determination was carried out as described in material and methods. Non-heme iron was calculated from the total iron content in each tissue, from which the endogenous iron content for the respective tissue from control animals (saline injected) was subtracted.

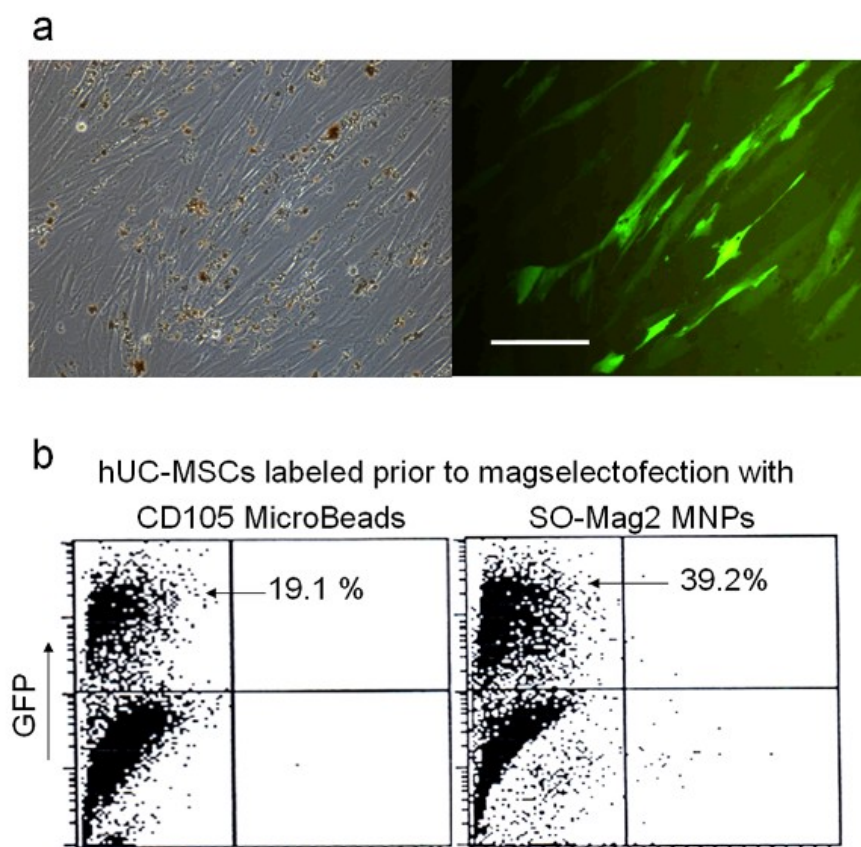


**Figure 38. eGFP reporter gene expression in hUC-MSCs after viral magselectofection of the cells magnetically labelled with CD105 MicroBeads or with SO-Mag2 MNPs prior to magselectofection.**  $10^6$  hUC-MSCs per LS Column were magnetically labelled just before magselectofection with CD105 MicroBeads or 24 h prior to magselectofection with SO-Mag2 magnetic nanoparticles at a dose of 50 pg Fe/cell and transduced at MOI of 0.2 pfu/cell with viral magnetic complexes SO-Mag2/LV.eGFP formulated at MNPs-to-VP ratio of 20 fg Fe/VP using the magselectofection procedure. The cells were analysed for eGFP expression 2 days post-magselectofection. (a) Bright field and fluorescence microscopy (490/509 nm) images of hUC-MSCs labelled with CD105 MicroBeads prior to magselectofection. Bar=200  $\mu$ m. (b) FACS data on the percentage of eGFP positive hUC-MSCs for the cells labelled prior to magselectofection with CD105 Microbeads (left graph) or with SO-Mag2 MNPs (right graph).

**Table 6. Exogenic iron ( $\mu$ g/g trissue) biodistribution**

	M1	M2	M3	M4	M5	M6
Liver	0	0	0	0	0	0
Left Lung	9	5	0	0	137	0
Right Lung	114	93	35	0	105	200
Spleen	70	81	69	232	64	0
Kidney	6	0	17	12	37	6
Heart	0	0	0	12	0	0
Brain	0	0	1	0	6	0
Muscle	3	5	0	0	2	0

M5: control mice



In table 6 the biodistribution of exogenic iron is summarized. Changes in iron levels varied from tissue to tissue. The highest exogenic iron levels were found in the right lung followed by spleen and kidney. No exogenic iron was found in the liver and other analysed organs. The results from exogenic iron analysis correlated with the histological results of Prussian blue staining (Figure 39).

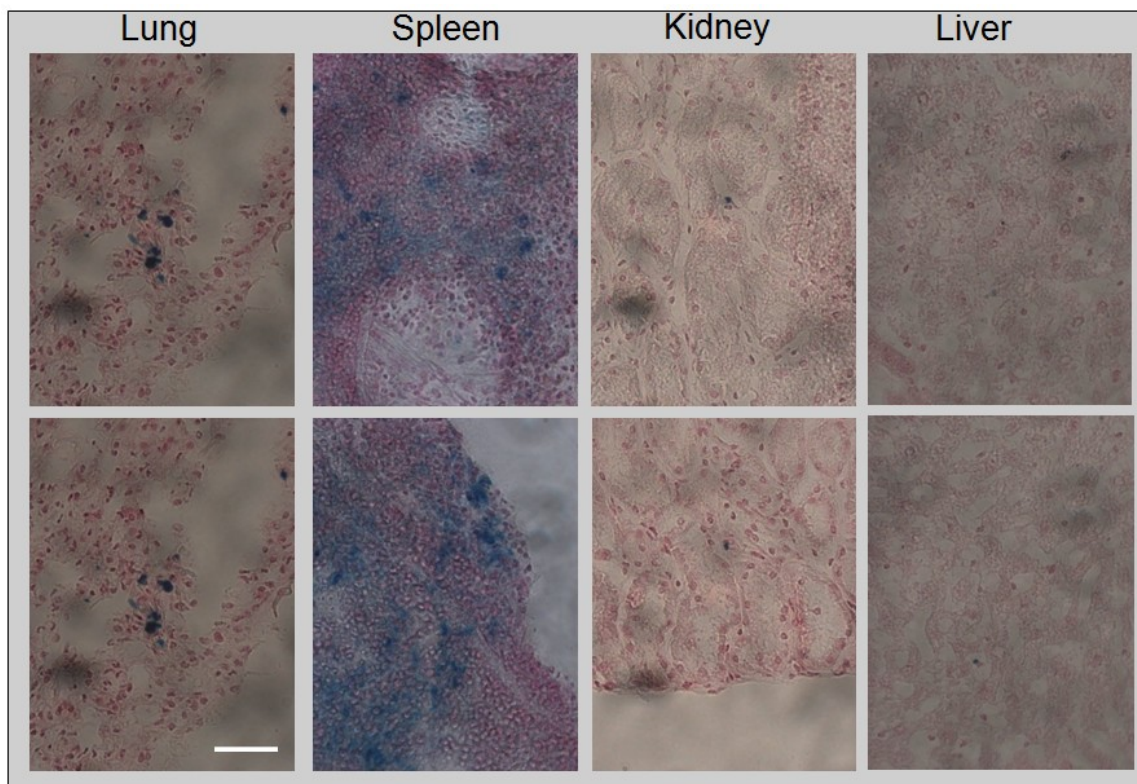


**Figure 39. Bright field microscopy images of the lung, spleen, kidney and liver tissue sections of the mice r after Prussian Blue staining for non-heme iron, bar= 100  $\mu$ m.**

From the exogenic iron results and taken into account that the injected cells contained on average 28.3 pg Fe/cell we were able to calculate the amount of hUC-MSCs per organ. In Figure 40 the cell biodistribution is represented. We can observe that hUC-MSCs were primarily found in lung and spleen and very few in kidneys. The result correlates with the histological results (Figure 41).

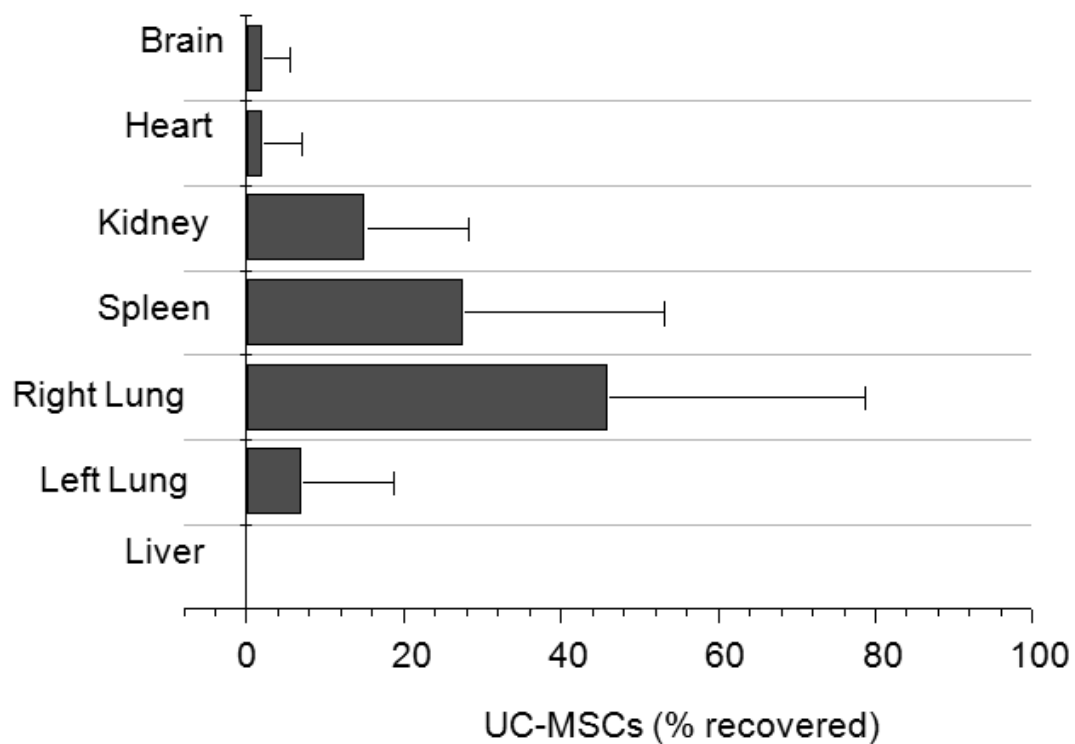


**Figure 40. Biodistribution of hUC-MSCs in mouse tissues.** Evaluation of the cell distribution in mice tissues derived from the data on the exogenic iron concentration in tissues with account for the iron content in the cells of 28.3 pg Fe/cell.

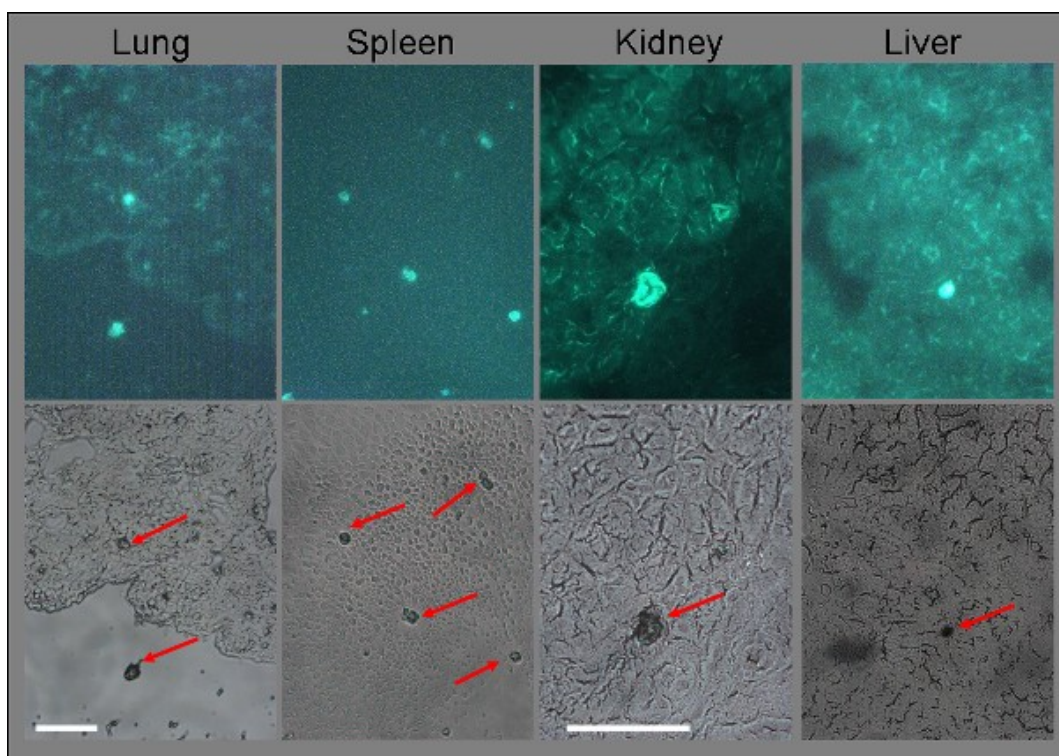


**Figure 41. Microscopy images of the tissue sections of the mice after i.v. injection of the hUC-MSCs transduced using magselectofection technology, bar= 100  $\mu$ m.**



### 3.7.2. Biodistribution of hCB-HSCs post- magnetic cell labeling

hCB-HSCs were magnetically labelled with SO-Mag2 magnetic nanoparticles using 50pg Fe/cell. Microscopy revealed that hCB-HSCs were magnetically labelled (Figure 42). Cells were injected into mice 24 h post-labeling. 24 h post injection animals were sacrificed. The entire harvested organs were weighed, transferred to a cryovial with freeze tissue liquid and immersed in liquid nitrogen to allow fast freezing. Then, cryovials were stored at -80°C until analysis. These tissues were used for determination of iron content and histological examination.

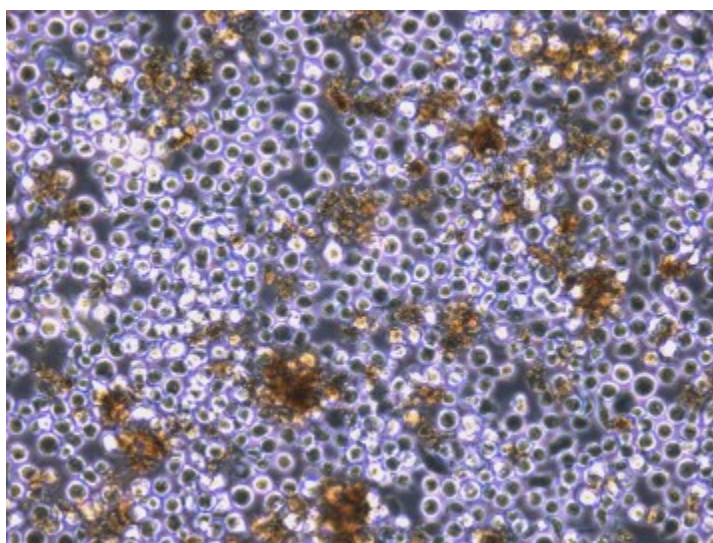


**Figure 42. Bright field microscopy image of magnetically labelled hCB-HSCs using 50pg Fe/cell of the SO-Mag2 magnetic nanoparticle.**

Non-heme iron determination was carried out as described in material and methods. Non-heme iron was calculated from the total iron content in each tissue, from which the endogenous iron content for the respective tissue from control animals (saline injected) was subtracted.

In Table 7, the biodistribution of exogenic iron is summarized. Changes in iron levels varied from tissue to tissue. The highest exogenic iron levels were found in the right lung followed by kidney. No exogenic iron was found in liver or other analysed organs. The results from exogenic iron analysis correlated with the histological results of Prussian blue staining (Figure 43).

**Table 7. Exogenic iron ( $\mu\text{g/g}$  trissue) biodistribution**

	M8	M9	M10	M11	M12
Liver	0	0	0	0	0
Left Lung	9	0	0	0	19
Right Lung	0	50	22	46	142
Spleen	0	0	0	42	0
Kidney	0	12	9	8	18
Heart	0	8	0	1	2
Brain	0	0	1	1	0
Muscle	14	0	5	0	4

M10: control mice

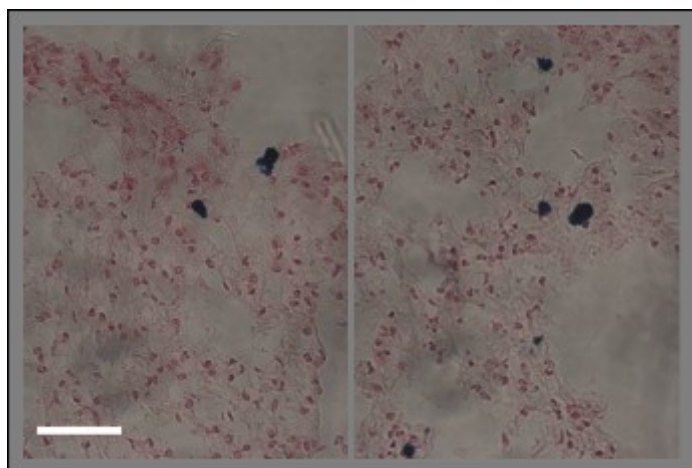


**Figure 43. Bright field microscopy images of the lung, spleen, kidney and liver tissue sections of the mice r after Prussian Blue staining for non-heme iron, bar= 100  $\mu\text{m}$ .**

From the exogenic iron results and taken into account that the injected cells contained on average 15.1 pg Fe/cell we were able to calculate the amount of hCB-HSCs per organ. In Figure 44 the cell biodistribution is represented. We can observe that hCB-HSCs were primarily found in lung and kidney and very few in the other organs.

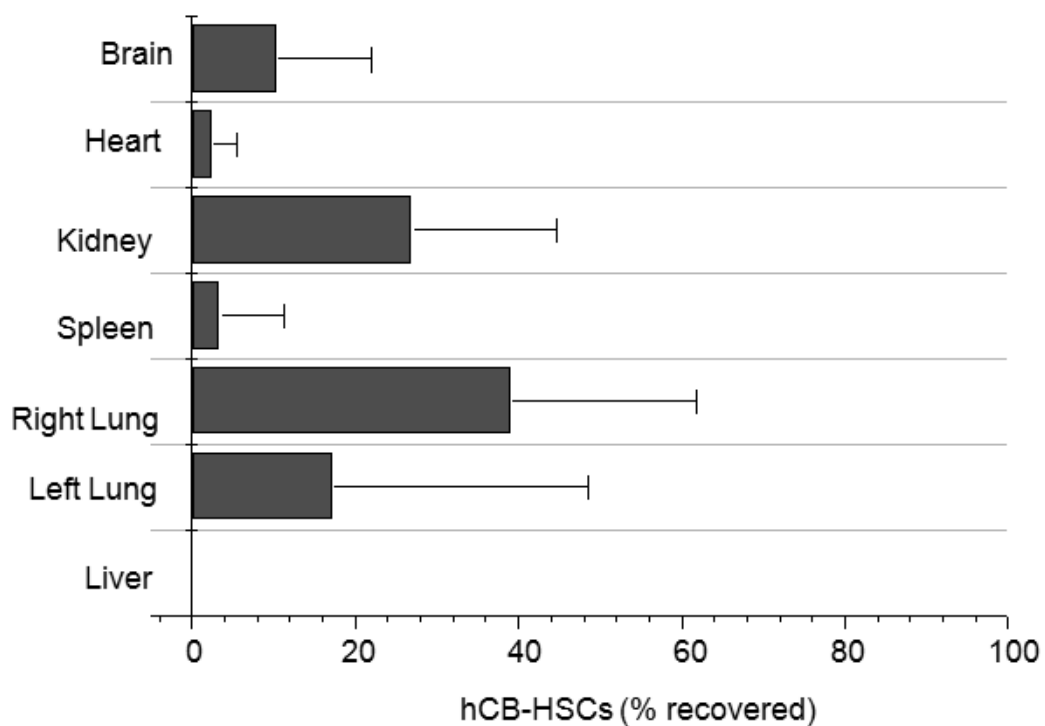


**Figure 44. Biodistribution of the hCB-HSCs in mice tissues derived from tissue analysis for exogenic non-heme iron.** Evaluation of the cell distribution in mice tissues derived from the data on the exogenic iron concentration in tissues with account for the iron content in the cells of 15.1 pg Fe/cell.

## 4. DISCUSSION

In recent years, cellular engineering using viral and non-viral technologies has emerged as a potential tool for the treatment of various diseases (Aiuti et al., 2009), (Cavazzana-Calvo and Fischer, 2007), (Williams, 2008). Given this tremendous potential, an obvious question lies in why these therapies with *ex vivo* engineered cells have not become widely practiced state-of-the-art treatments. The answer is that the full potential of cellular engineering can only be realized if efficient, safe, affordable and standardized technologies for cell manipulation are available. No single technology known today fulfills all of these requirements. The current technologies for cellular engineering with viral vectors have proven potential for clinical therapy but are faced with labor-intensive, time-consuming and inefficient processing, resulting in high production costs. The advantage of the high transfection rates achieved with electroporation or nucleofection for non-viral nucleic acid delivery is counteracted by the discontinuous working process and the unavailability of closed devices. Given these challenges, there is a need to investigate and develop new technologies that allow the production of engineered cells in an efficient, simple and practical way (Goverdhana et al., 2005). This is indeed the focus of this thesis.

Here, we have established a new method to separate and genetically modify target cell populations in a single procedure using magnetic cell separation columns. We demonstrate that this new approach works efficiently for both viral and non-viral vectors, allowing a high transfection/transduction efficiency in several cell lines and primary hematopoietic and mesenchymal stem cells from the umbilical cord. We show that the performance of cell sorting and cell recovery are not affected by magselectofection and that the function, viability and differentiation potential of the cells are not impaired.

### *4.1. The role of magnetic nanoparticles and enhancers in gene delivery efficiency*

As a parameter of genetic modification efficiency, the percentage of transgene-expressing cells is of primary importance. The steady-state intracellular concentration of the reporter protein does not have to be high, but ideally would be adjustable to a threshold that allows the desired effect, as, for example, in the case of the alpha subunit of the interleukin-2 receptor (CD25) (Ellery and Nicholls, 2002). Magnetic lipoplexes formulated with Df-Gold lipid and SO-Mag2 nanoparticles have shown the

highest percentage of eGFP-expressing cells using magselectofection compared to other magnetic lipoplexes (see Figure 25 A). In contrast, relatively low efficiency was obtained using magnetic lipoplexes formulated using SO-Mag2 with SM4-31 as the lipid (see Figure 25 A). However, SO-Mag2/SM4-31 magnetic lipoplexes yielded higher transfection efficiency in terms of luciferase expression (see Figure 25 B). Commercially available CombiMag nanoparticles are another useful example. The complexes formulated with these particles ensure the highest luciferase expression levels but a relatively low percentage of transfected cells when compared to other “leaders” (see Figure 13). From this point of view, we speculate that it is advantageous to have a spectrum of magnetic nanoparticles and lipids available for formulating magnetic vectors and hence for flexibly regulating the level of transgene expression post-magnetofection/magselectofection.

#### 4.2. *Development of magnetic vectors*

The first essential steps for efficient magselectofection are the generation of nanomagnetic vector formulations and magnetically-labeled cells. We have determined that magnetic lipoplexes with Dreamfect-Gold and suitable MNPs at iron:DNA (w/w) ratios of 0.5 and 1 with non-viral vectors yield high magnetofection and magselectofection efficiency, respectively. For magnetic viral vectors, it is essential to formulate the compositions in terms of iron weight per *physical* virus particle, and *not* per infectious virus particle, taking into account that both infectious and non-infectious virus particles associate with appropriate MNPs. Therefore, once a suitable ratio that allows quantitative virus particle binding has been identified, this ratio can be applied to any other virus preparation even without knowing its biological titer. We speculate that it is advantageous to have a spectrum of magnetic nanoparticles available for formulating viral and non-viral magnetic vectors. In our study, we have used in-house synthesized magnetic nanoparticles (Mykhaylyk et al., 2007a; Mykhaylyk et al., 2010), but magselectofection can be carried out by anyone with commercially available magnetofection reagents ((see Figure 15; (Hofmann et al., 2009; Kadota et al., 2005)). The complexes synthesized in this study present binding efficiencies between nucleic acid and magnetic nanoparticles comparable to other published studies (Mykhaylyk et al., 2007a), (Mykhaylyk et al., 2009b), (Mykhaylyk et al., 2010). Although several research groups have used magnetofection for viral infection (Bhattarai et al., 2008), (Sacha et al., 2007), no data

can be found about the binding efficiency between a virus and magnetic nanoparticles. We have demonstrated that more than 94% of the virus can be bound with magnetic nanoparticles (Cengizeroglu, 2008).

Efficient magnetic lipoplexes used for magnetofection and magselectofection were relatively large (from about 500 nm to 3  $\mu\text{m}$ ) compared to non-magnetic lipoplexes (about 700 nm), with surface charges ranging from slightly negative to slightly positive (about +25 eV) when measured in the absence of serum (see Tables 2 and 3). Thus, we can say that the net charge of the complex does not affect their internalization or the final gene expression level. An interesting result was obtained when the size and the electrokinetic potential of the magnetic lipoplexes were measured under conditions mimicking our transfection experiments (in the presence of 10% FCS; Table 3). Size was greatly increased for all complexes, indicating that in the presence of FCS, the magnetic complexes tend to aggregate. The complexes show negative charges (about -10 eV). According to magnetophoretic mobility measurements, 30,000-40,000 up to 400,000 MNPs were associated with the lipid component and plasmid in a complex, resulting in an average magnetic moment at the saturation magnetization of about  $(4-5)\times 10^{-15}$  to  $(1-2)\times 10^{-13}$   $\text{Am}^2$ , depending on whether the magnetic complexes were prepared for magnetofection or for magselectofection. Ogris *et al.* (Ogris *et al.*, 1998) reported that aggregated DNA/Tf-PEI complexes with an average size greater than 500 nm resulted in more efficient gene transfer than did smaller particles. Ross *et al.* (Ross and Hui, 1999) provided evidence that the size of the DOTAP/DOPE lipoplexes was the major determinant of the internalization and transfection efficiency and found the largest complexes (of 2.2  $\mu\text{m}$ ) to be the most efficient in Chinese hamster ovary (CHO) cells. Li *et al.* (Li *et al.*, 2005) found size, and not surface charge, to be a major determinant of the *in vitro* lipofection efficiency of a TFL-3 cationic lipid composed of lipid components in a pDNA/TFL-3 complex. We observe a direct relationship between the size of the complex and transfection efficiency, but complexes as large as 2  $\mu\text{m}$  can deliver genes very efficiently. Nevertheless, complexes with an average hydrodynamic diameter of about 200-400 nm can also be very efficient, like those formulated with the PEI-Mag3 nanoparticles. These results indicate that the size and charge of the magnetic vectors tested here were not of critical importance for gene delivery to cells. Apparently, fine differences in the composition of the surface layer of the particles cause more significant differences in the efficiency of the derived magnetic

lipoplexes, as observed for the NDT-Mag1, PEI-Mag2, PEI-Mag3, SO-Mag2, PalD1-Mag1 and PL-Mag1 particles.

### *4.3. Establishment of the magselectofection procedure*

#### **4.3.1. Modification of LS Miltenyi's columns with magnetic vectors**

Magselectofection turned out to be an extraordinarily simple procedure after we had established a method of quantitative and reversible magnetic vector retention on commercially available MACS cell separation columns that enabled more than 80% association between vectors and magnetically-labeled target cells (see Figure 19). We demonstrate here that immobilization of the complexes on the column is reversible, depending on the column preparation procedure. For a standard column preparation, the complexes are reversibly bound to the column, which enables further efficient association with magnetically labeled cells. In contrast, irreversible binding of the complexes to the column was observed using a freeze-drying procedure for column preparation, resulting in a low recovery of DNA after elution and low DNA cell association (see Figure 19). This gives an explanation for the low transfection efficiency observed when magselectofection was performed using the lyophilized column (see Figure 24 E). The irreversible binding of the complexes to the column can be explained by the high magnetization of the complexes due to their overnight exposure to a magnetic field. Therefore, the standard column preparation procedure was selected for further experiments.

The essential parameters in magnetic cell sorting are cell recovery, purity of target cells, viability and biological functionality. Magselectofection meets all of these parameters and also provides efficient transfection/transduction of the target cells.

To obtain maximum target cell purity, protocols for magnetic cell sorting recommend two steps of magnetic selection. Nevertheless, when establishing magselectofection with the Jurkat/K562 model system, we were interested in determining whether or not a one-column system would work. We found that while transfection efficiency was high, the resulting target cell purity was better when using the two column procedure, although cell retention, separation efficiency and recovery were not affected compared to the unmodified column. However, the one-column procedure turned out to be an excellent method when working with cell lines or already purified cells. For an integrated protocol with a cell mixture, the two-column format turned out to be

optimal. Cells are sorted on the first column and then brought in contact with transfection/transduction complexes on a second column. In this case, the cell separation efficiency was as high as when using the cell separation-only protocol of the manufacturer (ca. 95%, Figures 22 and 23), and cell recovery was quantitative. This was not only true for the model Jurkat/K562 mixture, but also for Sca-1<sup>+</sup> mouse hematopoietic stem cells isolated from the bone marrow of C57BL/6 mice (see Figure 31). Importantly, the selectivity of the transfection/transduction process for the target cell population was excellent (Figures 22 and 23).

Recently, a novel stem cell Tag-Less sorting method has been published (Roda et al., 2009). The advantage of magselectofection over other cell separation/sorting technologies is that when using magselectofection, the cells are separated and genetically modified in one integrated step.

#### **4.3.2. Genetic modification of different cell types using magnetofection and magselectofection procedures**

The data for the percentage of eGFP-expressing cells reported in this work are calculated from FACS data using the corresponding magnetic and non-magnetic lipoplexes, with luciferase plasmid as a reference to account for the weak fluorescence of the enhancer. The subtraction of this background gives a “true” percentage of eGFP-expressing cells. The results calculated in this way were in agreement with time-consuming quantification of combined bright and fluorescent microscopy images (see Figure 11). It is known that various cationic lipids frequently exhibit a white to orange color fluorescence when added to cells (personal communication at the website <http://www.bio.net/bionet/hypermail/methds-reagnts/1998-August/069931.html>), but this problem is rarely discussed and apparently often neglected, thus leading to overestimation of the achieved transfection efficiency.

##### **4.3.2.1. Jurkat T cells**

The highest reported efficiency for the transfection of Jurkat T cells with non-viral vectors is 19% (Uduehi et al., 2003), which was achieved using triplexes of integrin-binding peptide, Lipofectin and pDNA for cells stimulated with 1 ng/mL of phorbol 12-myristate 13-acetate (PMA) during or after transfection. This stimulation increased



the transgene expression for luciferase plasmid complexes 3- to 5-fold. Guillem et al. (Guillem et al., 2002) achieved  $9.7 \pm 1.2\%$  eGFP-positive Jurkat T cells after transfection with anti-CD3 immunopolyplexes. The vector was formulated using a streptavidin-polyethyleneimine conjugate associated with biotin-labeled CD3 antibodies associated with the eGFP plasmid, N/P=10. Additional treatment of cells 4 h post-transfection with the “Booster #1” lipid transfection reagent resulted in 15% eGFP-positive cells. Puls et al. (Puls and Minchin, 1999) found that anti-CD4 antibody-polylysine-DNA complexes selectively and efficiently transfect Jurkat T cells. The luciferase expression in Jurkat T cells was enhanced 3-fold by treatment with 100 ng/mL PMA upon transfection with luciferase plasmid immunopolyplexes. The authors claimed that 95% of the post-transfection Jurkat T cells were eGFP-positive using eGFP plasmid immunopolyplexes combined with PMA treatment, according to confocal microscopy eGFP fluorescence images. Supporting quantitative FACS data on the percentage of eGFP-positive cells were not provided in the article, making it difficult to unambiguously estimate the transfection efficiency of Jurkat T cells achieved with this approach.

The first experiment in this work was to analyze whether Jurkat T cells, chosen in this work as a model of suspension cells, can be genetically modified using the magnetofection procedure. For this purpose, we compared the ability of PEI-25<sub>Br</sub> polyplexes, Lipofectamine 2000 and DF-Gold lipoplexes and those combined with the PEI-Mag2 nanoparticles to transfect Jurkat T cells. The resulting low transfection efficiency of both the magnetic and non-magnetic vectors of polyethylenimin and Lipofectamine 2000 could be attributed to the membrane damage and apoptosis in Jurkat T cells reported by Moghimi et al. (Moghimi et al., 2005) for polyethyleneimines and to the toxicity of Lipofectamine 2000 lipoplexes (Nguyen et al., 2007). In contrast, DF-Gold lipoplexes efficiently transfected Jurkat T cells using magnetofection.

Commercial CombiMag, PolyMag and several domestic magnetic nanoparticles (either positively or negatively charged), which were associated with DNA in the presence of DF-Gold at a DF-Gold-to-plasmid v/w ratio of 4 and iron-to-DNA w/w ratio of 0.5, were tested for transfection efficiency upon magnetofection. Selected magnetic DF-Gold lipoplexes prepared at an iron-to-plasmid w/w ratio of 0.5 using NDT-Mag1, PEI-Mag1 and PalD1-Mag1 nanoparticles increased the transfection

efficiency considerably compared to lipofection without causing cell toxicity. At applied eGFP plasmid doses of 250-500 ng per 20,000 cells, up to 28% and 9% of the cells expressed eGFP post-magnetofection and post-lipofection, respectively. These results clearly show that the magnetofection procedure is a more efficient method for transfecting Jurkat T cells than other conventional transfection methods.

Lipoplexes formulated with our synthesized nanoparticles resulted in at least a 2-fold-higher percentage of eGFP-positive Jurkat T cells compared to lipoplexes formulated with commercially available CombiMag or PolyMag (see Figure 13).

In order to increase the transfection efficiency in Jurkat T cells, the magnetofection procedure was combined with some compounds that destabilize cell membranes, such as glycerol and DMSO. Glycerol has been reported to increase the transfection efficiency of ligand-coupled polyplexes in different cell lines as well as in some primary human fibroblasts under specific conditions (Zauner et al., 1996). In another study, mouse L cells were first transfected with DEAE-dextran polyplexes of the reporter gene, followed by a short, 2-min shock with 10% DMSO 4-20 h after transfection (Lopata et al., 1984). This treatment resulted in a 50-fold improvement of transgene expression. Neither glycerol nor DMSO augmented gene transfer by magnetofection in Jurkat T cells and resulted in high toxicity. These data are in agreement with the findings of Zauner et al. (Zauner et al., 1996), who observed no positive effect from a glycerol shock on transfection efficiency when using the lipid transfection reagent DOTAP, the cationic lipopolyamine Transfectam® (Zauner et al., 1996).

Once we demonstrated that the magnetofection procedure can be applied for genetic modification of Jurkat T cells, the transfection efficiency of the novel magselectofection procedure was evaluated. Transfection efficiency using the magselectofection and magnetofection procedures was comparable in terms of the percentage of transfected cells. In contrast, large differences in transfection efficiency can be seen in terms of protein expression (see Figure 25). The magnetic field of the MidiMACS magnet in the vicinity of the cells could be higher than those at the magnetic plate during the standard magnetofection procedure. The difference in the magnetic field gradient could explain why more copy numbers of pDNA are delivered into the cells using magselectofection and why those cells produce higher amounts of protein.

At this point, a proof-of-principle of the magselectofection procedure was demonstrated.

#### **4.3.2.2. Primary and stem cells**

Having established a magselectofection method yielding high target cell purity and cell recovery, as well as high efficiency and specificity of transfection/transduction with a model mixture of cell lines, its utility with primary cells remained to be proven. We chose to study human mesenchymal and hematopoietic stem cells from the umbilical cord, because these cells are relevant in ongoing and future clinical applications of genetically engineered cell therapies (Cartier and Aubourg, 2008), (Song et al., 2010), (Bordignon, 2006), (Cavazzana-Calvo and Fischer, 2007). Magselectofection of hUC-MSCs with non-viral magnetic complexes, at a low vector dose of 8 pg plasmid/cell, resulted in more than 85% cell viability and yielded 29% of the cells expressing the eGFP reporter gene 3 to 7 days post-magselectofection (see Figures 26 A and B). This compares favorably with standard transfections, as reported by Yang et al. (Yang et al., 2009), who obtained 27% transfected cells with 40 pg DNA/cell. Among the non-viral methods, only electroporation (nucleofection) was reported to be superior in terms of transfection efficiency; however, it was at the expense of cell viability (Aslan et al., 2006). Hence, magselectofection and nucleofection yield approximately the same number (about 25%) of viable genetically modified hUC-MSC from an original cell number. The transient transgene expression in hUC-MSCs observed in our experiments is in agreement with the literature (Aslan et al., 2006), (Papapetrou et al., 2005). The reason for the transient gene expression may be due to the fact that common plasmids are unable to replicate in mammalian cells and are usually rapidly lost from cells during cell division (Papapetrou et al., 2005). Stable non-viral gene delivery can be achieved using a *Streptomyces* bacteriophage-derived  $\phi$ C31 integrase. It has been recently shown that the  $\phi$ C31 integrase system could have potential for the treatment of lung diseases (Aneja et al., 2007). Unfortunately, this system did not work with hematopoietic cells (Maucksch et al., 2008).

It has been reported that using electroporation, around 16 and 5% of PBMC and HSCs were positively transfected with 1.3 pg DNA/cell, respectively, with low toxicity (< 5%) (Van Tendeloo et al., 2000). We present that an increase in the DNA dose, up to 8 pg DNA/cells, does not increase the transfection efficiency.

High efficiency was also observed for viral magselectofection of hUC-MSCs (Figure 27) and hUC-HSCs (Figure 30), which, as expected, yielded higher percentages of genetically modified cells than the non-viral counterpart. Importantly, lentiviral magselectofection performed with hUC-HSCs at a low cell density resulted in 21% eGFP-positive cells, while the standard infection failed under these conditions (Figures 30 a and c). This is relevant because a low cell number and density of hUC-HSCs reflects a situation with clinical isolates. Lentiviral magselectofection also yielded excellent results with Sca-1<sup>+</sup> Lin<sup>-</sup> mouse cells, which are used in Il2rg<sup>-/-</sup> mouse models (Orschell-Traycoff et al., 2000). Here, MOIs of only 3 during magselectofection yielded 35% to 50% transduced cells (Figures 30 d and e) compared to only 9.5% with an MOI of 5 to 8 using a standard transduction protocol for Lin<sup>-</sup> bone marrow cells, as reported previously (Cai et al., 2008).

Under optimized transduction conditions, viral magselectofection of hUC-MSCs at an MOI as low as 0.5 pfu/cell (as determined using CMS5 cells and a standard polybrene infection) resulted in 60-100% transduced cells, depending on the donor (Figure 27). Reporter gene expression upon lentiviral magselectofection in hUC-MSCs was stably maintained for one month for most of the donors, whereas for some of the donors a gradual decrease in the transgene expression was observed (Figure 27 B, left graph). Significant inter-donor variations in the transduction efficiency and in the persistence of transgene expression for hUC-MSCs have previously been reported (Kyriakou et al., 2006), (Pannell et al., 2000). A similarly high transduction efficiency to that obtained with lentiviral magselectofection of hUC-MSCs was reported earlier, but only for infection at a high MOI of 20 (Koponen et al., 2007). The cell viability upon adenoviral or lentiviral magselectofection was high (> 85% living cells). The apparently paradoxical result of achieving 100% transduction for hUC-MSCs at 0.5 MOI clearly demonstrates that the infectivity of the virus is determined by both the concentration of infectious particles in the preparation and the internalization efficiency of the particles. This suggests that the measured virus titers are highly dependent on the method of virus titration. Magnetofection and magselectofection lead to rapid contact between the target cells and the applied vector dose ((Furlani and Ng, 2008) and Figure 19) and also lead to improved vector uptake ((Mykhaylyk et al., 2010) and figures 17 and 21). With standard protocols, transfection/transduction kinetics and efficiency are dominated by diffusion (Luo and Saltzman, 2000). Hence, protocols that do not promote vector-target cell contact will

necessarily lead to an underestimation of biological vector titers. We propose that magselectofection or magnetofection can be used as a tool to estimate the biological virus titers more realistically.

Importantly, as shown in Figures 26 and 28, the differentiation potential of hUC-MSCs into an osteogenic lineage was not impaired by the magselectofection procedure. Our results are in accordance with those obtained by Kalajzic et al. (Kalajzic et al., 2001), who demonstrated that VSV-G pseudotypes retroviral vectors are suitable for introducing genes into osteoprogenitor cells without affecting osteoprogenitor lineage progression. The same result was observed with hCB-HSCs (see Figure 30). This is important, especially considering that cellular engineering with stem cells has the potential to be used to cure diseases like SCID or used for bone or myocardial regeneration.

Our findings suggest that magselectofection yields superior results to many other transfection/transduction procedures (see Figure 34), and it is broadly applicable with non-viral and viral vectors. It is already known that the application of a gradient magnetic field to different cell lines can deliver a high concentration of transfection vectors at the cell membrane (Huth et al., 2004), (Mykhaylyk et al., 2009b), (Mykhaylyk et al., 2010). Enhancement of viral gene delivery to suspension cells using magnetofection with cationic chitosan-coated iron oxide nanoparticles has also been reported (Bhattarai et al., 2008). This could explain why magselectofection and magnetofection are more efficient than standard infection procedures. Interestingly, adenoviral magselectofection outperformed the same procedure carried out in a 2-dimensional format (magnetofection) (see Figure 34). This may be due to the stronger magnetic forces prevailing in a high gradient field magnetic separation column, and also to the high concentration of “reactants” (vectors and cells) under magselectofection conditions.

#### *4.4. Internalization of the magnetic complexes*

Our results imply that the magnetic nanoparticles not only play a “vehicle” role, by enhancing internalization and increasing the intracellular concentration of the plasmid, but can also stimulate endosomal escape, modulate further turnover of the complexes, stabilize the plasmid and ultimately increase the transfection efficiency. This statement is supported by the fact that magnetofection results in a 1.5-fold

increase in the percentage of cells that have internalized the complexes, but leads to a 3- to 4.5-fold enhancement in transgene expression levels, depending on the type of particles used to formulate the complexes. Up to 50 and 60% of the Jurkat T cells had internalized the magnetic complexes 48 h post-magselectofection or magnetofection, respectively, and up to 45% of the cells internalized the non-magnetic lipoplexes (see Figure 17 and 21). In addition, up to 28-30% and 9% of the Jurkat T cells express the eGFP reporter gene post-magnetofection/magselectofection and post-lipofection, respectively. Moreover, in our results one can see that magnetic complexes formulated with SO-Mag2, PEI-Mag2 and PEI-Mag 3 magnetic nanoparticles are equally internalized into Jurkat T cells (see Figure 25). However, transfection efficiency is different for each one. Indeed, slight differences in the surface composition of the particles lead to differences in the percentage of reporter-expressing cells and the level of transgene expression (Figure 13 and 25). Sauer et al. (Sauer et al., 2009) reported that the increase in transfection efficiency using magnetofection is suggested to be caused by an increased amount of complexes bound to the cell surface, because magnetofection does not seem to influence the internalization mechanics, and magnetofection does not seem to induce efficient endosomal release. Pradhan et al. (Pradhan et al., 2010) recently showed that no enhancing effect from folate receptor targeting was observed in FACS analysis of uptake in both KB and HeLa cells, unless the uptake was supported by magnetic targeting. In this work, it is shown that when biologic and magnetic targeting were combined, the enhancement of uptake was synergistic, being about 8-fold in KB and 42-fold in HeLa cells. Other authors have recently reported (Kim et al., 2008), (Yang et al., 2008) that the uptake can be enhanced due to the combined effects of receptor targeting and a magnetic field on the cellular uptake of folate-targeted multifunctional compositions comprising magnetic nanoparticles and doxorubicin.

Internalization experiments for magnetic virus complexes were not performed. Nevertheless, the difference in transduction efficiency observed using standard infection, magnetofection and the magselectofection procedure is indicative of an unequal internalization efficiency or internalization pathway of the virus particles. A magnetic field can deliver a high concentration of transfection vectors at the cell membrane, and this can explain why magselectofection and magnetofection are more efficient than the standard infection procedure. The high magnetic field gradient of the MidiMACS magnet used for magselectofection can lead a higher concentration

of magnetic complexes to the cells than is achieved using magnetofection, which leads to higher internalization of virus particles.

#### *4.5. Critical parameters in optimizing magselectofection*

The data in Figure 24 D show that the addition of the magnetic complex before the cells were loaded on the column gave the best transfection results. A white-powder was observed in the surround of the beginning of the column after a 30-minute incubation time at the MidiMACS magnet when the cells were added to the column before the complex. This powder corresponds to the dried complex. An explanation for this phenomenon could be that the column is blocked when the cells are added. Then, when the magnetic complex solution is applied, it cannot diffuse through the column. Hence, the cells are not in contact with the magnetic complexes. We also observed that increasing the number of target cells used for transfection in the LS columns resulted in a reduction in transfection efficiency, possibly due to the fact that the DNA becomes limited. If the number of cells is increased, the amount of vector also has to be increased. However, our results imply that higher amounts of DNA improved transfection efficiencies, although a high level of toxicity was detected (> 30%) (Figure 24 A). Thus, there is a need to find a balance between transfection efficiency and toxicity.

In this work, a 30-min incubation time on the column was found to be enough to achieve successful transfection efficiency. Longer incubation times at the MidiMACS magnet not only did not increase the transfection efficiency, but actually decreased it. It is possible that long incubation times on the column become toxic for the cells.

Scaling up from an LS to an XS column and CliniMACS device is possible (see Figures 35 and 37). It should be noted that while the cell number to be transfected in the XS columns has been increased by a factor 10, the amount of transfection complex has only been increased by a factor of 4, while the total column volume is in fact 18 times larger. These variables should be further investigated to see whether additional performance increases in XS columns are possible. The current partial reagent upscale was chosen mainly to limit the reagent consumption. XS columns are chosen for magnetic cell separation using the CliniMACS device. Further modification of the CliniMACS device will allow rapid and efficient genetic modification of the target cell line directly at the separation column. The only protocol

difference between the XS column process and the CliniMACS process is that a wash step occurs before the elution of the magselectofected cells. If this wash step is too rigorous, it could account for the reduction in transfection efficiencies. This factor could be eliminated by suitable changes to the CliniMACS software.

#### *4.6. Other applications of magselectofection*

Magselectofection is not only a promising integrated procedure for combined magnetic cell separation and genetic modification, but also a versatile and highly efficient tool for transfecting/transducing cell lines and primary monocell cultures. For this purpose, magnetic cell labeling of the entire cell population can also be carried out in a non-specific manner, as described previously (Wilhelm and Gazeau, 2008) (Mykhaylyk et al., 2009b). For example, labeling of hUC-MSCs with SO-Mag2 nanoparticles before magselectofection resulted in a two-fold increase in the percentage of transduced cells compared to magselectofection of the same cells labeled with CD105 MicroBeads (see Figure 38), presumably due to the limited availability of the target CD105 cell surface molecule. The increase in transfection efficiency observed after magnetically labeling the cells may be due to the fact that the magnetic moment of the labeled cells in the applied magnetic field increases the local gradient of the field in the vicinity of the cell. In this way, it may exert enough force on the neighboring magnetic vectors to magnetize them and, as a result, be attracted to the cell surface (the so-called avalanche effect). This phenomena was utilized in another context (Avilés et al., 2009) to improve the targeting of magnetic drugs using insertable or implantable ferromagnetic elements, such as wires, needles, catheters, or stents, to increase the magnetic force locally by increasing the gradient of the field close to the cell. As a consequence of this effect, the magnetic vectors are not only sedimented at the cell surface when they are incubated in magnetic field gradients, but they are also further extracted from the surroundings when the field is removed. This leads to the appearance of an “exhausted area” in the vicinity of the cell surface.

We demonstrate that the magselectofection procedure allows us to magnetically label and genetically modify hUC-MSCs. Cells manipulated in this manner can be used for a variety of purposes, such as magnetic positioning and magnetically-enforced engraftment in target tissues, which is potentially useful in delivering cell-based therapies (Wilhelm et al., 2007), (Mykhaylyk et al., 2009b), (Hofmann et al., 2009).



Mykhaylyk et al. (Mykhaylyk et al., 2009b) showed that the magnetic responsiveness of H441 cells loaded with NDT-Mag1 MNPs (20-38 pg Fe/cell) was sufficient to engraft these magnetically-labeled cells onto the luminal surface of a 3D cell culture system (tube). Moreover, cell loading of 38 pg Fe/cell of NDT-Mag1 MNPs resulted in high transverse relaxivities  $r_2^*$ , thus allowing the MRI detection of cell concentrations that were equivalent to (or higher than) 1.2  $\mu\text{g Fe/mL}$ .

A critical factor for determining the therapeutic efficacy is whether transplanted cells can home into the injured site. Therefore, it is crucial to monitor stem cell behavior in real time in live tissues. Recently, Cao et al. (Cao et al., 2009) have established a novel 7T micromagnetic resonance imaging (7T micro-MR) system specifically designed for small animals that enables imaging with high contrast and excellent spatiotemporal resolution up to micrometers in size. In this way, rat bone marrow mesenchymal cells (BMSCs) were isolated and cultured, subsequently dual-labeled with magnetic SPIO nanoparticle and fluorescent Dil dye *in vitro*, and transplanted into recipient animals in a posterior homing study. In another study (Loebinger et al., 2009), MSCs were labeled *in vitro* with superparamagnetic iron oxide nanoparticles and injected into the lateral tail vein of mice at day 35 after cancer models had been initiated. Then, MRI to track the MSCs to lung metastases *in vivo* was performed. This work demonstrated that labeling of MSCs with iron oxide nanoparticles has the potential to show MSC integration into human tumors, allowing early-phase clinical studies examining MSC homing in patients with metastatic tumors (Loebinger et al., 2009). These studies show how MRI allows dynamic monitoring of magnetically-labeled stem cells following transplantation and provides a feasible method to evaluate biological behaviors of transplanted cells during cell-based therapy. Moreover, targeted technologies may become an important adjuvant to the use of ionizing radiation and chemotherapeutic agents, opening up a variety of possibilities for the future of cancer treatment.

We demonstrated that non-heme iron analysis is a powerful tool to study cell biodistribution (Tables 6 and 7; Figures 40 and 44). The histological analysis by fluorescence microscopy (Figure 41) revealed that the percentage of positively infected cells is enough to find them in lungs, followed by spleen, kidney and liver. We found that hUC-MSCs were loaded with 28.3 pg Fe/cell. From our studies

(Mykhaylyk et al., 2009a), we can conclude that we will be able to monitor hUC-MSCs by MR imaging.

#### 4.7. Conclusions

During this work, a novel non-viral and viral technology for *ex vivo* gene therapy has been established. Magselectofection is a versatile integrated procedure of cell sorting and genetic modification. Highly efficient magnetic vectors have been designed and selected. The comprehensive characterization of nanoparticles with controlled surface properties provided here can be used for the further development of new magnetic nanoparticles and vectors containing particles for the genetic modification of cells that are difficult to transfect. Further development may include a search for new MNPs and modification of particles with affine molecules to formulate magnetic vectors.

During this work, a vector loading column procedure which allows magnetic vector immobilization on Miltenyi columns and association with/internalization into target cells has been developed. With a minimal number of *ex vivo* handling steps, and with low vector consumption, magselectofection yields high target cell purity and recovery of target cells with excellent cell viability and biological functionality. Moreover, we demonstrate that genetic modification using magselectofection is specific to the target cells. Using viral and non-viral magselectofection, a high efficiency in genetic modification of hUC-MSCs, hCB-HSCs and hPBMCs can be achieved. Furthermore, the differentiation potential of the genetically modified stem cells is not impaired.

Magselectofection is not only a promising integrated procedure for combined magnetic cell separation and genetic modification but is also a versatile and highly efficient tool for transfecting/transducing cell line populations and primary monocell cultures.

We demonstrate that the magselectofection procedure allows us to label cells magnetically. Cells manipulated in this manner can be used for a variety of purposes, such as magnetic positioning and magnetically enforced engraftment in target tissues, which is potentially useful in delivering cell-based therapies. Moreover, we expect that the behavior of magnetically-labeled cells after magselectofection can be monitored (by MRI) in real time in live tissues.

As magnetic cell sorting is already implemented in an automated manner and approved for some clinical applications, we envision that magselectofection can become an affordable and standardized tool for future cell therapies involving genetically engineered cells.

## 5. SUMMARY

Research applications and cell therapies involving genetically modified cells require reliable, standardized and cost-effective methods for cell manipulation. The goal of this work is to provide a novel methodology that produces, in a single standardized technology, genetic modification and cell isolation. We have named this novel procedure “Magselectofection”. The approach is based on magnetic cell separation and magnetically-guided gene delivery (magnetofection). Optimized gene vectors associated with novel magnetic nanoparticles were formulated to transfect/transduce target cells while they are passaged and separated through a high gradient magnetic field cell separation column. Magnetofection of the Jurkat T cells using selected vector formulations resulted in a significant (up to 4.5-fold) enhancement in both luciferase reporter gene expression and the percentage of cells expressing eGFP, as compared to lipofection. A procedure for vector loading on LS Miltenyi columns was developed that enables up to 100% retention for both non-viral and viral magnetic complexes. We demonstrate, using a model cell mixture of K562 and Jurkat T cells, that the integrated method is highly efficient and specific for the target cell population. This was not only true for the model Jurkat/K562 mixture, but also for Sca-1<sup>+</sup> mouse hematopoietic stem cells. With human umbilical cord mesenchymal stem cells (hUC-MSCs), we achieve up to 30% transfected cells with non-viral vector doses as low as 8 pg plasmid DNA per cell and up to 100% transduced cells with a multiplicity of infection of 0.5 TU/cell using lentivirus. Similarly, we obtain 22% eGFP-positive human cord blood hematopoietic stem cells (hCB-HSCs) upon lentiviral magselectofection compared to 0.15% eGFP-positive cells post-standard infection. We achieve up to 50% transduced Sca-1<sup>+</sup> mouse stem cells at a lentiviral MOI of 1-3. Up to 5-15% and 20% genetic modified PBMC were found using non-viral and viral magselectofection, respectively. After genetic modification using magselectofection differentiation potential of hCB-HSCs and hUC-MSCs was maintained. Magselectofection requires a minimal number of manipulation steps and results in efficient and specific gene delivery to target cells. This minimizes the necessary vector material while maintaining the cellular differentiation potential of modified stem cells. Magselectofection may become a useful tool for nucleic acid therapy approaches involving ex-vivo genetically modified cells.

## 6. ABBREVIATIONS

AAV	adeno-associated virus
ADA	adenosine desaminase
Ads	Adenovirus
ATCC	American Type Culture Collection
BSA	bovine serum albumin
CBMC	cord blood mononuclear cell
CFC	colony forming cell
CGD	chronic granulomatous disease
CMV	cytomegalovirus
DF-Gold	Dreamfect-Gold
DNA	Deoxyribonucleic acid
DMEM	Dulbecco's Minimum Essential Medium
DMSO	dimethyl sulfoxide
DSMZ	Deutsche Sammlung von Mikroorganismen und Zellkulturen
DRK	Deutsches Rotes Kreuz
<i>E. coli</i>	<i>Escherichia coli</i>
EDTA	ethylene diamine tetraacetic acid
e.g.	for example (abbr.of latin <i>exempli gratia</i> )
eGFP	enhanced Green Fluorescent Protein
ELISA	Enzyme-Linked ImmunoSorbent Assay
<i>env</i>	„envelope“ gene encoding for viral core glycoproteins
FACS	Fluorescence Activated Cell Sorter
FBS	fetal bovine serum
FCS	fetal calf serum
fg	femtogramm
FITC	fluorescein isothiocyanate
FIV	feline immunodeficiency virus
Flt3	FMS-like tyrosine kinase 3
FSA	fluorinated surfactant
<i>gag</i>	„group-specific antigen“ gene encoding for core structural proteins
GFP	Green Fluorescent Protein
HBS	HEPES Buffered Saline

---

HEK	Human embryonic kidney cells
HEPES	N-2-hydroxyethylpiperazine-Ni-2-ethanesulfonic acid
HIV	human immunodeficiency virus
hPBMCs	human peripheral blood mononuclear cells
HLA	Human leukocyte antigen
HSC	hematopoietic stem cells
hCB-HSCs	human cord blood haematopoietic stem cells
hUC-MSCs	human umbilical cord mesenchymal stem cells
kDa	kilo Dalton
LCA	Leber's congenital amaurosis
LV	lentiviral vector
LVP	lentiviral particle
MACS®	magnetic cell separation
MOI	multiplicity of infection
MNP	magnetic nanoparticle
MSC	mesenchymal stem cell
mRNA	messenger ribonucleic acid
MRI	magnetic resonance imaging
MTT	methylthiazoyldiphenyl-tetrazolium
mV	millivolt
PBS	Phosphate Buffered Saline
PE	phycoerythrin
PEI	polyethylenimine
PEI <sub>Br</sub>	branched polyethylenimine
pfu	plaque forming unit
PI	propidium iodide
<i>pol</i>	„polymerase“ gene encoding for viral polymerase
rcf	relative centrifugal force
Rev	regulator of expression of virion proteins
RNA	Ribonucleic acid
rpm	rounds per minute
RPMI	Roswell Park Memorial Institute
RT	room temperature
SCF	Stem cell factor

---

SCID-X1	X-linked severe combined immune deficiency
SDS	sodium dodecyl sulfate
SIN	self inactivating
siRNA	small interfering ribonucleic acid
SIV	Simian immunodeficiency viruses
S/MARs	scaffold/matrix attachment regions
SV40	Simian Virus 40
T	Tesla
TCR	T-cell receptors
TPO	Thrombopoietin
TU	transducing units
untx	untreated (negative control)
VP	virus particle
VSV-G	envelope glycoprotein G from Vesicular stomatitis virus
w/v	percentage solution

## 7. REFERENCES

- Aiuti, A., Cattaneo, F., Galimberti, S., Benninghoff, U., Cassani, B., Callegaro, L., Scaramuzza, S., Andolfi, G., Mirolo, M., Brigida, I., *et al.* (2009). Gene therapy for immunodeficiency due to adenosine deaminase deficiency. *N Engl J Med* **360**, 447-458.
- Andre, F. M., Gehl, J., Sersa, G., Preat, V., Hojman, P., Eriksen, J., Golzio, M., Cemazar, M., Pavselj, N., Rols, M. P., *et al.* (2008). Efficiency of high- and low-voltage pulse combinations for gene electrotransfer in muscle, liver, tumor, and skin. *Hum Gene Ther* **19**, 1261-1271.
- Aneja, M. K., Imker, R., and Rudolph, C. (2007). Phage phiC31 integrase-mediated genomic integration and long-term gene expression in the lung after nonviral gene delivery. *J Gene Med* **9**, 967-975.
- Antoine, C., Muller, S., Cant, A., Cavazzana-Calvo, M., Veys, P., Vossen, J., Fath, A., Heilmann, C., Wulffraat, N., Seger, R., *et al.* (2003). Long-term survival and transplantation of haemopoietic stem cells for immunodeficiencies: report of the European experience 1968-99. *Lancet* **361**, 553-560.
- Aslan, H., Zilberman, Y., Arbeli, V., Sheyn, D., Matan, Y., Liebergall, M., Li, J. Z., Helm, G. A., Gazit, D., and Gazit, Z. (2006). Nucleofection-based ex vivo nonviral gene delivery to human stem cells as a platform for tissue regeneration. *Tissue Eng* **12**, 877-889.
- Avilés, M. O., Ebner, A. D., and Ritter, J. A. (2009). In vitro study of magnetic particle seeding for implant-assisted-magnetic drug targeting: Seed and magnetic drug carrier particle capture. *Journal of Magnetism and Magnetic Materials* **321**, 1586.
- Bainbridge, J. W., Smith, A. J., Barker, S. S., Robbie, S., Henderson, R., Balaggan, K., Viswanathan, A., Holder, G. E., Stockman, A., Tyler, N., *et al.* (2008). Effect of gene therapy on visual function in Leber's congenital amaurosis. *N Engl J Med* **358**, 2231-2239.
- Barry, S. C., Harder, B., Brzezinski, M., Flint, L. Y., Seppen, J., and Osborne, W. R. (2001). Lentivirus vectors encoding both central polypurine tract and posttranscriptional regulatory element provide enhanced transduction and transgene expression. *Hum Gene Ther* **12**, 1103-1108.
- Baum, C., Dullmann, J., Li, Z., Fehse, B., Meyer, J., Williams, D. A., and von Kalle, C. (2003). Side effects of retroviral gene transfer into hematopoietic stem cells. *Blood* **101**, 2099-2114.
- Bhattacharai, S. R., Kim, S. Y., Jang, K. Y., Lee, K. C., Yi, H. K., Lee, D. Y., Kim, H. Y., and Hwang, P. H. (2008). Laboratory formulated magnetic nanoparticles for enhancement of viral gene expression in suspension cell line. *Journal of virological methods* **147**, 213-218.
- Blaese, R. M., Culver, K. W., Miller, A. D., Carter, C. S., Fleisher, T., Clerici, M., Shearer, G., Chang, L., Chiang, Y., Tolstoshev, P., *et al.* (1995). T lymphocyte-directed gene therapy for ADA- SCID: initial trial results after 4 years. *Science* **270**, 475-480.
- Blessing, T., Kursa, M., Holzhauser, R., Kircheis, R., and Wagner, E. (2001). Different strategies for formation of pegylated EGF-conjugated PEI/DNA complexes for targeted gene delivery. *Bioconjug Chem* **12**, 529-537.



- Boeckle, S., Wagner, E., and Ogris, M. (2005). C- versus N-terminally linked melittin-polyethylenimine conjugates: the site of linkage strongly influences activity of DNA polyplexes. *J Gene Med* 7, 1335-1347.
- Bordignon, C. (2006). Stem-cell therapies for blood diseases. *Nature* 441, 1100-1102.
- Boussif, O., Lezoualc'h, F., Zanta, M. A., Mergny, M. D., Scherman, D., Demeneix, B., and Behr, J. P. (1995). A versatile vector for gene and oligonucleotide transfer into cells in culture and in vivo: polyethylenimine. *Proc Natl Acad Sci U S A* 92, 7297-7301.
- Brunner, S., Furtbauer, E., Sauer, T., Kursa, M., and Wagner, E. (2002). Overcoming the nuclear barrier: cell cycle independent nonviral gene transfer with linear polyethylenimine or electroporation. *Mol Ther* 5, 80-86.
- Brunner, S., Sauer, T., Carotta, S., Cotten, M., Saltik, M., and Wagner, E. (2000). Cell cycle dependence of gene transfer by lipoplex, polyplex and recombinant adenovirus. *Gene Ther* 7, 401-407.
- Cai, S., Ernstberger, A., Wang, H., Bailey, B. J., Hartwell, J. R., Sinn, A. L., Eckermann, O., Linka, Y., Goebel, W. S., Hanenberg, H., and Pollok, K. E. (2008). In vivo selection of hematopoietic stem cells transduced at a low multiplicity-of-infection with a foamy viral MGMT(P140K) vector. *Experimental hematology* 36, 283-292.
- Cao, A. H., Shi, H. J., Zhang, Y., and Teng, G. J. (2009). In vivo tracking of dual-labeled mesenchymal stem cells homing into the injured common carotid artery. *Anat Rec (Hoboken)* 292, 1677-1683.
- Cartier, N., and Aubourg, P. (2008). Hematopoietic stem cell gene therapy in Hurler syndrome, globoid cell leukodystrophy, metachromatic leukodystrophy and X-adrenoleukodystrophy. *Curr Opin Mol Ther* 10, 471-478.
- Castel-Barthe, M. N., Jazat-Poindessous, F., Barneoud, P., Vigne, E., Revah, F., Mallet, J., and Lamour, Y. (1996). Direct intracerebral nerve growth factor gene transfer using a recombinant adenovirus: effect on basal forebrain cholinergic neurons during aging. *Neurobiol Dis* 3, 76-86.
- Cavazzana-Calvo, M., and Fischer, A. (2007). Gene therapy for severe combined immunodeficiency: are we there yet? *J Clin Invest* 117, 1456-1465.
- Cavazzana-Calvo, M., Lagresle, C., Hacein-Bey-Abina, S., and Fischer, A. (2005). Gene therapy for severe combined immunodeficiency. *Annu Rev Med* 56, 585-602.
- Cengizeroglu, A. (2008). Establishment of lentiviral magnetofection and magselectofection in adherent and suspension cells. Master thesis.
- Chan, L., Nesbeth, D., Mackey, T., Galea-Lauri, J., Gaken, J., Martin, F., Collins, M., Mufti, G., Farzaneh, F., and Darling, D. (2005). Conjugation of lentivirus to paramagnetic particles via nonviral proteins allows efficient concentration and infection of primary acute myeloid leukemia cells. *J Virol* 79, 13190-13194.
- Clay, T. M., Custer, M. C., Spiess, P. J., and Nishimura, M. I. (1999). Potential use of T cell receptor genes to modify hematopoietic stem cells for the gene therapy of cancer. *Pathol Oncol Res* 5, 3-15.

- Cohen, C. J., Li, Y. F., El-Gamil, M., Robbins, P. F., Rosenberg, S. A., and Morgan, R. A. (2007). Enhanced antitumor activity of T cells engineered to express T-cell receptors with a second disulfide bond. *Cancer Res* 67, 3898-3903.
- Conese, M., Auriche, C., and Ascenzioni, F. (2004). Gene therapy progress and prospects: episomally maintained self-replicating systems. *Gene Ther* 11, 1735-1741.
- Conwell, C. C., Liu, F., and Huang, L. (2008). Several serum proteins significantly decrease inflammatory response to lipid-based non-viral vectors. *Mol Ther* 16, 370-377.
- Cooper, L. J., Kalos, M., Lewinsohn, D. A., Riddell, S. R., and Greenberg, P. D. (2000). Transfer of specificity for human immunodeficiency virus type 1 into primary human T lymphocytes by introduction of T-cell receptor genes. *J Virol* 74, 8207-8212.
- Dahm, R. (2005). Friedrich Miescher and the discovery of DNA. *Dev Biol* 278, 274-288.
- de Bruin, K. G., Fella, C., Ogris, M., Wagner, E., Ruthardt, N., and Brauchle, C. (2008). Dynamics of photoinduced endosomal release of polyplexes. *J Control Release* 130, 175-182.
- Dobson, J. (2006). Gene therapy progress and prospects: magnetic nanoparticle-based gene delivery. *Gene Ther* 13, 283-287.
- Dudley, M. E., Wunderlich, J. R., Yang, J. C., Sherry, R. M., Topalian, S. L., Restifo, N. P., Royal, R. E., Kammula, U., White, D. E., Mavroukakis, S. A., *et al.* (2005). Adoptive cell transfer therapy following non-myeloablative but lymphodepleting chemotherapy for the treatment of patients with refractory metastatic melanoma. *J Clin Oncol* 23, 2346-2357.
- Dunbar, C. E., and Larochele, A. (2010). Gene therapy activates EVI1, destabilizes chromosomes. *Nat Med* 16, 163-165.
- Editorial (2003). Express delivery. *Nat Med* 9, 977.
- Ellery, J. M., and Nicholls, P. J. (2002). Possible mechanism for the alpha subunit of the interleukin-2 receptor (CD25) to influence interleukin-2 receptor signal transduction. *Immunol Cell Biol* 80, 351-357.
- Engelhardt, J. F., Litzky, L., and Wilson, J. M. (1994). Prolonged transgene expression in cotton rat lung with recombinant adenoviruses defective in E2a. *Hum Gene Ther* 5, 1217-1229.
- Fahrmeir, J., Gunther, M., Tietze, N., Wagner, E., and Ogris, M. (2007). Electrophoretic purification of tumor-targeted polyethylenimine-based polyplexes reduces toxic side effects in vivo. *J Control Release* 122, 236-245.
- Farag, S. S. (2002). Therapeutic applications of immunomagnetic cell selection: A review. *Eur Cells Mater* 3, 37-40.
- Felgner, P. L. (1997). Nonviral strategies for gene therapy. *Sci Am* 276, 102-106.
- Fella, C., Walker, G. F., Ogris, M., and Wagner, E. (2008). Amine-reactive pyridylhydrazone-based PEG reagents for pH-reversible PEI polyplex shielding. *Eur J Pharm Sci* 34, 309-320.
- Floch, V., Le Bolc'h, G., Audrezet, M. P., Yaouanc, J. J., Clement, J. C., des Abbayes, H., Mercier, B., Abgrall, J. F., and Ferec, C. (1997). Cationic phosphonolipids as non viral

vectors for DNA transfection in hematopoietic cell lines and CD34+ cells. *Blood Cells Mol Dis* 23, 69-87.

Furlani, E. P., and Ng, K. C. (2008). Nanoscale magnetic biotransport with application to magnetofection. *Phys Rev E Stat Nonlin Soft Matter Phys* 77, 061914.

Godbey, W. T., Wu, K. K., and Mikos, A. G. (1999). Tracking the intracellular path of poly(ethylenimine)/DNA complexes for gene delivery. *Proc Natl Acad Sci U S A* 96, 5177-5181.

Goverdhana, S., Puntel, M., Xiong, W., Zirger, J. M., Barcia, C., Curtin, J. F., Soffer, E. B., Mondkar, S., King, G. D., Hu, J., *et al.* (2005). Regulatable gene expression systems for gene therapy applications: progress and future challenges. *Mol Ther* 12, 189-211.

Guilbert, L. J., and Iscove, N. N. (1976). Partial replacement of serum by selenite, transferrin, albumin and lecithin in haemopoietic cell cultures. *Nature* 263, 594-595.

Guillem, V. M., Tormo, M., Revert, F., Benet, I., Garcia-Conde, J., Crespo, A., and Alino, S. F. (2002). Polyethyleneimine-based immunopolyplex for targeted gene transfer in human lymphoma cell lines. *J Gene Med* 4, 170-182.

Hacein-Bey-Abina, S., Garrigue, A., Wang, G. P., Soulier, J., Lim, A., Morillon, E., Clappier, E., Caccavelli, L., Delabesse, E., Beldjord, K., *et al.* (2008). Insertional oncogenesis in 4 patients after retrovirus-mediated gene therapy of SCID-X1. *J Clin Invest* 118, 3132-3142.

Hacein-Bey-Abina, S., von Kalle, C., Schmidt, M., Le Deist, F., Wulffraat, N., McIntyre, E., Radford, I., Villeval, J. L., Fraser, C. C., Cavazzana-Calvo, M., and Fischer, A. (2003). A serious adverse event after successful gene therapy for X-linked severe combined immunodeficiency. *N Engl J Med* 348, 255-256.

Haj-Ahmad, Y., and Graham, F. L. (1986). Development of a helper-independent human adenovirus vector and its use in the transfer of the herpes simplex virus thymidine kinase gene. *J Virol* 57, 267-274.

Hawley, R. G. (2001). Progress toward vector design for hematopoietic stem cell gene therapy. *Curr Gene Ther* 1, 1-17.

Hoare, M., Greiser, U., Schu, S., Mashayekhi, K., Aydogan, E., Murphy, M., Barry, F., Ritter, T., and O'Brien, T. (2010). Enhanced lipoplex-mediated gene expression in mesenchymal stem cells using reiterated nuclear localization sequence peptides. *J Gene Med*.

Hofmann, A., Wenzel, D., Becher, U. M., Freitag, D. F., Klein, A. M., Eberbeck, D., Schulte, M., Zimmermann, K., Bergemann, C., Gleich, B., *et al.* (2009). Combined targeting of lentiviral vectors and positioning of transduced cells by magnetic nanoparticles. *Proc Natl Acad Sci U S A* 106, 44-49.

Horellou, P., Vigne, E., Castel, M. N., Barneoud, P., Colin, P., Perricaudet, M., Delaere, P., and Mallet, J. (1994). Direct intracerebral gene transfer of an adenoviral vector expressing tyrosine hydroxylase in a rat model of Parkinson's disease. *Neuroreport* 6, 49-53.

Hughes, C., Galea-Lauri, J., Farzaneh, F., and Darling, D. (2001). Streptavidin paramagnetic particles provide a choice of three affinity-based capture and magnetic concentration strategies for retroviral vectors. *Mol Ther* 3, 623-630.

- Huth, S., Lausier, J., Gersting, S. W., Rudolph, C., Plank, C., Welsch, U., and Rosenecker, J. (2004). Insights into the mechanism of magnetofection using PEI-based magnetofectins for gene transfer. *J Gene Med* 6, 923-936.
- Hyndman, L., Lemoine, J. L., Huang, L., Porteous, D. J., Boyd, A. C., and Nan, X. (2004). HIV-1 Tat protein transduction domain peptide facilitates gene transfer in combination with cationic liposomes. *J Control Release* 99, 435-444.
- Ikeda, Y., Yonemitsu, Y., Miyazaki, M., Kohno, R., Murakami, Y., Murata, T., Tabata, T., Ueda, Y., Ono, F., Suzuki, T., *et al.* (2009). Stable retinal gene expression in nonhuman primates via subretinal injection of SIVagm-based lentiviral vectors. *Hum Gene Ther* 20, 573-579.
- Isalan, M., Santori, M. I., Gonzalez, C., and Serrano, L. (2005). Localized transfection on arrays of magnetic beads coated with PCR products. *Nat Methods* 2, 113-118.
- Jenke, B. H., Fetzer, C. P., Stehle, I. M., Jonsson, F., Fackelmayer, F. O., Conradt, H., Bode, J., and Lipps, H. J. (2002). An episomally replicating vector binds to the nuclear matrix protein SAF-A in vivo. *EMBO Rep* 3, 349-354.
- Kadota, S., Kanayama, T., Miyajima, N., Takeuchi, K., and Nagata, K. (2005). Enhancing of measles virus infection by magnetofection. *Journal of virological methods* 128, 61-66.
- Kalajzic, I., Stover, M. L., Liu, P., Kalajzic, Z., Rowe, D. W., and Lichtler, A. C. (2001). Use of VSV-G pseudotyped retroviral vectors to target murine osteoprogenitor cells. *Virology* 284, 37-45.
- Kaneko, S., Mastaglio, S., Bondanza, A., Ponzoni, M., Sanvito, F., Aldrighetti, L., Radrizzani, M., La Seta-Catamancio, S., Provasi, E., Mondino, A., *et al.* (2009). IL-7 and IL-15 allow the generation of suicide gene-modified alloreactive self-renewing central memory human T lymphocytes. *Blood* 113, 1006-1015.
- Kappes, J. C., and Wu, X. (2001). Safety considerations in vector development. *Somat Cell Mol Genet* 26, 147-158.
- Kichler, A., Leborgne, C., Coeytaux, E., and Danos, O. (2001). Polyethylenimine-mediated gene delivery: a mechanistic study. *J Gene Med* 3, 135-144.
- Kim, J., Lee, J. E., Lee, S. H., Yu, J. H., Lee, J. H., Park, T. G., and Hyeon, T. (2008). Designed Fabrication of a Multifunctional Polymer Nanomedical Platform for Simultaneous Cancer- Targeted Imaging and Magnetically Guided Drug Delivery. *Advanced Materials* 20, 478-483.
- Klein, C., and Baum, C. (2004). Gene therapy for inherited disorders of haematopoietic cells. *Hematol J* 5, 103-111.
- Koponen, J. K., Kekarainen, T., S, E. H., Laitinen, A., Nystedt, J., Laine, J., and Yla-Herttuala, S. (2007). Umbilical cord blood-derived progenitor cells enhance muscle regeneration in mouse hindlimb ischemia model. *Mol Ther* 15, 2172-2177.
- Kowalski, J. B., and Tallentire, A. (1999). Substantiation of 25 kGy as a sterilization dose: a rational approach to establishing verification dose. *Radiat Phys Chem* 54, 55-64.

- Kronick, P. L., Campbell, G. L., and Joseph, K. (1978). Magnetic microspheres prepared by redox polymerization used in a cell separation based on gangliosides. *Science* *200*, 1074-1076.
- Kyriakou, C. A., Yong, K. L., Benjamin, R., Pizzey, A., Dogan, A., Singh, N., Davidoff, A. M., and Nathwani, A. C. (2006). Human mesenchymal stem cells (hMSCs) expressing truncated soluble vascular endothelial growth factor receptor (tsFlk-1) following lentiviral-mediated gene transfer inhibit growth of Burkitt's lymphoma in a murine model. *J Gene Med* *8*, 253-264.
- Lee, C. H., Kim, E. Y., Jeon, K., Tae, J. C., Lee, K. S., Kim, Y. O., Jeong, M. Y., Yun, C. W., Jeong, D. K., Cho, S. K., *et al.* (2008). Simple, efficient, and reproducible gene transfection of mouse embryonic stem cells by magnetofection. *Stem Cells Dev* *17*, 133-141.
- Lewis, P. F., and Emerman, M. (1994). Passage through mitosis is required for oncoretroviruses but not for the human immunodeficiency virus. *J Virol* *68*, 510-516.
- Li, W., Ishida, T., Okada, Y., Oku, N., and Kiwada, H. (2005). Increased gene expression by cationic liposomes (TFL-3) in lung metastases following intravenous injection. *Biol Pharm Bull* *28*, 701-706.
- Liu, F., Qi, H., Huang, L., and Liu, D. (1997). Factors controlling the efficiency of cationic lipid-mediated transfection in vivo via intravenous administration. *Gene Ther* *4*, 517-523.
- Loebinger, M. R., Kyrtatos, P. G., Turmaine, M., Price, A. N., Pankhurst, Q., Lythgoe, M. F., and Janes, S. M. (2009). Magnetic resonance imaging of mesenchymal stem cells homing to pulmonary metastases using biocompatible magnetic nanoparticles. *Cancer Res* *69*, 8862-8867.
- Lopata, M. A., Cleveland, D. W., and Sollner-Webb, B. (1984). High level transient expression of a chloramphenicol acetyl transferase gene by DEAE-dextran mediated DNA transfection coupled with a dimethyl sulfoxide or glycerol shock treatment. *Nucleic Acids Res* *12*, 5707-5717.
- Luo, D., and Saltzman, W. M. (2000). Enhancement of transfection by physical concentration of DNA at the cell surface. *Nat Biotechnol* *18*, 893-895.
- MacKenzie, T. C., Kobinger, G. P., Kootstra, N. A., Radu, A., Sena-Esteves, M., Bouchard, S., Wilson, J. M., Verma, I. M., and Flake, A. W. (2002). Efficient transduction of liver and muscle after in utero injection of lentiviral vectors with different pseudotypes. *Mol Ther* *6*, 349-358.
- Maguire, A. M., Simonelli, F., Pierce, E. A., Pugh, E. N., Jr., Mingozzi, F., Bennicelli, J., Banfi, S., Marshall, K. A., Testa, F., Surace, E. M., *et al.* (2008). Safety and efficacy of gene transfer for Leber's congenital amaurosis. *N Engl J Med* *358*, 2240-2248.
- Mah, C., Fraitas, T. J., Jr., Zolotukhin, I., Song, S., Flotte, T. R., Dobson, J., Batich, C., and Byrne, B. J. (2002). Improved method of recombinant AAV2 delivery for systemic targeted gene therapy. *Mol Ther* *6*, 106-112.
- Maucksch, C., Aneja, M. K., Hennen, E., Bohla, A., Hoffmann, F., Elfinger, M., Rosenecker, J., and Rudolph, C. (2008). Cell type differences in activity of the *Streptomyces* bacteriophage phiC31 integrase. *Nucleic Acids Res* *36*, 5462-5471.

- Merchav, S., and Wagemaker, G. (1984). Detection of murine bone marrow granulocyte/macrophage progenitor cells (GM-CFU) in serum-free cultures stimulated with purified M-CSF or GM-CSF. *Int J Cell Cloning* 2, 356-367.
- Meyer, M., Zintchenko, A., Ogris, M., and Wagner, E. (2007). A dimethylmaleic acid-melittin-polylysine conjugate with reduced toxicity, pH-triggered endosomolytic activity and enhanced gene transfer potential. *J Gene Med* 9, 797-805.
- Meyers, P. H., Cronin, F., and Nice, C. M. J. (1963). Experimental Approach in the Use and Magnetic Control of Metallic Iron Particles in the Lymphatic and Vascular System of Dogs as a Contrast and Isotopic Agent. *Am J Roentgenol Radium Ther Nucl Med* 90.
- Miltenyi, S., Muller, W., Weichel, W., and Radbruch, A. (1990). High gradient magnetic cell separation with MACS. *Cytometry* 11, 231-238.
- Mir, L. M. (2009). Nucleic acids electrotransfer-based gene therapy (electrogenetherapy): past, current, and future. *Mol Biotechnol* 43, 167-176.
- Miyoshi, H., Takahashi, M., Gage, F. H., and Verma, I. M. (1997). Stable and efficient gene transfer into the retina using an HIV-based lentiviral vector. *Proc Natl Acad Sci U S A* 94, 10319-10323.
- Moghimi, S. M., Symonds, P., Murray, J. C., Hunter, A. C., Debska, G., and Szewczyk, A. (2005). A two-stage poly(ethylenimine)-mediated cytotoxicity: implications for gene transfer/therapy. *Mol Ther* 11, 990-995.
- Mykhaylyk, O., Antequera, Y. S., Vlaskou, D., and Plank, C. (2007a). Generation of magnetic nonviral gene transfer agents and magnetofection in vitro. *Nat Protoc* 2, 2391-2411.
- Mykhaylyk, O., Sanchez-Antequera, Y., Vlaskou, D., Hammerschmid, E., Anton, M., Zelphati, O., and Plank, C. (2010). Liposomal magnetofection. *Methods Mol Biol* 605, 487-525.
- Mykhaylyk, O., Steingötter, A., Perea, H., Aigner, J., Botnar, R., and Plank, C. (2009a). Nucleic Acid Delivery to Magnetically-Labeled Cells in a 2D Array and at the Luminal Surface of Cell Culture Tube and Their Detection by MRI. *Journal of Biomedical Nanotechnology* 5, 692-706.
- Mykhaylyk, O., Vlaskou, D., Tresilwised, N., Pithayanukul, P., Moller, W., and Plank, C. (2007b). Magnetic nanoparticle formulations for DNA and siRNA delivery. *Journal of Magnetism and Magnetic Materials*
- Proceedings of the Sixth International Conference on the Scientific and Clinical Applications of Magnetic Carriers - SCAMC-06 311, 275-281.
- Mykhaylyk, O., Zelphati, O., Hammerschmid, E., Anton, M., Rosenecker, J., and Plank, C. (2009b). Recent advances in magnetofection and its potential to deliver siRNAs in vitro. *Methods Mol Biol* 487, 111-146.
- Mykhaylyk, O., Zelphati, O., Rosenecker, J., and Plank, C. (2008). siRNA delivery by magnetofection. *Curr Opin Mol Ther* 10, 493-505.
- Naldini, L. (1998). Lentiviruses as gene transfer agents for delivery to non-dividing cells. *Curr Opin Biotechnol* 9, 457-463.

- Naldini, L., Blomer, U., Gally, P., Ory, D., Mulligan, R., Gage, F. H., Verma, I. M., and Trono, D. (1996). In vivo gene delivery and stable transduction of nondividing cells by a lentiviral vector. *Science* *272*, 263-267.
- Nanou, A., and Azzouz, M. (2009). Gene therapy for neurodegenerative diseases based on lentiviral vectors. *Prog Brain Res* *175*, 187-200.
- Neven, B., Leroy, S., Decaluwe, H., Le Deist, F., Picard, C., Moshous, D., Mahlaoui, N., Debre, M., Casanova, J. L., Dal Cortivo, L., *et al.* (2009). Long-term outcome after hematopoietic stem cell transplantation of a single-center cohort of 90 patients with severe combined immunodeficiency. *Blood* *113*, 4114-4124.
- Nguyen, L. T., Atobe, K., Barichello, J. M., Ishida, T., and Kiwada, H. (2007). Complex formation with plasmid DNA increases the cytotoxicity of cationic liposomes. *Biol Pharm Bull* *30*, 751-757.
- Nickoloff, J. A. (1995). *Electroporation Protocols for Microorganisms*. Totowa, New jersey: Humana press v-iv.
- Nishikawa, M., and Hashida, M. (2002). Nonviral approaches satisfying various requirements for effective in vivo gene therapy. *Biol Pharm Bull* *25*, 275-283.
- Ogris, M., Steinlein, P., Kursa, M., Mechtler, K., Kircheis, R., and Wagner, E. (1998). The size of DNA/transferrin-PEI complexes is an important factor for gene expression in cultured cells. *Gene Ther* *5*, 1425-1433.
- Ogris, M., and Wagner, E. (2002). Tumor-targeted gene transfer with DNA polyplexes. *Somat Cell Mol Genet* *27*, 85-95.
- Ogris, M., Wagner, E., and Steinlein, P. (2000). A versatile assay to study cellular uptake of gene transfer complexes by flow cytometry. *Biochim Biophys Acta* *1474*, 237-243.
- Orentas, R. J., Roskopf, S. J., Nolan, G. P., and Nishimura, M. I. (2001). Retroviral transduction of a T cell receptor specific for an Epstein-Barr virus-encoded peptide. *Clin Immunol* *98*, 220-228.
- Orschell-Traycoff, C. M., Hiatt, K., Dagher, R. N., Rice, S., Yoder, M. C., and Srour, E. F. (2000). Homing and engraftment potential of Sca-1(+)/lin(-) cells fractionated on the basis of adhesion molecule expression and position in cell cycle. *Blood* *96*, 1380-1387.
- Pandori, M., Hobson, D., and Sano, T. (2002). Adenovirus-microbead conjugates possess enhanced infectivity: a new strategy for localized gene delivery. *Virology* *299*, 204-212.
- Pannell, D., Osborne, C. S., Yao, S., Sukonnik, T., Pasceri, P., Karaiskakis, A., Okano, M., Li, E., Lipshitz, H. D., and Ellis, J. (2000). Retrovirus vector silencing is de novo methylase independent and marked by a repressive histone code. *EMBO J* *19*, 5884-5894.
- Papapetrou, E. P., Zoumbos, N. C., and Athanassiadou, A. (2005). Genetic modification of hematopoietic stem cells with nonviral systems: past progress and future prospects. *Gene Ther* *12 Suppl 1*, S118-130.
- Plank, C., Anton, M., Rudolph, C., Rosenecker, J., and Krotz, F. (2003a). Enhancing and targeting nucleic acid delivery by magnetic force. *Expert Opin Biol Ther* *3*, 745-758.

- Plank, C., Scherer, F., and Rudolph, C. (2005). Localized nucleic acid delivery: A discussion of selected methods. DNA Pharmaceuticals, M Schlee, ed (Weinheim, Wiley-VCH Verlag GmbH & Co KGaA), 55-116.
- Plank, C., Scherer, F., Schillinger, U., and Anton, M. (2000). Magnetofection: enhancement and localization of gene delivery with magnetic particles under the influence of a magnetic field. *J Gene Med* 2, 24.
- Plank, C., Scherer, F., Schillinger, U., Bergemann, C., and Anton, M. (2003b). Magnetofection: enhancing and targeting gene delivery with superparamagnetic nanoparticles and magnetic fields. *J Liposome Res* 13, 29-32.
- Plank, C., Schillinger, U., Scherer, F., Bergemann, C., Remy, J. S., Krotz, F., Anton, M., Lausier, J., and Rosenecker, J. (2003c). The magnetofection method: using magnetic force to enhance gene delivery. *Biol Chem* 384, 737-747.
- Pollard, H., Remy, J. S., Loussouarn, G., Demolombe, S., Behr, J. P., and Escande, D. (1998). Polyethylenimine but not cationic lipids promotes transgene delivery to the nucleus in mammalian cells. *J Biol Chem* 273, 7507-7511.
- Pradhan, P., Giri, J., Rieken, F., Koch, C., Mykhaylyk, O., Doblinger, M., Banerjee, R., Bahadur, D., and Plank, C. (2010). Targeted temperature sensitive magnetic liposomes for thermo-chemotherapy. *J Control Release* 142, 108-121.
- Prince, H. M., Wall, D., Rischin, D., Toner, G. C., Seymour, J. F., Blakey, D., Haylock, D., Simmons, P., Wolf, M., Januszewicz, E. H., *et al.* (2002). CliniMACS CD34-selected cells to support multiple cycles of high-dose therapy. *Cytotherapy* 4, 147-155.
- Puls, R., and Minchin, R. (1999). Gene transfer and expression of a non-viral polycation-based vector in CD4+ cells. *Gene Ther* 6, 1774-1778.
- Raper, S. E., Chirmule, N., Lee, F. S., Wivel, N. A., Bagg, A., Gao, G. P., Wilson, J. M., and Batshaw, M. L. (2003). Fatal systemic inflammatory response syndrome in a ornithine transcarbamylase deficient patient following adenoviral gene transfer. *Mol Genet Metab* 80, 148-158.
- Rebolledo, M. A., Krogstad, P., Chen, F., Shannon, K. M., and Klitzner, T. S. (1998). Infection of human fetal cardiac myocytes by a human immunodeficiency virus-1-derived vector. *Circ Res* 83, 738-742.
- Recillas-Targa, F., Valadez-Graham, V., and Farrell, C. M. (2004). Prospects and implications of using chromatin insulators in gene therapy and transgenesis. *Bioessays* 26, 796-807.
- Roda, B., Lanzoni, G., Alviano, F., Zattoni, A., Costa, R., Di Carlo, A., Marchionni, C., Franchina, M., Ricci, F., Tazzari, P. L., *et al.* (2009). A Novel Stem Cell Tag-Less Sorting Method. *Stem Cell Rev Rep*.
- Ross, P. C., and Hui, S. W. (1999). Lipoplex size is a major determinant of in vitro lipofection efficiency. *Gene Ther* 6, 651-659.
- Sacha, J. B., Chung, C., Reed, J., Jonas, A. K., Bean, A. T., Spencer, S. P., Lee, W., Vojnov, L., Rudersdorf, R., Friedrich, T. C., *et al.* (2007). Pol-specific CD8+ T cells recognize simian immunodeficiency virus-infected cells prior to Nef-mediated major histocompatibility complex class I downregulation. *J Virol* 81, 11703-11712.



- Sauer, A. M., de Bruin, K. G., Ruthardt, N., Mykhaylyk, O., Plank, C., and Brauchle, C. (2009). Dynamics of magnetic lipoplexes studied by single particle tracking in living cells. *J Control Release* 137, 136-145.
- Savoldo, B., Heslop, H. E., and Rooney, C. M. (2000). The use of cytotoxic t cells for the prevention and treatment of epstein-barr virus induced lymphoma in transplant recipients. *Leuk Lymphoma* 39, 455-464.
- Schaft, N., Willemsen, R. A., de Vries, J., Lankiewicz, B., Essers, B. W., Gratama, J. W., Figdor, C. G., Bolhuis, R. L., Debets, R., and Adema, G. J. (2003). Peptide fine specificity of anti-glycoprotein 100 CTL is preserved following transfer of engineered TCR alpha beta genes into primary human T lymphocytes. *J Immunol* 170, 2186-2194.
- Scherer, F., Anton, M., Schillinger, U., Henke, J., Bergemann, C., Kruger, A., Gansbacher, B., and Plank, C. (2002). Magnetofection: enhancing and targeting gene delivery by magnetic force in vitro and in vivo. *Gene Ther* 9, 102-109.
- Sebestyen, Z., Schooten, E., Sals, T., Zaldivar, I., San Jose, E., Alarcon, B., Bobisse, S., Rosato, A., Szollosi, J., Gratama, J. W., *et al.* (2008). Human TCR that incorporate CD3zeta induce highly preferred pairing between TCRalpha and beta chains following gene transfer. *J Immunol* 180, 7736-7746.
- Singh, H., Manuri, P. R., Olivares, S., Dara, N., Dawson, M. J., Huls, H., Hackett, P. B., Kohn, D. B., Shpall, E. J., Champlin, R. E., and Cooper, L. J. (2008). Redirecting specificity of T-cell populations for CD19 using the Sleeping Beauty system. *Cancer Res* 68, 2961-2971.
- Smith, T. A., Mehaffey, M. G., Kayda, D. B., Saunders, J. M., Yei, S., Trapnell, B. C., McClelland, A., and Kaleko, M. (1993). Adenovirus mediated expression of therapeutic plasma levels of human factor IX in mice. *Nat Genet* 5, 397-402.
- Sonawane, N. D., Szoka, F. C., Jr., and Verkman, A. S. (2003). Chloride accumulation and swelling in endosomes enhances DNA transfer by polyamine-DNA polyplexes. *J Biol Chem* 278, 44826-44831.
- Song, H., Song, B. W., Cha, M. J., Choi, I. G., and Hwang, K. C. (2010). Modification of mesenchymal stem cells for cardiac regeneration. *Expert Opin Biol Ther* 10, 309-319.
- Staal, F. J., Pike-Overzet, K., Ng, Y. Y., and van Dongen, J. J. (2008). Sola dosis facit venenum. Leukemia in gene therapy trials: a question of vectors, inserts and dosage? *Leukemia* 22, 1849-1852.
- Stein, S., Ott, M. G., Schultze-Strasser, S., Jauch, A., Burwinkel, B., Kinner, A., Schmidt, M., Kramer, A., Schwable, J., Glimm, H., *et al.* (2010). Genomic instability and myelodysplasia with monosomy 7 consequent to EVI1 activation after gene therapy for chronic granulomatous disease. *Nat Med* 16, 198-204.
- Suzuki, M., Mikami, T., Matsumoto, T., and Suzuki, S. (1977). Preparation and antitumor activity of o-palmitoyldextran phosphates, o-palmitoyldextrans, and dextran phosphate. *Carbohydr Res* 53, 223-229.
- Tatum, E. L. (1966). Molecular biology, nucleic acids, and the future of medicine. *Perspect Biol Med* 10, 19-32.

- Uduehi, A., Mailhos, C., Truman, H., Thrasher, A. J., Kinnon, C., and Hart, S. L. (2003). Enhancement of integrin-mediated transfection of haematopoietic cells with a synthetic vector system. *Biotechnol Appl Biochem* 38, 201-209.
- Van Tendeloo, V. F., Willems, R., Ponsaerts, P., Lenjou, M., Nijs, G., Vanhove, M., Muylaert, P., Van Cauwelaert, P., Van Broeckhoven, C., Van Bockstaele, D. R., and Berneman, Z. N. (2000). High-level transgene expression in primary human T lymphocytes and adult bone marrow CD34+ cells via electroporation-mediated gene delivery. *Gene Ther* 7, 1431-1437.
- Varela-Rohena, A., Carpenito, C., Perez, E. E., Richardson, M., Parry, R. V., Milone, M., Scholler, J., Hao, X., Mexas, A., Carroll, R. G., *et al.* (2008). Genetic engineering of T cells for adoptive immunotherapy. *Immunol Res* 42, 166-181.
- von Gersdorff, K., Ogris, M., and Wagner, E. (2005). Cryoconserved shielded and EGF receptor targeted DNA polyplexes: cellular mechanisms. *Eur J Pharm Biopharm* 60, 279-285.
- Wagner, J., Kean, T., Young, R., Dennis, J. E., and Caplan, A. I. (2009). Optimizing mesenchymal stem cell-based therapeutics. *Curr Opin Biotechnol*.
- Walter, E. A., Greenberg, P. D., Gilbert, M. J., Finch, R. J., Watanabe, K. S., Thomas, E. D., and Riddell, S. R. (1995). Reconstitution of cellular immunity against cytomegalovirus in recipients of allogeneic bone marrow by transfer of T-cell clones from the donor. *N Engl J Med* 333, 1038-1044.
- Ward, C. M. (2000). Folate-targeted non-viral DNA vectors for cancer gene therapy. *Curr Opin Mol Ther* 2, 182-187.
- Watson, J. D., and Crick, F. H. C. (1953a). Genetical implications of the structure of deoxyribonucleic acid. *Nature* 171, 964-967.
- Watson, J. D., and Crick, F. H. C. (1953b). Molecular Structure of Nucleic Acids: A Structure for Deoxyribose Nucleic Acid. *Nature* 171, 737-738.
- Weaver, J. C. (1995). Electroporation theory. Concepts and mechanisms. *Methods Mol Biol* 55, 3-28.
- Weissleder, R., Stark, D. D., Engelstad, B. L., Bacon, B. R., Compton, C. C., White, D. L., Jacobs, P., and Lewis, J. (1989). Superparamagnetic iron oxide: pharmacokinetics and toxicity. *AJR Am J Roentgenol* 152, 167-173.
- Wilhelm, C., Fortin, J. P., and Gazeau, F. (2007). Tumour cell toxicity of intracellular hyperthermia mediated by magnetic nanoparticles. *Journal of nanoscience and nanotechnology* 7, 2933-2937.
- Wilhelm, C., and Gazeau, F. (2008). Universal cell labelling with anionic magnetic nanoparticles. *Biomaterials* 29, 3161-3174.
- Wilhelm, C., Gazeau, F., and Bacri, J. C. (2002). Magnetophoresis and ferromagnetic resonance of magnetically labeled cells. *Eur Biophys J* 31, 118-125.
- Willemsen, R. A., Weijtens, M. E., Ronteltap, C., Eshhar, Z., Gratama, J. W., Chames, P., and Bolhuis, R. L. (2000). Grafting primary human T lymphocytes with cancer-specific chimeric single chain and two chain TCR. *Gene Ther* 7, 1369-1377.

- Williams, D. A. (2008). Sleeping beauty vector system moves toward human trials in the United States. *Mol Ther* 16, 1515-1516.
- Xenariou, S., Griesenbach, U., Ferrari, S., Dean, P., Scheule, R. K., Cheng, S. H., Geddes, D. M., Plank, C., and Alton, E. W. (2006). Using magnetic forces to enhance non-viral gene transfer to airway epithelium in vivo. *Gene Ther* 13, 1545-1552.
- Xu, Y., and Szoka, F. C., Jr. (1996). Mechanism of DNA release from cationic liposome/DNA complexes used in cell transfection. *Biochemistry* 35, 5616-5623.
- Yang, F., Green, J. J., Dinio, T., Keung, L., Cho, S. W., Park, H., Langer, R., and Anderson, D. G. (2009). Gene delivery to human adult and embryonic cell-derived stem cells using biodegradable nanoparticulate polymeric vectors. *Gene Ther* 16, 533-546.
- Yang, X. Q., Chen, Y. H., Yuan, R. X., Chen, G. H., Blanco, E., Gao, J. M., and Shuai, X. T. (2008). Folate encoded and Fe<sub>3</sub>O<sub>4</sub>-loaded polymeric micelles for dual targeting of cancer cells. *Polymer* 49, 3477-3485.
- Yee, C., Thompson, J. A., Byrd, D., Riddell, S. R., Roche, P., Celis, E., and Greenberg, P. D. (2002). Adoptive T cell therapy using antigen-specific CD8<sup>+</sup> T cell clones for the treatment of patients with metastatic melanoma: in vivo persistence, migration, and antitumor effect of transferred T cells. *Proc Natl Acad Sci U S A* 99, 16168-16173.
- Zauner, W., Kichler, A., Schmidt, W., Sinski, A., and Wagner, E. (1996). Glycerol enhancement of ligand-polylysine/DNA transfection. *BioTechniques* 20, 905-913.
- Zelphati, O., and Szoka, F. C., Jr. (1996a). Intracellular distribution and mechanism of delivery of oligonucleotides mediated by cationic lipids. *Pharm Res* 13, 1367-1372.
- Zelphati, O., and Szoka, F. C., Jr. (1996b). Mechanism of oligonucleotide release from cationic liposomes. *Proc Natl Acad Sci U S A* 93, 11493-11498.
- Zhu, N., Liggitt, D., Liu, Y., and Debs, R. (1993). Systemic gene expression after intravenous DNA delivery into adult mice. *Science* 261, 209-211.
- Zintchenko, A., Philipp, A., Dehshahri, A., and Wagner, E. (2008). Simple modifications of branched PEI lead to highly efficient siRNA carriers with low toxicity. *Bioconjug Chem* 19, 1448-1455.

## 8. ACKNOWLEDGEMENTS

Lots of thanks to Prof. Dr. Ernst Wagner for the supervision of this thesis and valuable discussions.

I want to thank PD Dr. Christian Plank for give me the opportunity to carry out my PhD in his lab, for his support during the time and for his intensive supervision and full discussions in writing the dissertation.

Many thanks also to Prof. Dr. Bernd Gänsbacher for the possibility to work in his “Institute of Experimental Oncology and Therapy Research” in Klinikum Rechts der Isar.

I want to thank specially Dr. Olga Mykhaylyk for her inconditionally help and friendship and for her intensive supervision in the experiments and manuscripts. Olga, thanks for continuously listening, helping and encouraging if something went wrong.

To fill me with enthusiasm for scientific work I always will be grateful to Dr. Cristian Plank and Dr. Olga Mykhaylyk.

I would like to thank all my colleagues in laboratory 1.39 for their help, support and joy, especially to Nittaya Tresilwised, Dr. Pallab Pradham, Dr. Dialekti Vlaskou and Sabine Brandt.

Because they always were ready to help me, I would like to thank all the colleagues in the Institute of Experimental Oncology and Therapy Reasearch for their help. Special thanks to Edelburga Hammerschmid, without you FACS results would not be possible.

Many thanks to Prof. Gerard Wagemaker, Prof. Zygmunt Pojda and Dr. Niek Van Til for introduce me in the stem cells world and their fruitful discussions. Many Thanks also to Ian Johnston (Miltenyi biotec) for his rich help with the PBMCs.

My very special thanks to my parents who always encouraged me in my plans and without whom all my education would not have been possible. Os quiero mucho.

Finnally, but not less, I would like to thank my husband. Jan, thanks a lot for listening all my problems, to be patient and support me during the last four years. Te quiero.

## 9. CURRICULUM VITAE

- Personal data**
- Subname: Sánchez-Antequera
- Name: Yolanda
- Date of birth: 08.05.1980
- Birthplace: Valencia
- Family status: Married, no children
- Nationality: Spanish
- Current Position
- Scientist at Comprehensive Pneumology Center (CPC),  
Institute of Lung Biology and Disease (iLBD), Helmholtz  
Zentrum München, Group of Drug delivery (Dr. Otmar Schmid)
- Tel.: +49 (0) 89 3187 3795
- E-Mail: [yolanda@harenburg.net](mailto:yolanda@harenburg.net);  
[yolanda.antequera@helmholtz-muenchen.de](mailto:yolanda.antequera@helmholtz-muenchen.de)
- Languages:** Spanish, Catalan, German und English
- Education**
- 09/1994 - 06/1998 High school “Dr. Simarro”, Xàtiva – Spain**
- Degree: Bachillerato (Comparable to a German Abitur)
- 10/1998 - 07/2003 University of Valencia - Spain**
- Degree: Licenciada en Biología
  - Equivalent title in Germany: Diplom-Biologin (Uni)
- 11/2003 – 03/2004 University of Valencia - Spain**
- Teacher training CAP (Curso Adaptación Pedagógica)
  - Course content: Theory and practical part of teaching in a high school
  - The CAP tends to result in Spain for the teaching license in secondary schools
- 10/2004 – 09/2005 Diploma thesis at ZIEL (TU München)**
- Topic “Essential genes of *Salmonella typhimurium*” as validation of the Spanish diploma at the TUM

**01/2006-03/2010** PhD student at the Klinikum rechts der Isar, Institut of Experimental Oncology and Therapy research, Group of PD Dr. Christian Plank.

Supervisors: Prof.Dr. Ernst Wagner and PD Dr. Christian Plank

**Since 04/2010** Scientist at Comprehensive Pneumology Center (CPC), Institute of Lung Biology and Disease (iLBD), Helmholtz Zenrum München, Group of Drug delivery (Dr. Otmar Schmid)

### Grants

- Grant as research student at the Department of Microbiology at the University of Valencia (Spain)
- Grant to perform Diplomarbeit at ZIEL TU München

### Stay abroad

- **04/2007 and 08/2009** Research cooperation in the framework of the EU Project "Magselectofection" at the Erasmus University Rotterdam, Erasmus Medical center, Department of Hematology
- **12/2007 and 05/2009** Research cooperation in the framework of the EU Project "Magselectofection" at the Erasmus University Rotterdam, Erasmus Medical center, Department of Hematology M. Skolodowska-Curie Memorial Cancer Center Warsaw, Department of Experimental Hematology and Cord Blood Bank
- **11/2008** Research cooperation in the framework of the EU Project "Magselectofection" at the Erasmus University Rotterdam, Erasmus Medical center, Department of Hematology Miltenyi Biotec

## 9.1. Publications

### 9.1.1. Original papers

- Olga Mykhaylyk, Yolanda Sánchez-Antequera, Dialekti Vlaskou and Christian Plank (2007). Generation of magnetic nonviral gene transfer agents and magnetofection in vitro. *Nature protocols*. 2:2391-2411.
- Olga Mykhaylyk, Yolanda Sánchez-Antequera, Dialekti Vlaskou, Edelburga Hammerschmid, Olivier Zelphati, Christian Plank. (2010) Liposomal magnetofection. *Methods Mol Biol*; 605: 487-525.
- Yolanda Sanchez-Antequera, Olga M. Mykhaylyk, Stefan Thalhammer, Christian Plank. Gene delivery to Jurkat T cells using non-viral vectors associated with magnetic nanoparticles (2010). Special Issue on Advances in Drug delivery Systems. *International Journal of Biomedical Nanoscience and Nanotechnology (IJBNN)*. Vol. 1, No.2/3/4: 202 – 229.
- Yolanda Sanchez-Antequera, Olga Mykhaylyk, Arzu Cengizeroglu, Niek P van Til, Martina Anton, Ian Johnston, Zygmunt Pojda, Gerard Wagemaker, Christian Plank. Magselctofection: an integrated method of nanomagnetic separation and genetic modification of target cells. Submitted

### 9.1.2. Oral presentations

- Sánchez-Antequera, Y, Arzu Cengizeroglu, Olga Mykhaylyk, Ian Johnston, Christian Plank. A novel non-viral and viral technology for ex-vivo gene therapy: Magselctofection. *CliniGene 2nd Training courses. Viral and non-viral vectors for gene therapy approaches to human diseases: new developments*. January 22-23, 2009. Barcelona, Spain.
- Olga Mykhaylyk, Yolanda Sánchez-Antequera, Nittaya Tresilwised, Stefan Thalhammer, Denis Adigüzel, Markus Döblinger, Thomas Bein, Per Sonne Holm, Christian Plank. Magnetic nanoparticles for gene delivery: some determinant of the efficient delivery vectors. 9<sup>th</sup> German Ferrofluid Workshop, p. 58-59, September 22-25, 2009. Benediktbeuern, Germany.

- Yolanda Sánchez-Antequera, Arzu Cengizeroglu, Aleksandra Kopera, Olga Mykhaylyk, Ian Johnston, Zygmunt Pojda and Christian Plank. A novel non-viral and vira technology for ex-vivo gene therapy: Magselectofection. Hum Gene Ther. 2009; 20(11):1222. Annual Meeting ESGCT: European Society of Gene and Cell Therapy. 20-25 November 2009. Hannover, Germany.
- Olga Mykhaylyk, Yolanda Sánchez-Antequera, Nittaya Tresilwised, Markus Döblinger, Stefan Thalhammer, Per Sonne Holm, Christian Plank. Physicochemical Platform of the Efficient Magnetic Gene Delivery Vectors. Hum Gene Ther. 2009; 20(11): 1516. Annual Meeting ESGCT, November 20-25, 2009. Hannover, Germany.
- Olga Mykhaylyk, Yolanda Sánchez-Antequera, Markus Döblinger, Stefan Thalhammer, Per Sonne Holm, Christian Plank. Optimizing virus-magnetic nanoparticle complexes for gene transfer in cell lines and stem cells. 8th International Conference on the Scientific and Clinical Applications of Magnetic Carriers took place in Rostock, Germany, May 25-29, 2010.

### 9.1.3. Poster presentations

- Sánchez- Antequera Y, Mykhaylyk O, Hammerschmid E, Plank C. Magselectofection - Combined magnetic cell separation and magnetofection. Hum Gene Ther. 2007;18:1048. ESGCT: European Society of Gene and Cell Therapy. October 2007. Rotterdam, Netherlands.
- Sánchez-Antequera, Y, Hammerschmid E, Mykhaylyk O, Plank C. Magselectofection – combined magnetic cell separation and magnetofection. Scientific and Clinical Applications of Magnetic Carriers. 21-24 May 2008. Vancouver, Canada.
- Olga Mykhaylyk, Nittaya Tresilwised, Yolanda Sánchez-Antequera, Arzu Cengizeroglu, Per Sonne Holm, and Christian Plank. Lentivirus and oncolytic adenovirus magnetic complexes: some determinants for biological efficacy *in vitro*. Consert symposium: Lentiviral vectors: concepts, practice, hope and reality. June 29th-July 5th, 2008. University of Evry-Val 'Essonne, Evry, France.



- 
- Sánchez-Antequera Y, Cengizeroglu A, Hammerschmid E, Mykhaylyk O, Plank C. Magselectofection – combined magnetic cell separation and magnetofection: a novel non-viral and viral technology for ex-vivo gene therapy. Hum Gene Ther. 2008; 19(10):1145. ESGCT: European Society of Gene and Cell Therapy. 13-16 November 2008. Brugge, Belgium.
  - Zygmunt Pojda, Eugeniusz K. Machaj, Yolanda Sánchez-Antequera, Paulina Adamczyk-Wojciechowska, Aleksandra Kopera, Marzena Korczak, Bartłomiej Noszczyk, Christian Plank, Romuald Dębski, Monika Turkowska. Stem cells of fetal origin — biology and the prospects of clinical applications. 43rd Annual Meeting of the Polish Biochemical Society and the 10th Conference of Cell Biology, 2008.
  - P. Adamczyk-Wojciechowska, E. K. Machaj, M. Korczak , Y. Sánchez-Antequera, C. Plank, A. Kopera, Z. Pojda. Umbilical cord stromal cells (UCSC) - Do they fulfill the criteria for cells useful for regenerative medicine applications? Annual Meeting ISCT 2008.
  - Sánchez-Antequera, Y, Arzu Cengizeroglu, Olga Mykhaylyk, Ian Johnston, Christian Plank. A novel non-viral and viral technology for ex-vivo gene therapy: Magselectofection. CliniGene 2nd Training courses. Viral and non-viral vectors for gene therapy approaches to human diseases: new developments. January 22-23, 2009. Barcelona, Spain.
  - Olga Mykhaylyk, Yolanda Sánchez-Antequera, Nittaya Tresilwised, Markus Döblinger, Stefan Thalhammer, Per Sonne Holm, Christian Plank. Engineering magnetic nanoparticles and formulations for gene delivery. 11th European Symposium on Controlled Drug Delivery. April 7-9, 2010. Egmond aan Zee, The Netherlands.